Economic, Greenhouse Gas, and Resource Assessment for Fuel and Protein Production from Microalgae: 2022 Algae Harmonization Update

Contributing Authors

Report Coordination: Ryan Davis,[1] Troy R. Hawkins[2]

Resource Assessment: Andre Coleman,[3] Song Gao[3]

Algae Farm TEA: Bruno Klein,[1] Matthew Wiatrowski[1]

HTL Conversion TEA: Yunhua Zhu,[3] Yiling Xu,[3] Lesley Snowden-Swan,[3] Peter Valdez[3]

System LCA: Jingyi Zhang,[2] Udayan Singh,[2] Longwen Ou[2]

[1] *National Renewable Energy Laboratory*
[2] *Argonne National Laboratory*
[3] *Pacific Northwest National Laboratory*

Argonne is a U.S. Department of Energy laboratory managed by UChicago Argonne LLC under contract DE-AC02-06CH11357. NREL is a national laboratory of the U.S. Department of Energy Office of Energy Efficiency & Renewable Energy operated by the Alliance for Sustainable Energy LLC under contract DE-AC36-08GO28308. Pacific Northwest National Laboratory is operated by Battelle for the U.S. Department of Energy under contract DE-AC05-76RL01830.

Technical Report
ANL/ESIA-23/7; NREL/TP-5100-87099; PNNL-35604
February 2024

Economic, Greenhouse Gas, and Resource Assessment for Fuel and Protein Production from Microalgae: 2022 Algae Harmonization Update

Contributing Authors

Report Coordination: Ryan Davis,[1] Troy R. Hawkins[2]

Resource Assessment: Andre Coleman,[3] Song Gao[3]

Algae Farm TEA: Bruno Klein,[1] Matthew Wiatrowski[1]

HTL Conversion TEA: Yunhua Zhu,[3] Yiling Xu,[3] Lesley Snowden-Swan,[3] Peter Valdez[3]

System LCA: Jingyi Zhang,[2] Udayan Singh,[2] Longwen Ou[2]

[1] *National Renewable Energy Laboratory*
[2] *Argonne National Laboratory*
[3] *Pacific Northwest National Laboratory*

Suggested Citation
National Renewable Energy Laboratory (NREL), Argonne National Laboratory (ANL), and Pacific Northwest National Laboratory (PNNL). 2024. *Economic, Greenhouse Gas, and Resource Assessment for Fuel and Protein Production from Microalgae: 2022 Algae Harmonization Update*. Golden, CO: National Renewable Energy Laboratory. NREL/TP-5100-87099. www.nrel.gov/docs/fy24osti/87099.pdf.

Technical Report
ANL/ESIA-23/7; NREL/TP-5100-87099; PNNL-35604
February 2024

NOTICE

This work was authored by the National Renewable Energy Laboratory, operated by Alliance for Sustainable Energy, LLC, for the U.S. Department of Energy (DOE) under Contract No. DE-AC36-08GO28308; Argonne National Laboratory, managed by UChicago Argonne, LLC, under DOE Contract No. DE-AC02-06CH11357; and Pacific Northwest National Laboratory, operated by Battelle under DOE Contract No. DE-AC05-76RL01830. Funding provided by the U.S. Department of Energy Office of Energy Efficiency and Renewable Energy Bioenergy Technologies Office. The views expressed in the article do not necessarily represent the views of DOE or the U.S. Government.

Nomenclature

AFDW	ash-free dry weight
BAT	Biomass Assessment Tool
BETO	Bioenergy Technologies Office
CAP	combined algae processing
CAPEX	capital expenses
CO_2	carbon dioxide
CO_2e	carbon dioxide equivalent
CONUS	conterminous United States
DAC	direct air capture
DAP	diammonium phosphate
DISCOVR	Development of Integrated Screening, Cultivar Optimization, and Verification Research
DLUC	direct land use change
DOE	U.S. Department of Energy
FAME	fatty acid methyl esters
FO	forward osmosis
FPCM	fat- and protein-corrected milk
GGE	gasoline gallon equivalent
GHG	greenhouse gas
GREET	Greenhouse Gases, Regulated Emissions, and Energy Use in Technologies
HDN	hydrodenitrogenation
HPH	high-pressure homogenization
HTL	hydrothermal liquefaction
ILUC	indirect land use change
JFC	jet fuel cut
LCA	life cycle analysis
LCI	life cycle inventory
LHSV	liquid hourly space velocity
LUC	land use change
MBSP	minimum biomass selling price
MFSP	minimum fuel selling price
MM	million
OPEX	operating expenses
NREL	National Renewable Energy Laboratory
PC	protein concentrate
PEA	protein-extracted algae
PNNL	Pacific Northwest National Laboratory
SAF	sustainable aviation fuel
TDC	total direct cost
TEA	techno-economic analysis
USDA	U.S. Department of Agriculture

Executive Summary

This report presents an updated "harmonization study" documenting the collaborative analysis of saline microalgae cultivation and conversion to fuels and products. Four national laboratory modeling teams reconvened to investigate the resource, economic, and environmental sustainability implications of integrated systems encompassing large-scale algae farms and conversion biorefineries. Relative to prior harmonization analyses conducted by these partners, the present effort focuses on more near-term technology potential based on the use of nutrient-replete, high-protein algal biomass compositions (more readily achievable today without sacrificing cultivation productivity) coupled with individual algae farms varying in size but generally smaller at 3,900 acres on average (more realistic in practice than a fixed 5,000-acre farm scale previously considered). Additionally, the present assessment adds further granularity around carbon dioxide (CO_2) sourcing and transport via carbon capture of nearby point sources, as well as handling of high-saline cultivation media and resultant blowdown/disposal processing. Finally, this assessment focuses on conversion opportunities to produce both fuel (prioritizing sustainable aviation fuel [SAF], in this case via hydrothermal liquefaction [HTL]) and protein products for the food and feed markets, recognizing growing needs for such products.

The overall approach taken in this report is generally consistent with prior harmonization efforts. A resource assessment of all potential algae farm sites is first established using the Biomass Assessment Tool (BAT), which uses geospatial and temporal models in combination with algae strain growth parameters to quantify the national scalability of algae biomass production. Outputs from the BAT model are then used in the algae farm techno-economic analysis (TEA) models, which subsequently tie into algae conversion TEA models to evaluate the biomass, fuel, and protein production implications for individual sites, compiled to national-scale outputs across the United States. Life cycle inventory (LCI) data for each identified facility site from the BAT, algae farm, and algae conversion models are utilized to perform a life cycle analysis (LCA) to determine the potential environmental sustainability impacts of fuel and protein production at the regional and national levels. Per the focus as a "harmonization" study, the key information flows were synchronized to the greatest practical extent between BAT biophysical/geospatial modeling, algae farm and conversion TEA modeling, and LCA modeling, such that the resulting outputs for resource, economic, and environmental sustainability potential were anchored to the same common framework and set of assumptions.

The BAT model identified several key biomass production parameters that varied spatially and temporally across the Southern United States, including unencumbered land available for cultivation, saline groundwater availability, modeled monthly biomass cultivation productivity rates, saline pond blowdown requirements as a function of evaporation and local groundwater salinity levels, and point-source waste CO_2 identification, supply, and energy requirements for capture and pipeline transport specific to a given industry process. A large portion of the viable production sites identified were shown to be in the South-Central region spanning Texas and Louisiana, accounting for roughly 75% of the total area identified and 74% of the total microalgae biomass potential. However, the regions supporting the most economical algae production were largely concentrated in the Southeast (Florida and nominally Georgia, 14% of total area and 13% of total biomass), driven by higher biomass productivities, lower seasonal variabilities, and larger algae farm scales. The remainder was identified in the Western region encompassing California and Arizona. Despite differences in biomass productivity potential,

salinity of the makeup water, salt disposal requirements, and delivered CO_2 costs between sites, the possibility of producing algal biomass at reasonable prices was demonstrated, with a weighted average minimum biomass selling price (MBSP) of $674 per ton (ash-free dry weight [AFDW] basis, excluding seasonal storage; all costs presented in 2020 dollars) across the entire collection of sites. **This corresponded to a total algal biomass production potential of 152 million tons per year AFDW across 3.9 million acres of total available cultivation pond area, representing a cumulative 268 million tons per year of CO_2 capture potential based on biomass uptake.**

Subsequent conversion of algal biomass to fuels and protein products, using an example conversion pathway via HTL with protein extraction pretreatment, was shown to hold promise pending market applications and volume constraints for the algal protein coproduct. The minimum fuel selling price (MFSP) for **fuel production alone was estimated at $8.69 per gasoline gallon equivalent (GGE) on average across the full site collection with a cumulative fuel potential of 14.4 billion GGE/year** (including SAF at 8.6 billion GGE/year). This would reduce under a "best-case" scenario to **$3.72/GGE with inclusion of algal protein coproduction**, valued for food applications currently served by products such as whey protein and other protein ingredient markets (without applying market volume constraints for such products at a cumulative 51 million tons/year of algal protein production), albeit at a lower fuel production potential of **7.7 billion GGE/year** (4.6 billion GGE/year of SAF). In between these bounds, two intermediate scenarios were also identified under algal protein market constraints for the 2030 projected global whey protein concentrate (PC) market (3.7 million tons/year) or the protein ingredients market (14 million tons/year). The former scenario would achieve an average **MFSP of $8.49/GGE and total fuel output of 13.9 billion GGE/year,** while the latter would reduce the average **MFSP to $7.89/GGE and total fuel output to 12.6 billion GGE/year**. The MFSP values for algae HTL facilities that include protein coproduction can be considerably reduced, owing to a substantial PC coproduct credit of approximately $13.4/GGE despite a lower fuel production rate and added costs for protein extraction.

For LCA modeling, a biorefinery-level analysis was conducted to quantify the total life cycle greenhouse gas (GHG) emissions from all products and their potential GHG emission reductions when displacing conventionally produced counterpart products. In this analysis, algal biorefinery fuel and protein coproduction do not achieve an overall GHG improvement when compared to conventional fuel and soy PC production, but they do demonstrate a significant improvement when compared to conventional fuel and whey PC production (given considerably higher GHG emissions for conventional production of whey PC versus soy PC). However, the current whey PC market is small, and as whey is a coproduct of the cheese industry, its production would not be prevented by replacement with algal PC. However, by replacing conventional grid electricity and natural gas with zero-carbon-intensity renewable energy sources, an approximately 80% reduction in biorefinery-level GHG emissions could be achieved for the overall algal biorefinery, which could enable lower GHG emissions than conventional fuel and soy PC production. Alternatively, fuel-only production demonstrates a modest 9.4% improvement in GHG emissions when compared to conventional fuel production, resulting in a CO_2 reduction potential of 41 million tons per year over the collection of sites that achieve GHG emissions less than conventional fuel. Alternatively, when considering allocation of impacts in the LCA, GHG impacts allocated to algal PC outweigh the effects of increased emissions and loss of nutrient recycling efficiencies when PC coproduction is included, leading to marginally lower GHG

emissions for fuels with PC coproduction relative to fuel production alone. Namely, GHG emissions from fuel and PC coproduction, without being constrained by market limits, range from 48 to 90 g carbon dioxide equivalent (CO_2e) per MJ, with a weighted average of 61 g/MJ when applying mass allocation, while GHG emissions from the fuel-only scenario range from 69 to 118 g/MJ, with a weighted average of 85 g/MJ (compared to a reference case for conventional fuels at 87 g/MJ).

Overall, the results from this study highlight the potential for commodity-scale production of biomass, biofuels, and protein products that could be enabled by cultivation of high-protein microalgae, though also reiterating challenges in fuel yields, costs, and carbon intensities for algal systems that could be significantly improved by moving to low-protein/high-lipid algae compositional targets as found in prior harmonization studies (recognizing this may reflect a longer-term objective to achieve). Additionally, further consideration of other protein food scenarios such as meat alternatives is warranted as market opportunities expand for such products in the future.

Table of Contents

1 Introduction

Over recent years, numerous analyses have been conducted highlighting the potential benefits of microalgae for production of renewable fuels, chemicals, and food/feed applications based on promising opportunities for decarbonization of such products while avoiding competition for land and water resources (Wiatrowski, Davis, and Kruger 2022; Zhu et al. 2020). Microalgae is a promising alternative source for protein owing to its nontoxic nature, high protein content, and low allergenicity (Becker 2007). Whole microalgae, such as *Spirulina* and *Aphanizomenon*, have been used as a human food supplement. In addition, approximately 30% of the world's microalgal biomass production is sold for animal feed applications (Caporgno and Mathys 2018; Saadaoui et al. 2021). Driven by the need for healthy and nutritious food with low fat, cholesterol, and sugar content, microalgae have great potential to become a healthy protein source (Soto-Sierra, Stoykova, and Nikolov 2018). As indicated in Becker (2007) and Wang, Tibbetts, and McGinn (2021), certain algae strains such as *Spirulina* have amino acid contents comparable to eggs and better than soybeans. In addition, using microalgae to produce protein-based food/feed does not incur food competition for protein production as with traditional food crops, such as soy and peas. More importantly, microalgae can yield higher protein per unit area (approximately 4–15 tons/ha/yr) compared to traditional terrestrial crops such as soy (approximately 0.6–1.2 tons/ha/yr) and wheat (approximately 1–2 tons/ha/yr), which makes it a more attractive protein source considering the near-term potential for farmland degradation (Bleakley and Hayes 2017; Koyande et al. 2019).

Collaborators from Argonne National Laboratory, the National Renewable Energy Laboratory (NREL), and Pacific Northwest National Laboratory (PNNL) have conducted a number of "harmonization analyses" seeking to quantify implications on environmental sustainability metrics, economics, and resource availability for the production and conversion of algal biomass. Initial harmonization efforts in 2012–2013 focused on evaluating such metrics as may be attributed to technology performance benchmarks as they stood at the time (e.g., biomass cultivation productivity rates), coupled with biomass conversion through a lipid extraction-based approach (Davis et al. 2012) and hydrothermal liquefaction (HTL) processing (Zhu et al. 2013). Subsequently, an updated harmonization assessment was conducted in 2017 focusing more on understanding the *long-term future potential* implications on those metrics moving beyond benchmark performance levels, while also highlighting opportunities for employing carbon capture of point-source carbon dioxide (CO_2) emissions to support more than 100 million tons per year of algal biomass production potential at the national scale (Davis et al. 2018).

The harmonization analyses helped present a clearer picture of costs, carbon intensity, and resource constraints for integrated algae biorefinery systems reflecting both current and future technology performance projections, based on a harmonized modeling framework employing consistent inputs and assumptions. However, past studies have all focused on prioritizing production of fuel (renewable diesel) as the primary output from the conversion processes, largely seeking to maximize fuel production by employing nutrient depletion before harvesting to shift biomass compositions from high-protein (typical in nutrient-replete cultivation) to high-carbohydrate and/or high-lipid compositions to enable higher fuel conversion yields. While this remains a viable approach warranting further research, it presents a more aspirational case that to date remains more challenging to achieve, given known trade-offs often incurring penalties in

lower cultivation productivity rates when moving to nutrient-deplete harvesting to shift the biomass composition to a lower-protein state (Sajjadi et al. 2018; Procházková et al. 2014). Additionally, it bypasses an opportunity for algae to contribute to other needs such as protein for food/feed applications, supporting agricultural decarbonization as another growing area of emphasis for the U.S. Department of Energy's (DOE's) Bioenergy Technologies Office (BETO) (DOE 2022).

In 2021, DOE, the U.S. Department of Transportation, the U.S. Department of Agriculture (USDA), and other federal government agencies launched a governmentwide memorandum of understanding to develop a comprehensive strategy for scaling up new technologies to produce sustainable aviation fuel (SAF) on a commercial scale (DOE 2021), resulting in the SAF Grand Challenge. SAFs are drop-in fuel blending components derived from renewable or waste-based feedstocks that, relative to petroleum-based fuels, provide reduced CO_2 emissions. The goals of the SAF Grand Challenge include achieving a minimum 50% reduction in life cycle greenhouse gas (GHG) emissions compared to conventional fuel and supplying sufficient SAF to meet 100% of aviation fuel demand, or 35 billion gallons per year, by 2050. A near-term goal of 3 billion gallons per year is established as a milestone for 2030. Most of the current research for algae conversion to fuel focuses on diesel and gasoline products. Limited work has been reported on jet fuel production from microalgae, and most research reports are focused on hydroprocessing of microalgae oils to produce SAF (Bwapwa, Anandraj, and Trois 2018; Gutiérrez-Antonio et al. 2018).

To address the potential for producing SAF from microalgae, Argonne National Laboratory, NREL, and PNNL reconvened for the present work to conduct a new algae harmonization study, this time focused on more near-term deployment potential based on cultivation of nutrient-replete algae for subsequent upgrading to both fuels and protein products. The work further pursues joint modeling efforts similar in nature to the previous harmonization activities focused on evaluating resource assessment, techno-economic analysis (TEA), and life cycle analysis (LCA) for algal biomass production and conversion extrapolated to national scalability potential. Relative to the 2017 harmonization assessment, which focused on longer-term future projections both for cultivation performance (elevated compositional quality enriching carbohydrates/lipids at reduced protein content) and commercial maturity (large 5,000-acre commercial-scale farms significantly exceeding current facility scales) centered around fuel production (Davis et al. 2018), the current effort focuses on nearer-term deployability and the role of microalgae in both fuel and agricultural decarbonization. The 2022 harmonization is focused on addressing the following five topics in particular:

1. **Smaller-scale farms** consisting of 1,000 acres of production pond area, as a more likely design to be deployed commercially in the near term (versus large 5,000-acre commercial-scale farms significantly exceeding current facility scales as considered in prior efforts).
2. Cultivation of **non-freshwater species** to prioritize brackish/saline algae production and reduce competition with freshwater resources (no freshwater scenario is considered here).
3. Increased granularity of model processes for resource assessment and LCA implications of waste **CO_2 capture and delivery**, as well as **blowdown salt management and disposal**.

4. **High-protein biomass compositions**, as more readily achievable in the near term at concomitant cultivation productivity goals approaching 25 g/m^2/day.
5. Conversion technology pathways centered on TEA and LCA **co-prioritizing production of fuels** (emphasizing SAF) **and food/feed** from algal protein.

In light of the differences summarized above (e.g., smaller farms producing higher-protein biomass), the results from the present harmonization study are expected to reduce fuel yields and increase fuel costs relative to the 2017 harmonization study. These results do not contradict the prior 2017 results, but rather supplement the picture to reflect what may be more readily achievable in the nearer term from farmed saline algae systems under nutrient-replete cultivation. The remainder of this report documents the key modeling inputs, assumptions, and results for this updated study, primarily highlighting updated or new methods and assumptions while deferring to our prior studies for other details that remain unchanged (Davis et al. 2018).

2 Methods

2.1 Modeling Approaches

Scope of Analysis

The scope of analysis spans algal biomass production through harvest, dewatering, seasonal storage, and conversion to fuels and protein food/feed coproducts. Process, TEA, and LCA modeling is conducted at the individual site level for a single integrated farm/conversion facility. This includes sourcing inputs for delivered CO_2 and water costs and energy demands, as well as saline pond blowdown disposal outputs, from resource assessment models at the local facility level of granularity. Likewise, process/TEA/LCA modeling is also conducted for the integrated conversion facility processing the dewatered biomass from the farm through HTL for production of fuels, evaluating scenarios with and without coproduction of algal protein concentrate (PC) across several scenarios for protein market volume capacities. The results at the individual facility level are compiled across all facility locations, identified from resource assessment modeling through a set of suitability criteria, to generate national-scale resource curves for costs and LCA metrics for production of algal biomass and subsequently fuels and protein coproducts. The overall workflow for the modeling approach is depicted in Figure 2.1.1.

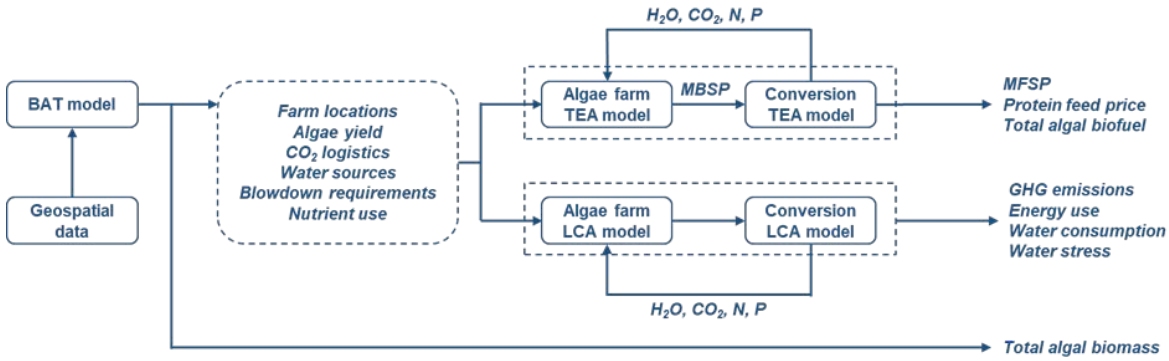

Figure 2.1.1. Workflow depicting key steps and handoffs between models

Algae Biomass Resource Assessment

Similar to prior harmonization efforts, the workflow is harmonized around high-spatiotemporal-resolution, national-extent resource assessment models identifying suitable algae farm locations throughout the conterminous United States (CONUS) subject to land, water, and CO_2 availability constraints. The resource assessment utilizes PNNL's Biomass Assessment Tool (BAT) modeling methodologies incorporating geospatial and biophysical models to predict 40 years of hourly cultivation productivities as a function of location, meteorological variables, and multicriteria screening using lab-derived parameterizations for strains of relevance to the BETO algae platform. The BAT is a modeling system comprising numerous spatial and numerical modules that incorporate (1) multiscale spatial and temporal modeling; (2) physics- and biophysical-based modeling to simulate pond temperature, strain-specific biomass productivity, and pond management; (3) least-cost transportation modeling for sourcing and moving required resources; (4) upstream and downstream resource demand and supply accounting; (5) partial techno-economics; and (6) other analyses performed using the best available climate, water, land, and infrastructure data, along with environmental constraints, biomass growth rates, and

other proximal resource requirements such as nutrient and CO_2 sources (Coleman et al. 2014; Venteris et al. 2014; Wigmosta et al. 2017; Sun et al. 2020; Xu et al. 2020; Ou et al. 2021).

A high-performing saline strain investigated under the Development of Integrated Screening, Cultivar Optimization, and Verification Research (DISCOVR) project was used in this assessment: *Tetraselmis striata* LANL 1001 (Huesemann et al. 2023). The modeled productivity of this algal strain is projected to achieve an annual average of 26 g/m^2/day, varying regionally across the collection of sites considered, which is in line with out-year performance targets of 25 g/m^2/day targeted by 2030 (DOE 2020). Outputs from the resource assessment models for the selected individual farm site locations are exported to algae farm TEA and LCA models and include site area, monthly biomass productivities, point-source-captured and pipeline-delivered CO_2 capital expenses (CAPEX) and operating expenses (OPEX), makeup water sourcing/pipeline distance/pumping CAPEX/OPEX and salinity, and saline pond water blowdown management CAPEX/OPEX considering forward osmosis (FO) processing, brine water disposal through deep-well injection, and freshwater recycling within the farm.

Building from prior harmonization efforts, the BAT modeling includes the following for the present assessment:

- New location siting (CONUS) for open pond cultivation of microalgae.
- Open pond temperature model including net consumptive water use tracking.
- Biomass productivity modeling for saline strains (validated with experimental data).
- Saline groundwater sourcing and pumping to ponds.
- Pond salinity tracking and blowdown management (inclusive of net evaporation).
- Treatment of blowdown water through FO, with freshwater fraction returned to pond to reduce groundwater pumping requirement.
- Disposal of FO brine concentrate through deep-well injection.
- Identification and use of variable-concentration point-source CO_2 for collocation and beneficial use including capture, transport, and mass balance accounting. This includes high-purity industrial sources and lower-purity, higher-volume sources such as power plants utilizing combustion of natural gas and coal.

Algae Farm Process Modeling and TEA

The key outputs from the BAT model noted above are next run through NREL's algae farm TEA model for each identified individual farm site. As described in prior reports (Davis et al. 2016, 2018), the algae farm model consists of a series of 10-acre open raceway ponds scaled to meet the total cultivation area identified by the BAT model—in this case varying between 1,000 and 38,500 acres according to each individual farm site (a deviation from prior harmonization studies that assumed a fixed farm size across all locations). The biomass is harvested at a rate (i.e., *tons/day*) consistent with the given farm's cultivation productivity and size (i.e., *tons/acre/day* × *production pond acres*), and routed to dewatering across a series of operations to concentrate the biomass up to 10 wt % solids in the case of downstream conversion to fuels and PC coproducts, or to 20 wt % in the case of downstream conversion to fuels alone (the former scenario requires protein extraction to be conducted at a lower biomass concentration). The dewatered biomass is then sent to seasonal storage during peak cultivation seasons (typically summer and a fraction of spring/fall seasons depending on the site), utilizing a wet anaerobic storage design to minimize

degradation, as a means of negating seasonal swings in throughput capacity through downstream conversion operations. Resulting capital/operating costs for these operations, as well as CO_2 pipeline delivery, makeup water delivery/disposal, and blowdown FO processing costs scaled from BAT model outputs, are calculated through published TEA tools (NREL 2023) to estimate the resultant minimum biomass selling price (MBSP) at each individual farm location.

Algae Conversion Process Modeling and TEA

The resulting MBSP and seasonal flowrate outputs from the farm models were subsequently sent through conversion models, leveraging PNNL's HTL model pathway as an example case. The addition of a protein extraction pretreatment step was included to quantify TEA metrics of fuel and protein food/feed selling prices. Predicted product yields at the individual facility scale were subsequently compiled into national-scale cost-versus-yield curves spanning all sites identified from the resource assessment models. NREL's combined algae processing (CAP) pathway was also evaluated across a number of model configuration scenarios, but was ultimately not included as none of the CAP scenarios were found to offer optimal solutions to achieve necessary GHG reduction levels within the confines of this study's fuel/feed focus under high-protein biomass compositions (driven primarily by challenging GHG results for animal feed coproduction targeted in the CAP cases, in contrast to the HTL pathway's focus on PC targeting food markets). Conversion scenarios consider two conversion pathways. The first is protein extraction and recovery to yield algal PC as a coproduct alongside fuels from HTL conversion of the residual protein-extracted algae material (requiring a more dilute 10 wt % concentration of biomass for protein extraction and accordingly reflecting a slightly lower MBSP from the farm model as the input biomass cost). The second is exclusive HTL processing to fuels alone (accommodating more concentrated biomass at 20 wt % to reduce HTL processing costs and accordingly a marginally higher MBSP reflective of additional dewatering in the upstream algae farm model). The TEA model ultimately yields a calculated minimum fuel selling price (MFSP) either with or without inclusion of PC sold at a fixed coproduct market value.

System LCA

The Greenhouse Gases, Regulated Emissions, and Energy Use in Technologies (GREET) model was used for the LCA modeling. The goal of the LCA is to provide life cycle GHG, fossil energy use, and water consumption results for algal biomass and biofuel production. The system boundary of this LCA study involves the relevant life cycle stages and supply chains of operational input, including the material and energy consumption for CO_2 capture and transport, algae growth, conversion to biofuel, PC coproduct production, fuel transportation, and fuel combustion. Capital infrastructure for CO_2 delivery, algae ponds, and the conversion facility is not included in the scope of the LCA. Two functional units are used: one ton of algal biomass on an ash-free dry-weight (AFDW) basis (following cultivation and dewatering) and one megajoule of algal biofuel (following subsequent conversion of the biomass through HTL). Global warming potential (GHG emissions) is characterized based on the Intergovernmental Panel on Climate Change's Sixth Assessment Report 100-year characterization factors (CH_4: 29.8; N_2O: 273). Fossil energy and freshwater resource consumption are reported on an inventory basis without further characterization (i.e., as the sum of coal, natural gas, and petroleum resource extraction and the sum of freshwater use across the life cycle). Freshwater use is considerably lower in this study than the prior 2017 algae harmonization study, as cultivation is based only on saline water inputs (not included in the calculation of freshwater consumption). The GREET model was

tailored to the algae farm/conversion operations as reflected in this study, with the application of several coproduct handling methods in scenarios involving coproduction of algal PC alongside fuels.

2.2 System Description

Algae Cultivation System

Open Pond System

Figure 2.2.1 presents the general algae farm cultivation framework devised for this study. The model is largely based on the set of operations and assumptions in NREL's 2016 algae farm design report (Davis et al. 2016) and the more recent 2017 harmonization report (Davis et al. 2018), with several modifications. In brief, the inoculum train provides biomass inocula to multiple large-scale raceways (10 acres each), in which algae grow until a target density of 0.5 g/L is achieved. The microalgae suspension is drawn semi-continuously from the raceways and sent to a sequential dewatering system composed of settlers, membranes, and centrifuges to sequentially increase biomass concentration from 0.05 wt % (0.5 g/L) up to 20 wt % solids (200 g/L); dewatering system capital costs are scaled to match the harvest rates reflecting maximum seasonal productivities in the ponds (specific to each individual farm site). The final dewatering step reaches 20 wt % solids, which aligns with cases that only implement HTL conversion downstream for fuel production, although for cases that first include protein extraction, the final centrifugation step is eliminated to deliver the slurry at 10 wt % solids to downstream conversion. As implemented in the 2017 harmonization study, pond circulation is shut off during night hours. Seasonal biomass storage, an operation usually considered on the biomass conversion side of the supply chain as a means to equalize algae flowrates entering the biorefinery (Wiatrowski et al. 2022), was moved into the algae farm boundary for this work to facilitate consistent data handoff between teams after accounting for storage costs and degradation losses. Costs for additional site development within the farm boundary, such as roads and stormwater mitigation, are included in the cultivation system costs from the 2016 design report.

For this assessment, the NREL algae farm model was configured to consider monthly inputs for biomass productivity and evaporation rate based on BAT outputs (instead of seasonal averages as in previous work). Algae farm simulations considered several parameters at fixed values for all site locations, such as minimally lined raceway ponds for costing purposes, individual pond size of 10 acres, CO_2 uptake efficiency of 75% (Huntley et al. 2015), algae strain salinity tolerance of 55,000 mg/L, and harvested density of 0.5 g/L. Additionally, to better account for elevated pH conditions necessary to achieve CO_2 retention efficiencies on the order of 75%, urea was implemented as the primary nitrogen fertilizer source in place of historical models that have assumed ammonia (which would be lost to outgassing at elevated levels under such pH conditions supporting good CO_2 retention). Another key modification in this analysis was to allow the total farm size to vary based on BAT outputs for local resource availabilities, primarily dictated by CO_2 availability, discussed in further detail below. This translated to individual farm sizes ranging between 1,000 and 38,500 acres (with an average farm size of 3,940 acres, compared to a fixed farm size of 5,000 acres assumed in the 2017 harmonization). Other parameters (e.g., the basis for inoculum train sizing, on-site CO_2, and water circulation) were set consistent with Davis et al. (2016). Similar to the 2017 harmonization, CO_2 is sourced via carbon

capture and high-pressure pipeline transport from off-site flue gas point sources, but now reflecting more granular cost and energy demand details specific to the local source, as described further below.

The open pond was established under saline operating conditions with a target salinity set at 55,000 mg/L, which matches the maximum salinity for lab trials conducted on the saline strains considered without detrimental impacts in productivity observed to date (Klein and Davis 2023). Each site has a unique groundwater salinity and well depth to access the saline groundwater as its primary water source. A key addition in the present harmonization study that was not utilized in prior studies is the use of FO to process blowdown water, given the high-salinity conditions reflected in this design. The BAT pond temperature and microalgae growth model is run from 1979 to 2019 at an hourly time step. If the pond salinity exceeds the established 55,000-mg/L salinity threshold, a volume of water is removed from the pond (blowdown) and replaced with new source water, first from any available FO freshwater recovered from blowdown processing, with the remaining volume fulfilled from the saline groundwater source to close water balances after accounting for salinity/temperature-dependent evaporation. The objective is to maintain pond salinity as close to the established operating threshold as possible. The blowdown water is modeled through a simplified FO water treatment model that yields 82% of the blowdown water as freshwater and is recycled within the system. The remaining 18% of the blowdown is sent to an on-site deep injection well. CAPEX and OPEX are established for the source water and brine injection wells, as well as the FO system, which are all scaled according to the site-specific water demand. For the FO system, we assume an operational treatment cost at \$0.60/bbl and 5 kWh/m^3 of blowdown water treated. The FO system will concentrate brines to 230,000 mg/L and provide a permeate at 300 mg/L for recycle in the farm system.

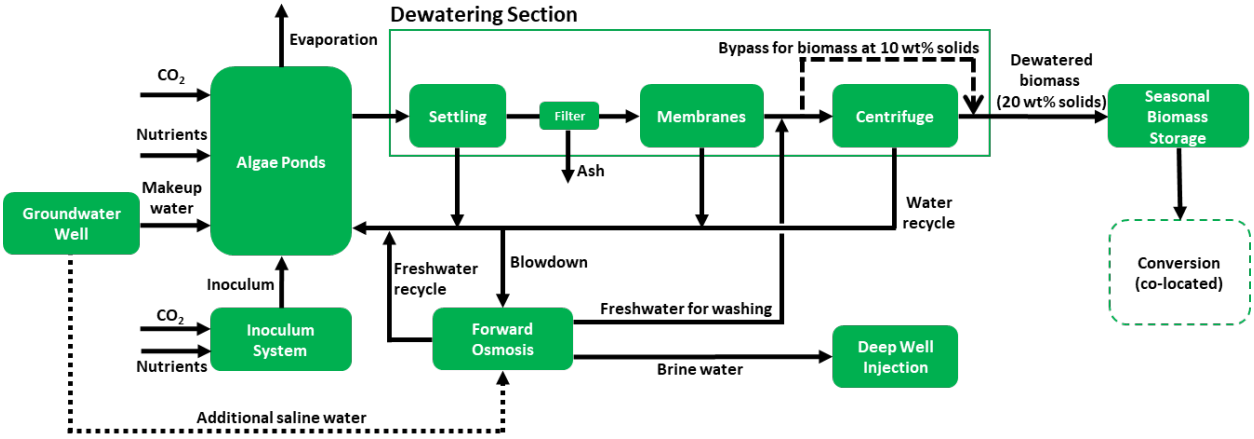

Figure 2.2.1. Framework of the algae farm model employed in this study. The centrifuge can be bypassed so the algae farm delivers 10 wt % solids for conversion in scenarios with protein coproduction.

The dewatering section of the algae farm was slightly modified in this study by adding two minor intermediate operations. First, a basket strainer was added prior to the secondary membrane step to reduce exogenous ash/inorganic suspended solids, assumed to reduce total ash content by 50%. Additionally, in order to control salt concentrations to a manageable level for downstream conversion equipment protection (e.g., high-pressure homogenization [HPH] utilized in HTL pretreatment) and in consideration for the resultant protein coproduct destined

for food applications, a solids washing operation with freshwater was added before the centrifugation step to reduce salt content from 55,000 mg/L down to 15,000 mg/L. To avoid externally sourced freshwater demands in an otherwise saline-focused cultivation model, the freshwater required for this washing step was sourced by splitting the treated water from the on-site FO unit (already in use to process the blowdown water), routed both to the salt washing step and for internal recycle to the ponds. It is noteworthy that the sizing of the FO unit is deeply connected to the washing operation, with the former scaled to fully offset the freshwater requirements in the latter. In higher-salinity cases (approximately 12% of all assessed points), all freshwater demand for washing can be supplied by the FO output from blowdown management alone, with the remainder of the freshwater sent to the ponds for salinity reduction. However, in the remaining 88% of cases with lower salinity, additional saline water must be pumped from the groundwater source and sent to the FO unit strictly to meet washing demands. This strategy increases both CAPEX and OPEX tied to salinity management (scaling FO and blowdown disposal costs and energy demands from BAT model values), but eliminates the need for procuring freshwater from outside the boundaries of the algae farm as a higher priority in this work. The costs for makeup saline groundwater (capital costs and pumping power for the groundwater well) were likewise scaled from the BAT model, specific to each individual farm site and associated local sourcing/delivery details for those inputs. Makeup groundwater was not assumed to require filtration for supply to the production or inoculum ponds (such a cost would likely be minimal if it were required in specific locations).

To better represent the individual characteristics of each algae farm under evaluation, several parameters have been either pulled directly as provided by the BAT model or calculated using mass balance outputs from the NREL algae farm combined with dimensioning parameters provided by the BAT team, as detailed in Table 2.2.1. Algae biomass composition based on experimental data for nutrient-replete cultivations of *Tetraselmis striata* LANL 1001 (Klein and Davis 2022; Huesemann et al. 2023; Song et al. 2023) was considered in this work, as provided in Table 2.2.2 (further discussion and parameterization of this strain is provided in the next section). While the composition assumed here reflects high-protein biomass typically cultivated under nutrient-replete conditions as the most direct way to maximize productivity in the near term, several performers in industry have achieved elevated lipid compositions of 25%–35% or higher while maintaining high productivity rates, as would translate to higher fuel yield potential and lower dependency on protein coproducts (Klein and Davis 2023; Hazlebeck 2023). Calculation of mass and energy balances follows the same practices as presented elsewhere (Davis et al. 2016).

Table 2.2.1. Origin of Parameters for Algae Farm Simulations

Algae Farm	BAT Model
Technical Parameters	
Pond design and individual pond size (10 acres) Harvested density Cultivation nutrient demands based on biomass composition Net saline makeup water based on BAT evaporation + blowdown rates vs. FO freshwater recycles	Individual farm size (>1,000 acres, based on total production pond area) Monthly biomass productivity (g/m^2/day) Monthly evaporation rate (translated to cm/day) Salinity of makeup water (mg/L) Salinity tolerance of algae strain (mg/L) Salinity blowdown removal rates
CAPEX Items	
Inoculum train Algae production ponds CO_2 on-site storage and piping On-site water circulation Dewatering (including basket strainer and water wash for inorganic solids/salt removal, respectively) Seasonal biomass storage	FO unit ($/vol throughput) Deep-well injection system ($/vol injection) Saline groundwater well ($/vol extraction)
OPEX Items	
Nutrients (urea, diammonium phosphate) Power required by the inoculum train, production ponds, and dewatering system Chiller utility (photobioreactor inoculum cooling) Fixed operating costs (labor, maintenance)	Delivered farm-gate CO_2 price ($/t) Power required by the FO unit and the groundwater well system (kWh/m^3) Power required for brine well injection (kWh/m^3)

Table 2.2.2. Composition Assumed for Nutrient-Replete *T. striata* (Klein and Davis 2022)

Component Composition (AFDW)	
Fatty acid methyl ester (FAME) lipids	10.6%
Non-FAME lipids	5.7%
Sterol	0.6%
Fermentable carbohydrates	7.7%
Non-fermentable carbohydrates	1.5%
Protein	44.2%
Cell biomass	29.8%
Total	**100%**
Ash (% dry weight)	20.4%
Elemental Composition	
Carbon	48.1%
Hydrogen	7.4%
Oxygen	33.9%
Nitrogen	9.2%
Sulfur	0.2%
Phosphorus	1.2%
Total	**100%**

Table 2.2.3 presents the main outputs of the algae farm model provided to the conversion TEA teams. The main metrics include the MBSP of algae cultivated both before and after inclusion of long-term seasonal storage, biomass output on daily and yearly bases, and biomass composition before and after seasonal storage. All costs were updated to 2020 dollars for this work. Apart from these parameters, the algae farm model also provided detailed process input and output inventories to the LCA team for the environmental assessment of algal biomass production.

Table 2.2.3. Main Metrics Supplied from the Algae Farm Model for Downstream Conversion TEA

Parameter	Description
MBSP ($/ton AFDW)	Before and after long-term storage, given in 2020 dollars
Total biomass output (tons/day, million tons/yr, and tons/acre/yr AFDW)	Average and seasonal values, before and after long-term storage
Biomass concentration (wt % AFDW)	Concentration after two-stage dewatering (for protein extraction/coproduction scenario) or three-stage dewatering (for fuel-only scenario)
Average biomass compositional profile	Before and after long-term storage

The life cycle inventory (LCI) for algae cultivation used for the LCA includes the use of electricity, urea, diammonium phosphate (DAP), CO_2, the blowdown of saline water, and emissions. Taking the site with median GHG emissions as an example, the detailed inventories for 10 wt % and 20 wt % solids AFDW, both with (net) and without (gross) recycling from downstream conversion, are illustrated in Table 2.2.4. In the case of 10 wt % solids AFDW, the material is routed to conversion for production of both protein and fuel. On the other hand, the scenario with 20 wt % solids processes the material through HTL alone and only produces fuel. Table 2.2.4 shows that more CO_2 and nitrogen (urea) can be recycled when only fuel is produced. For all the selected sites, in the scenario involving both PC and fuel production (without constraining protein coproduct market limitations), recycling from conversion reduces CO_2 demand by 0.670 to 0.681 kg, urea demand by 0.0592 to 0.0602 kg, and DAP demand by 0.0416 to 0.0423 kg. In the scenario that only produces fuel, recycling from conversion reduces CO_2 demand by 0.887 to 0.902 kg, urea demand by 0.154 to 0.157 kg, and DAP demand by 0.0402 to 0.0408 kg. Additionally, there is no external freshwater consumption in the algae farm model, as only saline makeup water is utilized (including via FO desalination to provide supplemental freshwater for salt washing when required).

Table 2.2.4 An Example for LCI of the Algae Farm Based on the Median GHG Site, With and Without Consideration of Recycles From Downstream Conversion

	10 wt % solids AFDW (whey PC without market limit)		20 wt % solids AFDW (fuel only)	
	Without recycling	Net, with recycling	Without recycling	Net, with recycling
Resource consumption, kg/kg AFDW				
CO_2 (counted as biogenic)	2.3	1.6	2.3	1.4
Urea	0.17	0.12	0.17	0.020
DAP	0.051	0.009	0.051	0.011
Total process water input (freshwater)	0	0	0	0
Electricity demand, kWh/kg	0.60	0.60	0.61	0.61
Output streams, kg/kg AFDW				
Water in biomass product stream	9.0	9.0	4.0	4.0
Water sent to blowdown	228	228	223	223
Algae lost in blowdown	0.0019	0.0019	0.0017	0.0017
Air emissions, kg/kg AFDW				
Water lost to evaporation	215	215	215	215
CO_2 outgassing from ponds (counted as biogenic)	0.58	0.58	0.58	0.58
O_2 to atmosphere	1.4	1.4	1.4	1.4

Strain Parameterization

For BAT modeling strain parameterization, two high-performing saline strains of investigation under the DISCOVR project were considered in this assessment: *Picochlorum celeri* (generally optimal for warm seasons) and *Tetraselmis striata* LANL 1001 (generally optimal for cold seasons), as described in Huesemann et al. (2023) and Song et al. (2023). These strains were lab characterized using a bench-scale photobioreactor, MC-1000 multi-cultivator. The light intensity for each column in the MC-1000 was programmed individually, ranging from 20 to 2,000 µmol $m^{-2} \cdot s^{-1}$. The light cycle for all the columns was set to 14 hours light and 10 hours dark. The cultures were sparged with 0.5% CO_2-enriched air, and the pH was kept near 7.5. The temperature levels tested were 5°C, 10°C, 15°C, 20°C, 25°C, and 30°C for *T. striata* and 20°C, 25°C, 30°C, and 35°C for *P. celeri*.

The biomass concentration of eight tested cultures, measured in optical density at 720 nm (OD720), was maintained between 0.1 and 0.3 by automatic optical density reading and dilution during the light period. The maximum specific growth rate (μ_{max}) was calculated by taking the slope of the logarithm of optical density versus time curve for each growth period when optical density increased from 0.1 to 0.3. Similarly, the dark respiration rate (μ_d) was also calculated using the slope of the logarithm of optical density versus time curve. This calculation was done only using the data during the dark period. At each temperature, the cultures were grown for at least 7 days, which allowed repeated dilution and determination of μ_{max} and μ_d. The μ_{max} is plotted as a function of temperature and light intensity. For example, in Figure 2.2.2, at each temperature, μ_{max} of *T. striata* increases with increasing light intensity. Apparent photoinhibition was observed at low temperatures (e.g., 5°C, 10°C, 15°C) with light intensity above 1,000 µmol·$m^{-2} \cdot s^{-1}$. The highest μ_{max} observed was 4.0 day^{-1}, measured in the 1,500-µmol·$m^{-2} \cdot s^{-1}$, 30°C culture.

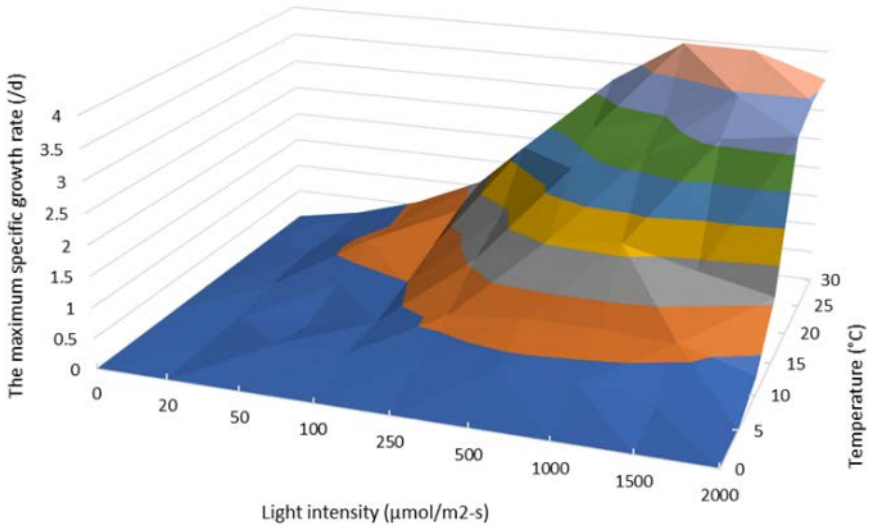

Figure 2.2.2. The maximum specific growth rate of *T. striata* LANL1001 as a function of light intensity and temperature

Prior to integrating the biomass growth model into the BAT, the model was validated against growth data collected from outdoor raceway ponds at the Arizona Center for Algae Technology

and Innovation (AzCATI) during the DISCOVR consortium project. In total, 83 batch culture runs were simulated for *P. celeri* and 96 batch culture runs were simulated for *T. striata.* The simulated biomass productivity showed an error of ±20% compared to observations, but on average, it was below 10% for both strains. This is significant considering differences in photobioreactor lab conditions and outdoor raceway ponds. In the BAT, the biomass growth model was run independently for each site in the CONUS, followed by running a strain rotation process based on a site-specific cumulative monthly total unit-area biomass output (kg/ha). Sites with a modeled annual average biomass productivity potential of ≥25 g/m^2/day were used in the remainder of the analysis. We recognize the current state of performance from DISCOVR for either of these strains has not yet reached such productivity levels, being most recently demonstrated closer to an annual average of 18 g/m^2/day (Klein and Davis 2022). No additional explicit biomass productivity numerical scaling was performed as was done in past harmonization efforts. It is noted, however, that the pond temperature model, biomass growth model, and strain rotation process did not threshold or bin the pond temperatures to the lab-characterized values of 5°C–30°C (*T. striata*) and 20°C–35°C (*P. celeri*), and it is expected that the modeled biomass may be somewhat overpredicted for *T. striata*, as modeled pond temperatures exceeded what was lab parameterized. Accordingly, *T. striata* was predicted by the BAT algae productivity model to be the optimal strain in all months/locations, and *P. celeri* was not utilized in the BAT models through a seasonal rotation approach (in contrast with optimal performance observed in DISCOVR trials to date [Klein and Davis 2022]). We emphasize that this is not to imply that *T. striata* in fact should be implemented year-round at all sites, but rather that there was an implied extrapolation in parameterization values relative to outdoor trials. This is in part due to lab testing that was not able to capture temperature ranges at all modeled sites across the country. This led to the universal selection of *T. striata* in this assessment, although this ultimately has minimal impact on the overall results given the threshold for >25-g/m^2/day annual productivity rates aligning with the goal in this study. (At the time of writing, the lab-parameterized values for both saline strains have been expanded to a broader temperature range, but these expanded strain parameterization tables were not available in time for a full rerun of the process/TEA/LCA harmonization analysis reported herein.) In the future, the strain rotation algorithm will be adapted to test for modeled pond temperature ranges before competing strains on monthly biomass productivity totals.

FO Membrane System

Desalination technologies are categorized into two types: thermal-based and membrane-based. For this study, the FO membrane system was chosen to desalinate saline groundwater due to its cost-effectiveness and lower energy when compared to other desalination technologies (Panagopoulos et al. 2019). The electricity used for saline water pretreatment and FO is 0.0055 kWh/L, while the electricity consumption for deep-well injection is 0.0012 kWh/L (Panagopoulos et al. 2020; Thiel et al. 2015). The electricity consumption for the FO membrane system has been accounted for in the total algae farm electricity demands. As noted above, 82% of the incoming water to FO is treated and internally recycled as freshwater for use in the algae farm (salt washing and return to ponds to reduce salt concentration). The remaining concentrated high-salinity wastewater is subsequently disposed of through deep-well injection.

The LCI for FO membrane fabrication is adapted from Coday et al. (2015) and adjusted to a flat sheet membrane configuration based on Zhang et al. (2019). We omitted the cleaning chemicals specified by Coday et al. (2015), as the feed for the FO membrane system is largely saline water with minimal biomass solids having first passed through primary clarification via settling, and as a result, it is assumed that freshwater is sufficient to wash the membrane periodically to avoid fouling. The life span of the FO membrane system is presumed to be 5 years based on Linares et al. (2016). The detailed LCI of the FO membrane system and the data sources are provided in Table S13, and the environmental impacts of FO membrane synthesis are provided in Table S28.

CO_2 Capture and Transport

The present analysis maintains the use of off-site point-source CO_2 capture and pipeline transport but incorporates further granularity to reflect local point-source capture costs and energy demands relative to the 2017 harmonization study. The CO_2 transport model is a location-allocation spatial network model that uses a point-source emission location, the source type, and the total annual CO_2 supply associated with that location. The CO_2 point-source data are assembled and deconflicted from numerous sources, including (1) the U.S. Environmental Protection Agency 2020 Greenhouse Gas Reporting Program, which limits reporting to ≥25 kt carbon dioxide equivalent (CO_2e) per year (U.S. Environmental Protection Agency 2020); (2) the National Energy Technology Laboratory's National Carbon Sequestration Database Atlas V database (Bauer et al. 2018); (3) Middleton et al. (2014) assembled data, which include sites <25 kt CO_2e per year and those identified with a beneficial use already; and (4) Homeland Infrastructure Foundation-Level Data (U.S. Department of Homeland Security 2019). Utilizing the combination of data sources, the resulting CO_2 point sources in the CONUS were manually validated against 2020 satellite imagery, Google web mapping services, business listings, and company websites for their spatial position and verification of active operations. This was a key process step, as most CO_2 point sources were mislocated from the actual facility (0.25–8 miles), or a headquarters office location was located instead of the actual facility. Numerous businesses had assumed new ownership or gone out of business, requiring subsequent updates to the data. Finally, new businesses came online, requiring additional validation activities. Some of these newly reported facilities serve as demonstration facilities, which were not retained for our purposes in this study due to the likely variable operations and higher uncertainty for future operation.

The 2020 annual CO_2 emissions data from the Greenhouse Gas Reporting Program were used where available, and other sites (<25 kt CO_2e per year) used the latest known CO_2 emissions data. Because annual data are reported, we assume an equal daily mass availability of CO_2, and pipeline calculations were established to hold 8 hours of additional CO_2 overnight, a process known as line packing. The model assumes that 80% of the reported annual emissions are available for transport. The transport model defines the most optimal route between the source and algae farm, preferentially using existing rights-of-way and other corridors and avoiding sensitive areas, off-limits areas, and urban areas, similar to what was defined in the land screening model. The pipeline distance and CO_2 transport mass dictate the pipeline diameter and any required mid-line pumping stations and assumes a 30-year design life. All the materials, labor installation costs, control systems, permitting, right-of-way damages, and other miscellaneous costs are incorporated into the CAPEX. The OPEX is established through annual labor, pipeline and pump maintenance, and energy costs. Details of the CO_2 transport model and CAPEX/OPEX costing are provided in the 2017 harmonization report, with the exception that

costs are adjusted to 2020 dollars (Davis et al. 2018). Alternative means of capturing flue gas CO_2 are also possible, such as a bicarbonate/carbonate shuttle approach employed historically by Global Algae Innovations (www.globalgae.com/). Such an approach could offer a lower-cost/lower-energy means of capturing CO_2 though would require being collocated with the flue gas source and was not included in the scope of this work.

The total hourly carbon demand is based on new biomass productivity for each time step, as established by the biomass growth model runs. The carbon demand is calculated by:

$$D_{CO2} = \frac{B \times W_{CBio}}{E_{CO2} \times W_{CCO2}} \quad \text{(Eq. 1)}$$

where:

D_{CO2} = CO_2 demand (kg/h)
B = AFDW biomass production rate per time step (kg/h)
W_{CBio} = Carbon fraction in biomass (0.55)
E_{CO2} = CO_2 utilization efficiency (0.75)
W_{CCO2} = Carbon fraction in CO_2 (0.273).

In the location-allocation model, pond sites that are closer to the CO_2 point source are given preferential access to the CO_2; as CO_2 supply remains, it is allocated to additional sites in order of transport distance. The carbon fraction in biomass assumed here for setting CO_2 demands (0.55) was set consistently with the prior 2017 harmonization study, although in this case this is somewhat conservative, as the carbon content for high-protein algae is somewhat lower (0.48 applied in the algae farm TEA model as noted in the open pond design description above).

It is notable that the E_{CO2} parameter in practice will have dynamic variability associated with it based on outgassing rates driven by pond pH, salinity concentrations, and pond temperature. The current version of the pond model does not simulate pH dynamics, but rather aligns with the 78% utilization rates in saline water open pond experiments documented in Huntley et al. (2015). A recent literature survey on the topic revealed CO_2 utilization efficiency ranges from 25% to 90%, with a median value of 66% across various experiments and pilot-scale implementations (Putt et al. 2011; Beal et al. 2012; Langley et al. 2012; De Godos et al. 2014; Huntley et al. 2015; Kuo et al. 2018; Schoenung, Efroymson, and Langholtz 2019; Eustance et al. 2020).

The CO_2 capture and compression costs and required energetics at the point source were updated from the previous harmonization effort, using values provided in Table 2.2.5 based on future projections extrapolated from literature spanning a range of sources including natural gas and coal-fired power plants, ethanol and renewable natural gas production, and a range of industrial manufacturing operations. The GIS point-source CO_2 data identify the source type, thus allowing for a joining of the capture and energetics. The CO_2 capture, compression, and transport modeling for sites that can be supplied according to the carbon supply and demand are then subject to a ≤$75/tonne (≤$83/ton) cost threshold based on delivered cost to the algae farm. Sites that exceeded this cost threshold were excluded. No further moisture removal is assumed for high-pressure CO_2 pipeline transport after cost/GHG burdens are assigned for carbon capture at the point source.

The estimates for future target (2040–2050) CO_2 capture and compression energy requirements presented in Table 2.2.5 are made using regression relationships between energy use and CO_2 concentrations based on results obtained from Carnegie Mellon University's Integrated Environmental Control Model (Integrated Environmental Control Model Team 2019; Singh, Banerjee, and Hawkins 2023). The future estimates assumed reduced energy use based on anticipated development of CO_2 capture technologies for the different CO_2 sources. We performed another regression between the future capture energy and the CO_2 concentration at 90% capture and obtained the following relationship:

$$Energy\ for\ capture\ \left(\frac{MJ}{kgCO_2}\right) = 10^{0.2183-0.3124log\beta} \quad \text{(Eq. 2)}$$

where:

β = CO_2 concentration in gas (mol%)

There were a few exceptions to the capture energy that we considered. For instance, two types of point sources considered here (ethanol and renewable natural gas processing) result in a nearly pure CO_2 stream. These two sources were therefore assigned a capture energy burden of about 0 MJ/kg CO_2. CO_2 compression energy of 0.38 MJ/kg CO_2 for all the sources was added to compress the CO_2 to a 137-bar pressure, suitable for pipeline transport. The energy use for CO_2 capture and compression ranged from 1.4 to 1.5 MJ/kg CO_2 for natural gas combined-cycle power plants with a flue gas CO_2 concentration of 3%–5%. For coal combustion power plants, total energy use was close to 1.1 MJ/kg CO_2. Coal power plants are the main CO_2 source for this study for use in algae ponds as identified from BAT. However, some other high-purity sources played a role. For instance, CO_2 can be captured and compressed from natural gas processing plants at 0.75 MJ/kg CO_2. Natural gas processing has the advantage of technological readiness, as most existing CO_2 capture facilities globally belong to this sector. Following carbon capture from the different CO_2 sources, the CO_2 stream is compressed to supercritical range and transported via pipelines for algae cultivation.

Direct air capture (DAC) of carbon is not currently considered as part of the scope of this study but may be evaluated in a future assessment. DAC could substantially increase the total algal biomass/biofuel potential relative to the results presented here, as it would decouple the farm siting constraints from nearby CO_2 point source availabilities; even sourcing 50% of CO_2 requirements from DAC would double the amount of available CO_2 for biomass cultivation relative to point-source capture and accordingly increase the total algal biomass resource potential, as CO_2 availability was the main constraining factor for algae farm siting in the BAT model. Moreover, if power and industrial decarbonization continue to progress over the coming decades (i.e., the algae system plant life of 30 years assumed in this study), there may be fewer CO_2 point sources on which algae farms can rely over that time frame, further shifting the priority to DAC deployment to support widescale algae farm development. Early assessment cost factors for DAC may be prohibitive, though, with current capture costs varying between $250 and $600 tonne/$CO_2$ ($276 and $661/ton) and future targets for the next decade suggesting capture costs of $100–$200 tonne/CO_2 ($110–$220/ton) (Baker et al. 2020; International Energy Agency 2022; DOE 2023).

Table 2.2.5. CO_2 Capture Cost and Energetics for Current and Future Scenarios by Source Type.

Zero values are artificially assigned for bioethanol and renewable natural gas; otherwise, values are sourced from Massachusetts Institute of Technology (2016); Esposito et al. (2019); and Pilorgé et al. (2020).

Source	CO_2 Concentration (mol%)	CO_2 Compression Energy (kWh/tonne CO_2)	Cost of Capture ($/tonne CO_2)		CO_2 Capture Energy (MJ/kg CO_2)	
			Current	Future	Current	Future
Natural gas combined cycle	3.5	Electrical energy: 107	76	51	3.51	1.06
Pulverized coal	12		47	31	2.42	0.69
Integrated gasification combined cycle	40		29	19	1.42	0.45
Bioethanol	99		0	0	0.00	0.00
Refining	15		43	29	1.39	0.64
Hydrogen	45		28	19	1.39	0.43
Ammonia	45		28	19	1.78	0.43
Steel	22.5		37	25	1.72	0.55
Cement	25		35	23	0.00	0.53
Renewable natural gas processing	99		0	0	0.00	0.00

For purposes of handling the CO_2 sourcing in LCA, the strategy used here for coproduct handling was a cutoff (or incremental) approach. In this approach, the benefits of avoided CO_2 emissions are entirely attributed to the biofuel. This approach has been used for most of the studies of CO_2 utilization to date within the Office of Energy Efficiency and Renewable Energy programs and is the one used in the previous algae harmonization report and BETO supply chain sustainability analysis studies (Cai et al. 2021). In this approach, the emissions arising from CO_2 capture, fuel processing, and ancillary steps are allocated to the biofuel. However, the emissions from fuel combustion are not considered because it is assumed that the CO_2 would have been emitted to the atmosphere had it not been captured. This approach is more useful in simplifying LCA data requirements, but it may have some shortfalls in considering future dynamics. More details may be found in Yoo et al. (2022) and Cooney et al. (2022).

Alternative approaches for coproduct handling with respect to CO_2 sourcing could be substitution (recommended by the National Energy Technology Laboratory in its CO_2 utilization LCA guidance [Skone et al. 2022]) or allocation. Considering these alternative approaches could be useful in future work but was outside the scope of this report. It is notable that in the business-as-usual case, system expansion yields identical result as the incremental approach (Cooney et al. 2022).

Algae Conversion via Protein Extraction and HTL

In this study, a preliminary economic analysis for an algae HTL conversion and biocrude upgrading system with protein extraction pretreatment was developed. High-protein saline algae biomass is assumed to be the feedstock for the system, as described above. Different from previous algae HTL techno-economic analysis studies by PNNL, for scenarios considering coproduction of algal protein, the system evaluated in this study includes protein extraction from an HPH pretreatment step followed by HTL conversion to SAF as one of the primary products. Alternatively, for scenarios considering only fuel production, conventional HTL conversion is modeled (processing the whole algal biomass material delivered from the farm models) without the additional HPH pretreatment and protein recovery steps. The purpose of this study is to

evaluate trade-offs of adding high-purity protein and SAF production to an algae HTL conversion system. The process design and cost analysis is based on PNNL's current experimental work, previous TEA studies, and relevant literature (Zhu et al. 2020, 2021, 2023; Jiang et al. 2019; Safi, Rodriguez, et al. 2017; Safi, Olivieri, et al. 2017; Parimi et al. 2015; Carullo et al. 2022; Gifuni et al. 2020; Bylund 1995). The previous sequential two-stage HTL testing conducted by PNNL (Zhu et al. 2021) reflected acid pretreatment for cell disruption to extract carbohydrate and other compounds and then HTL testing of acid-pretreated algae. Because both the acid and HPH pretreatment operations serve a similar function of cell disruption, the HTL testing results of the acid-pretreated algae verified the feasibility of HTL conversion of algae after HPH pretreatment. The biocrude yield of protein-extracted algae (PEA) is estimated based on the biocrude yield correlation relationship developed by Jiang et al. (2019) as a function of the biochemical composition of PEA taken from the process model.

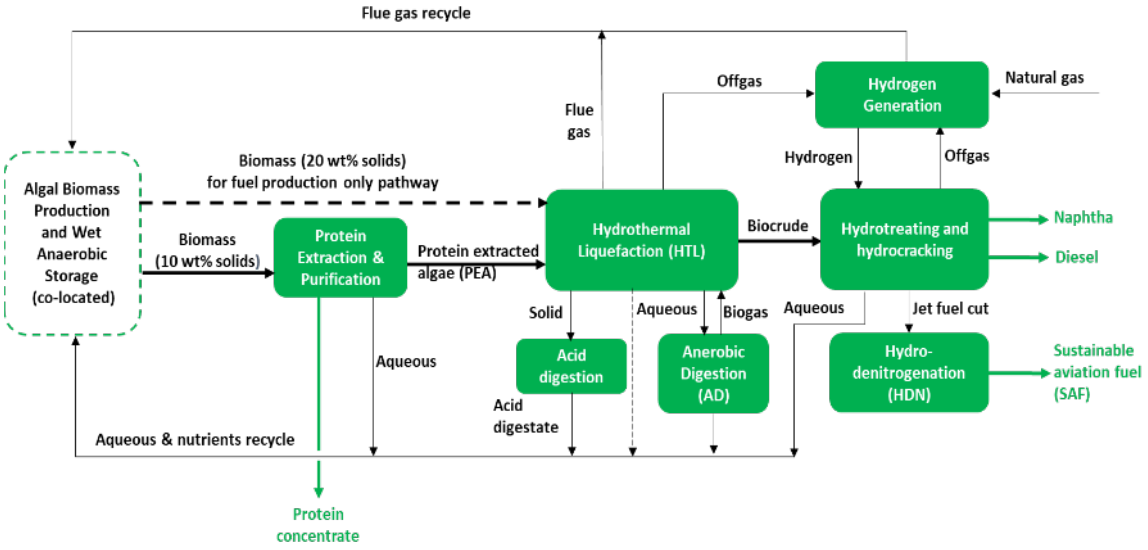

Figure 2.2.3. Block-flow diagram of the algae HTL conversion and biocrude upgrading system for fuel and protein production and fuel production only pathways

Figure 2.2.3 shows the simplified block-flow diagram of the algae HTL conversion system. In the pathway of coproducing algal protein alongside fuels, algal biomass with 10 wt % solids after dewatering and storage is sent to the conversion system. The 10 wt % or lower concentration of solids is required for efficient protein extraction (Safi, Olivieri, et al. 2017). The diluted algae slurry is pretreated via HPH for cell disruption to release intracellular protein and other components. The released protein is then extracted via alkaline solubilization followed by a solid-liquid separation step. The solid stream, referred to as PEA, is sent to the HTL unit for biocrude generation; alternatively, in the pathway considering only fuel production, the biomass dewatered to 20 wt % is routed directly from the algae farm to the HTL unit. The liquid stream is acidified to precipitate the solubilized protein, and then the stream is separated via filtration. The separated protein solids are spray dried to produce a dry protein powder to enable longer shelf life and lower transportation costs compared to liquid protein products (Carter et al. 2018). The aqueous stream from the protein extraction process, containing soluble organics, is assumed to be recycled to the algae farm.

PEA from the protein extraction process is roughly 35 wt % solid content following solid-liquid separation. Makeup water is added to reduce the solid content to 20 wt % to improve its pumpability. The PEA slurry (or alternatively the whole biomass slurry at 20 wt % from the algae farm model, in the case of fuel production only) is then pumped to the HTL reactor. Condensed-phase liquefaction then takes place through the effects of time, heat, and pressure. The resulting HTL products (biocrude, solid, aqueous, and gas) are separated. The aqueous phase is sent to an anaerobic digestion unit to generate biogas for process heating. For the fuel production only pathway, the HTL aqueous phase is directly recycled to the algae farm. The gas stream from HTL is also used for process heating. The HTL solid stream is subjected to acid digestion to recover phosphorus components from the ash. The acid digestate and the treated water from the anaerobic digestion unit are assumed to be recycled to the algae farm. The HTL biocrude is upgraded via hydrotreating and hydrocracking to remove oxygen, nitrogen, and other heteroatoms. The upgraded oil is then fractionated via distillation to generate diesel-, jet-, and naphtha-range fuels. Nitrogen levels of the jet fuel cut (JFC) in the hydrotreated oil were significantly higher than conventional petroleum-based jet fuel based on PNNL testing results. Therefore, a hydrodenitrogenation (HDN) step was assumed to remove excess nitrogen in the JFC. The JFC after HDN processing was assumed to be the final SAF product. While a nitrogen limit has not been established for SAF, this additional step has been incorporated into the TEA to account for the possibility that a final polishing step may be needed to reduce nitrogen to trace levels. The aqueous phase from the upgrading process is also assumed to be recycled to the algae farm. A hydrogen plant is included for hydrotreating, which is assumed to be collocated with the HTL conversion process. Flue gas containing CO_2 is recycled to the farm.

The major process design assumptions for the protein extraction pretreatment step are listed in Table 2.2.6. HPH was selected in this study for cell disruption based on its high protein release efficacy and relatively lower energy input for algae protein extraction compared to other methods, including bead milling and pulsed electric field (Safi, Rodriguez, et al. 2017; Safi, Olivieri, et al. 2017; Parimi et al. 2015; Soto-Sierra, Stoykova, and Nikolov 2018). Based on data from Parimi et al. (2015), increasing the pH from 8 to 12 was shown to increase the protein recovery from 78% to 88%. Considering the increase in protein recovery efficiency was only 10% for such a large swing from pH 8 to 12, a pH of 8 is assumed in this study to facilitate lower use of alkali and acid than would be required at pH 12, while still maintaining relatively high protein recovery. For other components in algae, HPH combined with alkali solubilization was assumed to release more than 60% of the lipid and 49% of the carbohydrates to the protein extract stream based on Carullo et al. (2022). The algae cell biomass is assumed to primarily report to the PEA after filtration. For different algae strains or operating conditions, including pH and slurry concentration, the recovery efficiencies for these components might be different, which need to be verified by future testing work.

Table 2.2.6. Major Design Assumptions for Protein Extraction Process

Processes	Model Assumptions	Sources
High-pressure homogenization		Safi, Rodriguez, et al. (2017); Safi, Olivieri, et al. (2017)
Feed slurry solid wt %, dry basis	10	
Temperature, °C	30	
Pressure, bar	1,500	
Pass	1	
Power consumption, kWh/kg dry basis	0.44	
Alkali solubilization and filtration		Parimi et al. (2015); Carullo et al. (2022)
pH	8 (by adding NaOH)	
Components recovery to the supernatant		
Protein, % of feedstock protein	77.8%	
Lipid, % of feedstock lipid	65%	
Carbohydrate and other components, % of these components in feedstock	24%	
Products yield, g/g feedstock dry basis		Estimated based on component recovery assumptions
Protein extract	0.54	
PEA	0.46	
Acid precipitation and filtration		Parimi et al. (2015); Gifuni et al. (2020)
pH	4 (by adding HCl)	
Component recoveries to the protein pellets		
Protein, % of protein in inlet stream	70.6%	
Lipid, % of lipid (FAME) in inlet stream	50%	
Carbohydrate and other components, % of components in inlet stream	50%	
Protein drying	Spray drying	Bylund (1995)
PC product composition, dry wt %		Estimated based on component recovery assumptions
Protein	72%	
Fat (FAME)	10%	
Carbohydrates and other compounds	16%	
Ash	1.3%	
Moisture, wt %	3.5	

After filtration, acid is added to the protein extract stream to reach a pH of 4 for protein precipitation at the isoelectric point (Parimi et al. 2015). The precipitated protein solids are then filtered from the solution. The filtrate containing non-precipitated proteins, carbohydrates, lipids, and other soluble components is assumed to be recycled to the algae cultivation farm as a nutrient source. Membrane filtration testing conducted by Gifuni et al. (2020) demonstrated that about 50% to 60% of algae carbohydrates, mainly polysaccharides, are retained together with proteins. Therefore, for the acid precipitation and filtration step, about 50% of carbohydrates and other components in the protein extract stream are assumed to be co-precipitated with the protein

solids. A similar percentage is assumed for the lipids (FAME) based on Parimi et al. (2015). The separated protein solids are then sent to a spray dryer to produce the final protein product powder.

The major design assumptions for HTL and biocrude upgrading are listed in Table 2.2.7. The design and evaluation of these processes are based on previous work (Zhu et al. 2021; Jiang et al. 2019) and current testing work by PNNL. The HTL product yields for PEA are predicted based on PEA feedstock composition and the correlation equation developed by Jiang et al. (2019). PEA has less protein and more carbohydrates, which leads to higher biocrude yield than untreated algae on a gram/gram feedstock basis. Upgrading experiments have been conducted at PNNL to investigate the hydrotreatment of HTL biocrude from algae biomass and the production and distillation of jet fuel products, and the JFC distribution reaches 22% of the hydrotreated oil based on the distillation range (Zhu et al. 2023). The design of hydrotreating and hydrocracking processes are based on current hydrotreating experiments and previous TEA work (Zhu et al. 2021, 2023). Protein extraction pretreatment leads to lower nitrogen content in the biocrude and thus lower hydrogen consumption and high hydrotreated oil yields based on solids sent to HTL compared to those of the fuel production only pathway. For this study, to maximize the production of jet fuel, both diesel and heavy oil cuts are assumed to be sent to the hydrocracking process to further convert these oils into naphtha and JFC products. This is different from previous algae HTL biocrude upgrading, which sends only the heavy cut (boiling point >340°C) to the hydrocracking unit. Based on this design, the optimal JFC distribution in final fuels can reach 60% to 65%, and the remaining products are diesel- and naphtha-range fuels. This JFC yield estimation is based on current hydrotreating testing results and optimal hydrocracking product yields predicted by expert judgement. Because no upgrading tests have been conducted for the HTL biocrude from PEA, the hydrogen consumption and hydrotreating yield for PEA HTL biocrude are assumed based on previous testing results for whole algae HTL. Bench experiments to upgrade HTL biocrude from PEA should be considered in the future to validate the assumptions for hydroprocessing yields. It is anticipated that the HTL biocrude will have a reduced nitrogen content, resulting in a lower hydrogen demand to remove nitrogen and other heteroatoms during hydrotreatment (Cronin et al. 2022).

Table 2.2.7. Major Design Assumptions for PEA and Whole Algae HTL Conversion and Upgrading Processes

Processes	Fuel and Protein Production	Fuel Production Only
HTL conversion		
Feedstock solid wt %, AFDW	20 (PEA)	20 (algae)
Temperature, °C	350	350
Pressure, psia	3,000	3,000
Liquid hourly space velocity (LHSV), L/L/h	4	4
Product yields, g/g PEA feed, AFDW		
Biocrude	0.41	0.39
Aqueous	0.31	0.39
Gas	0.25	0.19
Solid	0.03	0.03
Upgrading		
Hydrotreating		
Temperature, °C (outlet)	400 (main bed); 325 (guard bed)	400 (main bed); 325 (guard bed)
Pressure, psia (outlet)	1,500	1,500
Weight hourly space velocity, h^{-1}	0.5 (main bed); 0.72 (guard bed)	0.5 (main bed); 0.72 (guard bed)
H_2 consumption, g/g dry feed	0.057	0.071
Hydrotreated oil yields, g/g dry feed	0.88	0.83
Hydrocracking		
Temperature, °C (inlet)	390	390
Pressure, psia (inlet)	1,000	1,000
LHSV, h^{-1}	1	1
Hydrodenitrogenation of jet fuel cut		
Temperature, °C (outlet)	400	400
Pressure, psia (outlet)	1,500	1,500
LHSV, h^{-1}	0.5	0.5
Nitrogen removal, % of inlet nitrogen	99	99
Final fuels distribution, wt %		
Naphtha	23%	23%
SAF	60%	60%
Diesel	17%	17%

Based on current testing results of the algae HTL biocrude hydrotreating at PNNL, the nitrogen levels in the JFC (about 5,000 ppm) from the hydrotreated oil are significantly higher than conventional petroleum-based jet fuel. Although the impact of elevated nitrogen levels of jet fuel on engine/fuel performance has yet to be established, an HDN step is still assumed to remove most of the nitrogen in the JFC from the hydrotreated oil. Penner et al. (1999) mention that jet fuels contain only trace amounts of fuel-bound nitrogen and that higher levels can cause storage

stability problems and render the fuel unfit for use. A report by Chevron (Hemighaus et al. 2007) also mentioned that nitrogen in the petroleum-based fuel is neither controlled nor typically measured but can range from near zero to 20 ppm. To achieve a comparable nitrogen content as petroleum-based jet fuel, an initial HDN testing has been done at PNNL and demonstrated a 99% nitrogen removal efficiency (53 ppm after HDN processing) for the JFC from the wet sludge HTL biocrude hydrotreating (Snowden-Swan et al. 2022). Therefore, with HDN, the SAF generated from biomass HTL and upgrading has a nitrogen content of similar magnitude as petroleum-based jet fuel. The same HDN testing conditions and nitrogen removal efficiency are assumed in this study considering the compositional similarity of the hydrotreated biocrude from algae and wet sludge. The JFC after the HDN processing is assumed to constitute the final SAF product. Although the SAF product still has slightly higher nitrogen content than conventional jet fuel, SAF is generally used for blending with conventional jet fuel up to 50%, which will lead to a lower nitrogen content for the finished fuel blend. Future work can test the fuel storage stability and engine/fuel performance for jet fuel with different blending ratios of SAF from algae biomass to decide optimal nitrogen removal needs.

The capital cost estimation for the algae HTL conversion system is based on previous TEA studies for algae HTL (Zhu et al. 2020, 2021), with standard equipment costs sourced from Aspen Process Economic Analyzer (Al-Malah 2016) and special equipment costs for HPH and solid-liquid filtration based on prior NREL TEA studies. Variable operating costs are based on unit prices from industrial sources and previous work. The SAF is assumed to be sold together with naphtha and diesel cuts as the final fuel blendstock product. The yield of the final fuel product, including naphtha, SAF, and diesel cuts for each site group, is estimated on the basis of gasoline gallons equivalent (GGE), equal to the energy content of one gallon of gasoline on a lower heating value basis. The final fuel production cost was calculated as the MFSP by using a discounted cash flow rate of return calculation method in dollars per GGE. The methodology is identical to that used in previous TEA studies (Davis et al. 2018; Zhu et al. 2020).

For LCA modeling, the LCI of the HTL process includes material and energy consumption associated with fuel and PC coproduction, and the LCIs of HTL are consistent across all sites. LCI details can be found in Table 2.2.8. Considerations for coproduct handling methods are discussed below.

Table 2.2.8 Material and Energy Consumption Associated With the HTL Pathway

	Fuel + PC Without Market Limit	Fuel Only
Inputs		
Algae biomass (kg AFDW/MJ)	0.142	0.0764
Energy inputs		
Electricity demand (kWh/MJ)	0.0923	0.00596
Natural gas (utility) (MJ/MJ)	0.204	0.131
Natural gas (H_2 production) (MJ/MJ)	0.146	0.207
Chemical and water demand		
Sulfuric acid (kg/MJ)	0.0014	0.0021
Hydrotreating catalyst (HTL) (kg/MJ)	1.71E-05	1.83E-05
Hydrocracking catalyst (HTL) (kg/MJ)	3E-07	2.99E-07
Membrane flocculant (kg/MJ)	0.0016	0
NaOH (kg/MJ)	5.47E-05	2.31E-05
Water (process demands) (gal/MJ)	0.0356	0.0169
HCl (kg/MJ)	1.06E-05	0
Output		
Renewable diesel (MJ/MJ)	0.174	0.175
Naphtha (MJ/MJ)	0.223	0.226
SAF (MJ/MJ)	0.603	0.6
Protein coproduct	0.0495	0

Coproduct Handling in TEA and LCA Models

For TEA modeling, scenarios including algal PC coproduction assume that the protein coproduct is sold at market value, reducing fuel costs through the inclusion of coproduct revenues. Based on the process simulation, the purity of the final protein product is estimated to be 72 wt %. As shown in Table 2.2.9, this purity is comparable with currently marketed protein food products, including soy, pea, and whey PC. Therefore, the final protein product of the conversion system in this study is assumed to be sold as algae PC for human or animal consumption. Specifying the price of the algae PC product is challenging because the current market only includes whole microalgae for food/feed applications (Caporgno and Mathys 2018). Microalgae-based protein extract has only been tested for protein digestibility and toxicity and is not commercially available (Wang, Tibbetts, and McGinn 2021; Soto-Sierra, Stoykova, and Nikolov 2018). To specify the PC product price for this study, a summary of major PC products in the current protein market is collected to compare to the algae PC product, as listed in Table 2.2.9. The digestibility of whole microalgae ranges from 0.51 to 0.90 depending on the strain. For concentrated protein products, such as protein hydrolysate, the digestibility ranges from 0.9 to 0.97 (Wang, Tibbetts, and McGinn 2021; Soto-Sierra, Stoykova, and Nikolov 2018). Algae PC product has slightly lower protein content than protein hydrolysate (70 to more than 80 wt %), but much higher than whole cell algae (40 to 60 wt %). Therefore, the digestibility of algae PC product should be higher than pea PC when algae PC has higher protein content. Because algae PC is plant-based and the PC product of this study has similar protein content as the soy and pea PC, the selling price of the algae PC product in this study is assumed to be the average of the

selling prices of the two PCs, which is $1.0/lb. This price is higher than soy PC but much lower than pea and whey PC products (while noting that using saline microalgae avoids land and food conflicts associated with traditional food crops for protein generation, such as soy and pea).

Table 2.2.9 Protein Content, Digestibility, and Price of Different PC Products

Protein Products	Soy PC	Pea PC	Whey PC 34%	Whey PC 80%	Algae PC
Protein content, wt %	65	65	34	80	72 (this study)
Protein digestibility	0.96	0.72	1	1	Whole cell: 0.51–0.84; Protein hydrolysate: 0.9–0.97
Price, $/lb product	$0.59	$1.47	$0.9375 (2020 average)	$2.21 [a]	$1.0 (average of soy and pea PC prices)
Price, $/lb protein	$0.91	$2.27	$2.76 [b]	$2.76	$1.59 (average of soy and pea protein prices)
Source	Bashi et al. (2019)		USDA (2021)		Wang, Tibbetts, and McGinn (2021); Soto-Sierra, Stoykova, and Nikolov (2018)

[a] Estimated based on whey protein price and whey PC 80% protein content.

[b] Estimated based on whey PC 34% product price and its protein content.

For LCA modeling, the extracted PC can be used to replace high-protein products, such as whey PC and soybean PC. In this study, four coproduct handling methods have been employed: process-level mass allocation, process-level economic value allocation, system expansion (displacement), and an overall biorefinery-level method. Specifically, with process-level allocation, processes associated with both fuel and PC are allocated based on feedstock mass or economic values of products. Processes linked solely to fuel production or PC production are allocated accordingly. For simplicity in subsequent discussion, we use "mass allocation" and "economic value allocation" as abbreviations to represent the names of "process-level mass allocation" and "economic value allocation," respectively. According to ISO 14044 guidelines, allocation should be avoided in LCA whenever possible. This can be achieved by (1) subdividing multifunctional processes into two or more sub-processes and collecting input and output data for each sub-process, or (2) expanding the production system to encompass the additional functions related to coproducts. Additionally, when dealing with biofuel coproducts in transportation LCA models, the system expansion (displacement) method is recommended, particularly when the shares of non-fuel products are limited (Cai et al. 2018). However, liquid whey is the main feedstock for whey PC and a coproduct from cheese production. Due to uncertainties related to LCA credits for coproducts, we have chosen to use mass allocation as the default method in this report. Further discussion on the displacement of whey PC and soy PC and biorefinery-level analysis are also considered, with the aim of providing a foundation for future research on algae-based protein products.

Factors To Consider With the Introduction of Microalgae-Based Protein Products to the Market

Microalgae proteins have potential to replace whey PC or soy PC, but they may need to be further processed for flavor. Solubility, emulsification, gelation, and foaming are physicochemical properties of protein that directly impact the preparation, processing, storage,

and consumption of food. It has been found that microalgae proteins have comparable emulsifying and foaming properties with whey and soy proteins (Grossman, Hinrichs, and Weiss 2020). However, there is ongoing debate regarding the suitability of algae PC as a replacement for whey PC and meat, primarily due to flavor considerations and trends toward less processed food. In addition, there are many other factors that influence the replacement, such as increasing demand, current production and trade conditions of existing products and alternatives, and economic benefits associated with increasing protein demand.

Soy PC, extracted from soybeans, is used to represent the protein ingredient market. The LCI of soybean (13% water) farming, harvesting, and transportation to a soy PC production plant was obtained from the GREET model. The LCI of soy PC extraction from soybean (13% water) was obtained from Philis et al. (2018), and the LCI data were allocated based on mass or price as shown in Table S26. The protein content for soy PC is 62% according to literature (Philis et al. 2018), and it is assumed that the algae-based protein coproduct with protein content of approximately 75% can be used to replace it with three replacement metrics: mass, protein content, and digestible protein. The replacement ratio calculation is provided below, and the calculated replacement ratio for soybean PC can be found in Table 2.2.10.

Calculation of the replacement ratio (RR) by using protein content and digestible protein as the matching functional units:

$$RR(PC)_i = WP_C / WP_i \quad \text{(Eq. 3)}$$

$$RR(DP)_i = (PD_C \times WP_C)/(PD_i \times WP_i) \quad \text{(Eq. 4)}$$

$RR(PC)_i$ = Replacement ratio of replacing i with microalgae PC coproduct by using protein content.
WP_C = Weight percentage of protein in microalgae PC coproduct.
WP_i = Weight percentage of protein in i (whey PC, soybean PC, soybean meal, or alfalfa meal).
$RR(DP)_i$ = Replacement ratio of replacing i (whey PC, soybean PC, soybean meal, or alfalfa meal) with coproduct by using digestible protein.
PD_C = Protein digestibility of microalgae PC coproduct.
PD_i = Protein digestibility of i (whey PC, soybean PC, soybean meal, or alfalfa meal).

Table 2.2.10 Replacement Ratios Based on Protein Content and Digestible Protein

Parameter	Displacement				Coproduct From This Study
	Whey PC	Soybean PC	Soybean meal	Alfalfa meal	Microalgae PC
Protein content	60%	62%	49%	17%	72%
Protein digestibility	100%	95–98%	82%–87%	80%–99%	55%–80%
Average replacement ratio by using protein content	125%	121%	142%	136%	
Average replacement ratio by using digestible protein	~80%	~80%	113%	319%	
References	Qin et al. (2022)	Qin et al. (2022)	Ravindran, Abdollahi, and Bootwalla (2014)	Sheehan et al. (1998)	Devi et al. (1981) and Niccolai et al. (2019)

Commercial whey PC is derived from liquid whey through a series of processes involving ultrafiltration, evaporation, and drying (USDA 2015). From an LCA perspective, the displacement of whey PC presents a complex scenario. Liquid whey serves as a coproduct of cheese production, and the displacement of whey PC would not necessarily affect the production of liquid whey from cheese manufacturing. Given the projected growth in the cheese market, it is improbable that liquid whey will become obsolete. The displacement of liquid whey by microalgae PC may only become justifiable when liquid whey cannot meet the demand for whey PC. However, predicting the whey PC market is challenging due to multiple factors, including flavor acceptance, consumer preference for less processed foods, trade conditions, and more. Nevertheless, in this analysis, various coproduct calculation methods have been examined for liquid whey in order to offer a quantitative measure of environmental credits attributed to whey PC. The LCIs of whey PC and liquid whey and detailed allocation associated with cheese and liquid whey were obtained from literature (Bacenetti et al. 2018; Kim et al. 2013; Aguirre-Villegas et al. 2012), and detailed information can be found in the appendix. The replacement ratio for whey PC can be also found in Table 2.2.10.

2.3 Modeling of National Totals From Site-Specific Biomass Potential, Costs, and Greenhouse Gas Emissions

Multicriteria Land Screening

A nationally consistent geospatial resource database and modeling framework was redeveloped as a means to evaluate multicriteria spatial suitability, integrate numerical modeling, perform partial techno-economic modeling (primarily upstream and downstream of the farm gate, including CO_2 and makeup water delivery as well as saline blowdown disposal), and ultimately determine ideal locations for microalgae cultivation under a variety of scenarios and assumptions using the most recent available data (see Table 2.3.1). The land suitability model includes CONUS, Hawaii, and the U.S. territories, but this assessment is constrained to CONUS to maintain consistency with past model harmonization efforts (excluding international locations in keeping with the support for this study from DOE). The multicriteria land suitability model initially screens based on topography, particularly slopes <3%, then further considers protected lands such as state and national parks; environmentally sensitive lands such as forests, wetlands, and riparian areas; areas of high net primary productivity (kg C/m^2); and other lands deemed sensitive according to the 2021 World Database on Protected Areas. Further, high-productivity croplands, roadways, airports, and areas within urban area boundaries are removed from consideration; however low-productivity croplands, idle croplands, and pasturelands are retained, as are brownfield locations, even if they exist within an urban area boundary.

The model assumes a 1,000-acre minimum contiguous land area and does not enforce a maximum area threshold. For translation of these land screenings to the algae farm TEA model, this implies the selection of a stand-alone unit algae farm at least 1,000 acres in size based on production pond area. With no maximum area threshold, the unit algae farms were allowed to vary in size beyond 1,000 acres to match the suitable land area and locally available CO_2 and water reflected from the BAT model. Without further resource constraints, this analysis yielded 24,583 independent unit algae farms across the CONUS. These are further downselected as described next.

Table 2.3.1. Dataset Descriptions for the Multicriteria Land Screening for Determining Potential Algal Production Farms

Dataset	Year	Resolution (m)	Description and Processing	Source
Digital Elevation Model (National Elevation Dataset)	2021	10	Elevation data used to derive weighted slope dataset, where ≤1% slope is suitable (1), 1%–3% slope is weighted linearly, and ≥3% slope is not suitable (0). Digital Elevation Models were downloaded from The National Map.	U.S. Geological Survey
National Hydrography Dataset	2021	1:24,000 or better	Hydrography features, including rivers, streams, canals, lakes, ponds, and other open water. The database includes four datasets: areas, waterbodies, flowlines, and lines. The features are elevation-derived, and it is the most complete hydrological dataset for the United States, according to the U.S. Geological Survey.	U.S. Geological Survey
National Land Cover Database	2019	30	Standardized land cover with 25 categories over the CONUS. Open water; perennial ice/snow; developed (open space; low, medium, and high intensity), deciduous, evergreen, and mixed forest; lichens; moss; and woody and emergent herbaceous wetlands are not suitable. Barren land, dwarf shrub, shrub/scrub, grassland/herbaceous, sedge/herbaceous, pasture/hay, and cultivated crops are suitable.	Multi-Resolution Land Characteristics Consortium
Coastal Change Analysis Program Land Cover	2009–2016	1–5	Standardized land cover with 24 categories over coastal regions of the United States, including islands and territories. Classification deviates slightly from the National Land Cover Database. Developed (open space; low, medium, and high intensity), deciduous, evergreen, and mixed forest; scrub/shrub; palustrine (forested, scrub/shrub, emergent) wetland; estuarine (forested, scrub/shrub, emergent); wetland; unconsolidated shore; water; palustrine and estuarine aquatic bed; tundra; and snow/ice are not suitable. Cultivated, pasture/hay, grassland, scrub/shrub, and bare land are suitable.	National Oceanic and Atmospheric Administration
Cropland Data Layer	2020, 2019, 2018	30	Standardized land cover dataset including a wide variety of crops and general land cover classes over the CONUS. All crops, background, non-agricultural/undefined, barren, shrubland, and grass/pasture are suitable. Forest, developed, water, wetlands, aquaculture, open water, perennial ice/snow, developed (open space; low, medium, and high intensity), deciduous, evergreen, mixed forest, and woody and herbaceous wetlands are suitable. A long-term (3-year) idle cropland dataset was produced by isolating	USDA

Dataset	Year	Resolution (m)	Description and Processing	Source
			the fallow/idle class to a binary raster for each of the 2020, 2019, and 2018 datasets, then multiplying the rasters. The long-term idle cropland data are used to locate low-productivity croplands that may be ideal for siting an algal production facility.	
National Wetlands Inventory	2021	1:24,000 or better	Feature dataset that covers all wetlands and surface water features on the landscape. Wetland areas are converted to a binary raster and marked as unsuitable.	U.S. Fish & Wildlife Service
Urban Area Boundaries	2020	n/a	In accordance with new rules in the 2020 Census, any block group with a housing unit density of at least 385 per square mile, where at least one-third of the block has an imperviousness of at least 20% and the area is compact in nature. Additionally, at least 40% of its boundary is contiguous with qualifying territory. Urban areas are marked as unsuitable.	U.S. Census
TIGER/Line Roads	2020	n/a	TIGER/Line all roads file containing all linear street features, such as primary, secondary, local, private, and rural roads; city streets; vehicular trails; ramps; service drives; walkways; stairways; and alleys. Roadways are an essential piece of infrastructure for an algal production farm, and existing roadways may reduce upfront cost for a new facility. Road features are considered following the land screening.	U.S. Census
Aeroways	2021	n/a	An open crowdsourced dataset containing polygon features for any infrastructure related to aviation and spaceflight. This includes runways, terminals, heliports, spaceports, parking lots, and more. Aeroways are not fully screened out as unsuitable, as there is potential to utilize part of the open areas typically associated with airports. A dataset was produced to indicate the presence of aeroway built infrastructure.	OpenStreetMap contributors
World Database on Protected Areas	2021	n/a	A worldwide database containing protected areas, with emphasis on conservation. In an effort to preserve valuable habitat, all protected areas are marked unsuitable.	Protected Planet Initiative
Protected Areas Database of the United States	2021	n/a	All areas in the United States that are held in public trust. The dataset is considered functionally complete, though the estimated completion varies by state. These lands are marked as unsuitable.	U.S. Geological Survey
Military Installations, Ranges, and Training Areas	2021	n/a	Feature dataset containing major installations, ranges, and training areas in the United States and its territories. Similar to aeroways, there is potential to utilize part of	U.S. Department of Defense

Dataset	Year	Resolution (m)	Description and Processing	Source
			the land on military installations; thus, not all areas are screened as unsuitable.	
Brownfields	2021	n/a	Point feature dataset containing the location of brownfield sites in the United States. Brownfields are ideal for algal production facilities, as they are typically idle land that is open to development. The sites are considered after the land screening analysis.	U.S. Environmental Protection Agency
Net Primary Productivity	2018	960	Net primary productivity (NPP) derived from the Integrated Biosphere Simulator (IBIS) model in kg C/m^2. Data span 1971–2015, and the period of 1985–2015 was averaged for this analysis. NPP is considered, especially in grassland areas, to avoid removing grasslands that are effective in capturing and storing carbon.	U.S. Geological Survey

Downselection of Algae Farm Sites

The BAT model is used to provide locations, biomass production potential, and pertinent cost factors (CAPEX and energy for groundwater and brine injection wells, and CAPEX and energy for FO blowdown processing) used in the TEA and LCA tasks. This includes the following:

1. A CONUS-wide multicriteria land suitability analysis to identify potential land areas for algae cultivation (see Section 2.3: Multicriteria Land Screening).
2. Identification of saline groundwater resources that could reasonably support saline water pond operations at 55,000-mg/L concentrations. This focused on CONUS-wide saline groundwater resources at total dissolved solids of ≥2,000 and ≤40,000 mg/L retrievable at ≤500-m depth.
3. An hourly time-step pond temperature and water balance model run from 1979 to 2019 (40 years) to simulate water temperature, evaporative loss, and blowdown volumes. The pond model uses the North American Land Data Assimilation System Phase 2 1/8° gridded hourly time-step meteorology.
4. An hourly time-step biomass growth model run from 1979 to 2019 for the two identified saline strains (*Picochlorum celery* and *Tetraselmis striata*) along with a monthly maximum productivity model (i.e., strain rotation). The growth rate of microalgae is modeled as a function of light intensity and temperature under nutrient-replete conditions and diurnally fluctuating light intensities and water temperatures.
5. A point-source location-allocation spatial network model simulates the capture, compression to supercritical fluid, and pipeline transport of waste CO_2 to individual sites' farm gates. As in the 2017 harmonization study, we consider the location and carbon demand of individual farm sites in combination with the location and supply of waste CO_2 supplies. Further considering the industrial process generating the CO_2 (and subsequent CO_2 concentrations), the most cost-effective sources of CO_2 are supplied to a given farm first, followed by additional sources as required to fulfill the needs of a cultivation site (Davis et al. 2018). Additionally, multiple CO_2 sources can meet the carbon demand of a given site, or a single CO_2 source may feed multiple farm sites.

6. Salinity management of the cultivation pond by modeling evaporative water loss and subsequent salinity levels, and processing the resulting water through FO once the 55,000-mg/L pond salinity threshold is achieved. The FO freshwater fraction is recycled for use within the algae farm, and the brine water fraction is disposed of through deep-well injection.

When subsequently applying minimum groundwater salinity constraints of ≥2,000 and ≤40,000 mg/L at depths <500 m (Figure 2.3.1) in addition to ≥25-g/m^2/day productivity thresholds, this yields a total of 3,255 sites focused across the U.S. Southern-tier states. For this analysis, potential cultivation sites are further constrained by the availability of nearby, non-committed waste point-source CO_2 that can be captured and transported to the site for ≤$75 tonne (≤$83/ton), bringing the total down to 1,199 sites. Further eliminating a set of unique outlier cases in the TEA process, the sites were further downselected to a final total of 980 sites (Figure 2.3.2). For reporting purposes and to organize the results where practical, the individual sites are categorized regionally by "Western" (California and Arizona), "South-Central" (Texas and Louisiana), and "Southeast" (Florida and Georgia) regions.

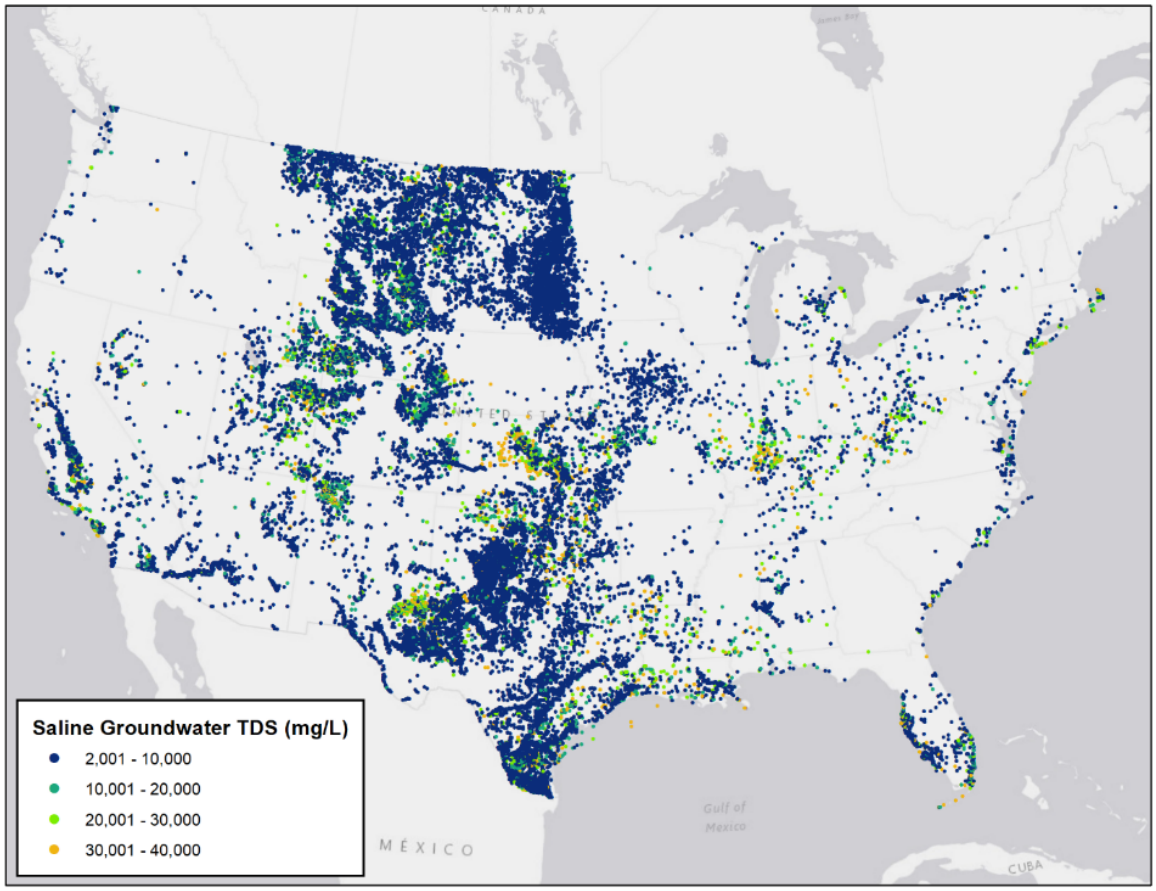

Figure 2.3.1. Groundwater salinity (mg/L) at 24,583 CONUS-wide land-screened sites constrained to ≥2,000 and ≤40,000 mg/L and depths ≤500 m

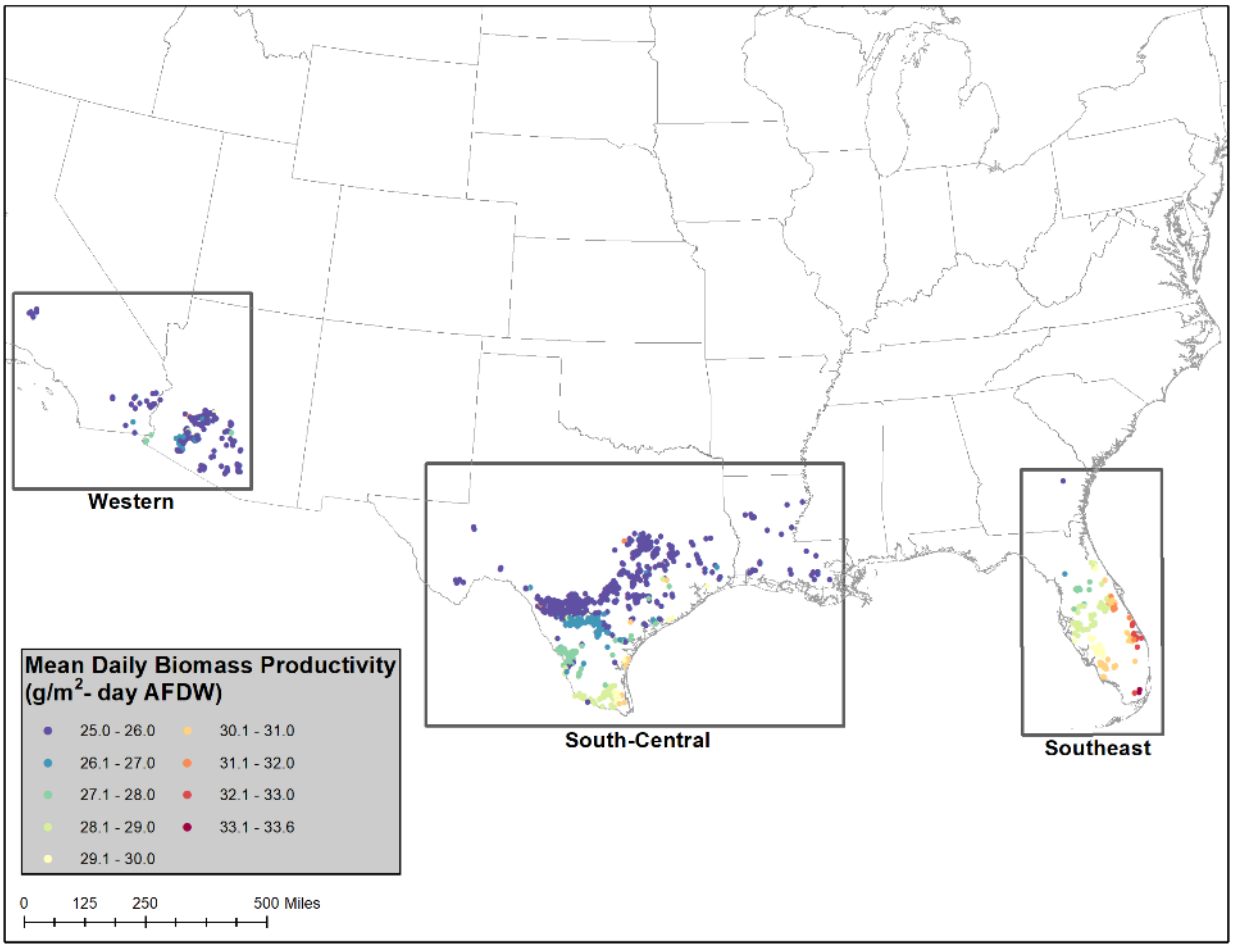

Figure 2.3.2. Final 980 land-screened sites meeting the 25-g/m^2/day AFDW threshold, saline groundwater constraints, and ≤$75/tonne (≤$83/ton) CO_2 collocation requirement

To help characterize the regional differences in productivity (g/m^2/day), annual total biomass production (MM tons/yr), and CO_2 pipeline transport distance (miles), sets of histograms are presented in Figures 2.3.3–2.3.5, respectively, for each region. A histogram of long-term average biomass productivity among the land-screened sites for each of the three regions is provided in Figure 2.3.3. Table 3.1.1 provides a summary of biomass productivity, cultivation area, and total biomass output for each region, as well as a total for CONUS.

With regard to unit biomass productivity, the Southeastern region shows the highest levels of productivity, with the vast majority of total sites (n = 137) performing at 30 g/m^2/day or greater. Out of the three regions, the Southeast has the fewest number of individual farm sites. The South-Central region has the largest number of sites (n = 675) by more than a factor of 3 compared to the other two regions. This region exhibits biomass productivity in the 26–27-g/m^2/day range and is the second-highest-performing region with regard to productivity. The Western region has the second highest number of sites (n = 168), with biomass productivity dominantly ranging in the 25–27-g/m^2/day range.

The total annual biomass production (MM tons/yr) reflects a combination of unit biomass productivity, total available land area for cultivation, and economically collocated CO_2 sources.

Among the three regions, the South-Central region provides a significantly greater amount of land area for cultivation (2,903,983 acres) than the other two regions, by more than a factor of 5. Accordingly, the South-Central region dominates in the total annual biomass output at 124.1 MM tons/yr. The Western region produces the second largest amount of annual biomass at 21.7 MM tons/yr on 521,395 acres, followed by the Southeastern region with 21.6 MM tons/yr on 434,091 acres. Among the three regions, the majority of individual sites within each region produce between 33,068 and 110,226 tons/yr.

The availability and supply of waste CO_2 is another key factor in the siting of cultivation farms. Without the availability of external CO_2, a cultivation site is not considered in this analysis, largely due to significantly reduced productivity without the sparged CO_2. Figure 2.3.6 shows the CO_2 point source locations used in this study and categorized across eight different sectors, including electricity generation, refinery and chemical production operations, petroleum and natural gas processing, cement production, fertilizer production, industrial applications, agricultural processing, and ethanol production. Further, the annual CO_2 mass availability applied in this study by sector and region of the collocated point-sources is presented in Figure 2.3.7, highlighting the electricity generation sector as by far the largest contributor, followed by refineries and chemical production. Each of these CO_2 sources is linked to one or many land screened algae cultivation sites based on carbon availability and carbon demand at the individual farm, as a function of biomass productivity and total production area. The sourcing and transport of CO_2 to an algal cultivation farm can have a considerable impact on overall production costs. Thus, in general, the shorter the pipeline transport distance, the more economical the availability of CO_2. However, with larger individual sources of CO_2, it can be advantageous to source a single site and capture and transport this across a longer distance as opposed to capturing and transporting from several smaller sources that may be closer in proximity. Recall that for this study, a $75/tonne ($83/ton) delivered CO_2 cost cap was placed to help keep the supplemental carbon costs manageable. Figure 2.3.5 is telling in that for all three regions, the majority of the pipeline distances fall in the 1–30 mile range, where the South-Central region has the most required pipelines, with a distance average of 24 miles and a total non-optimized pipeline network of 16,308 miles. These numbers are also reflective of the region's large availability of waste CO_2 sources. In comparison, the Western region's average pipeline distance is 28 miles, comprising a total network of 4,677 miles, and for the Southeastern region, the average pipeline distance is 18 miles with a total network of 2,463 miles.

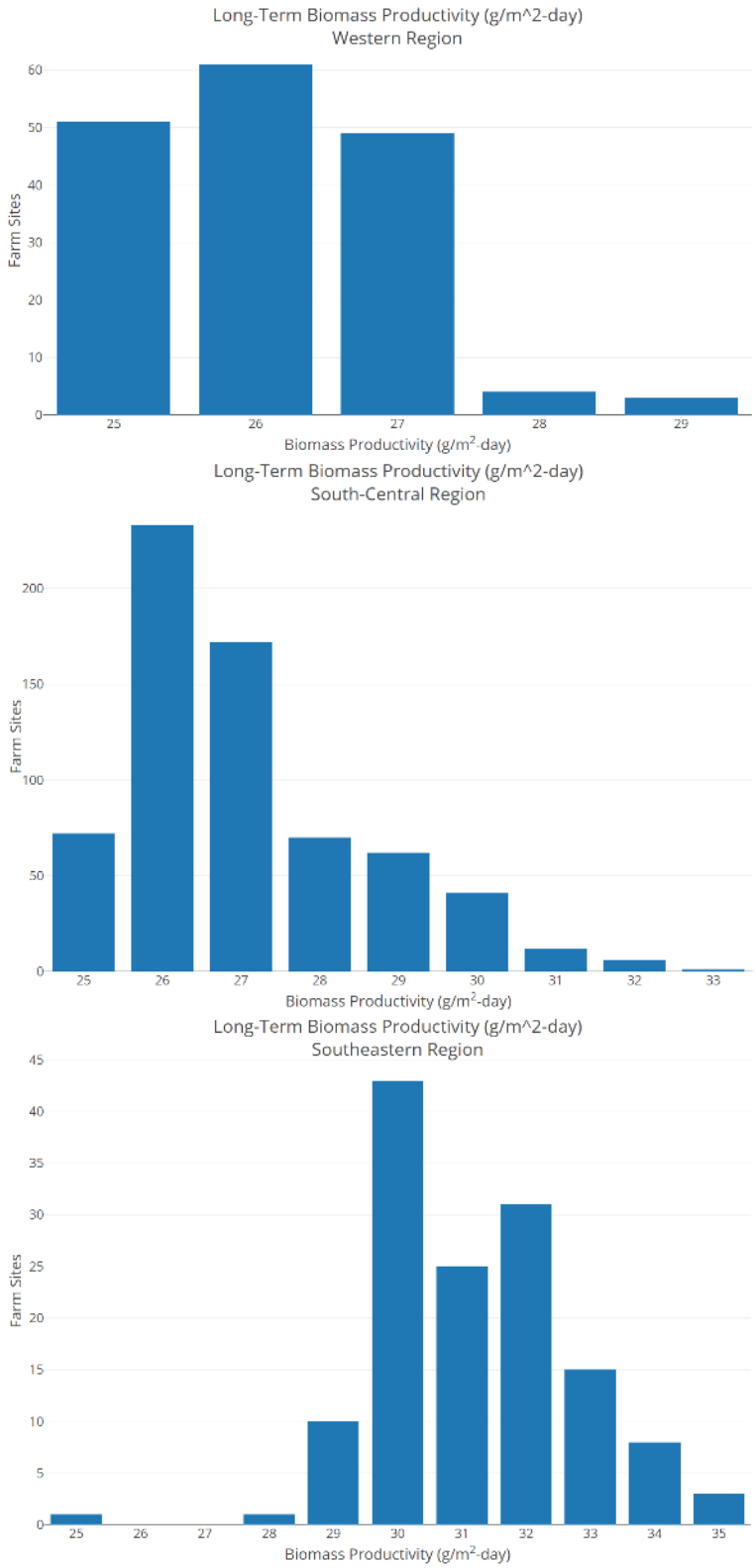

Figure 2.3.3. Histograms of long-term average biomass productivity (g/m^2/day) for sites within each of the three regions (Western, South-Central, and Southeastern)

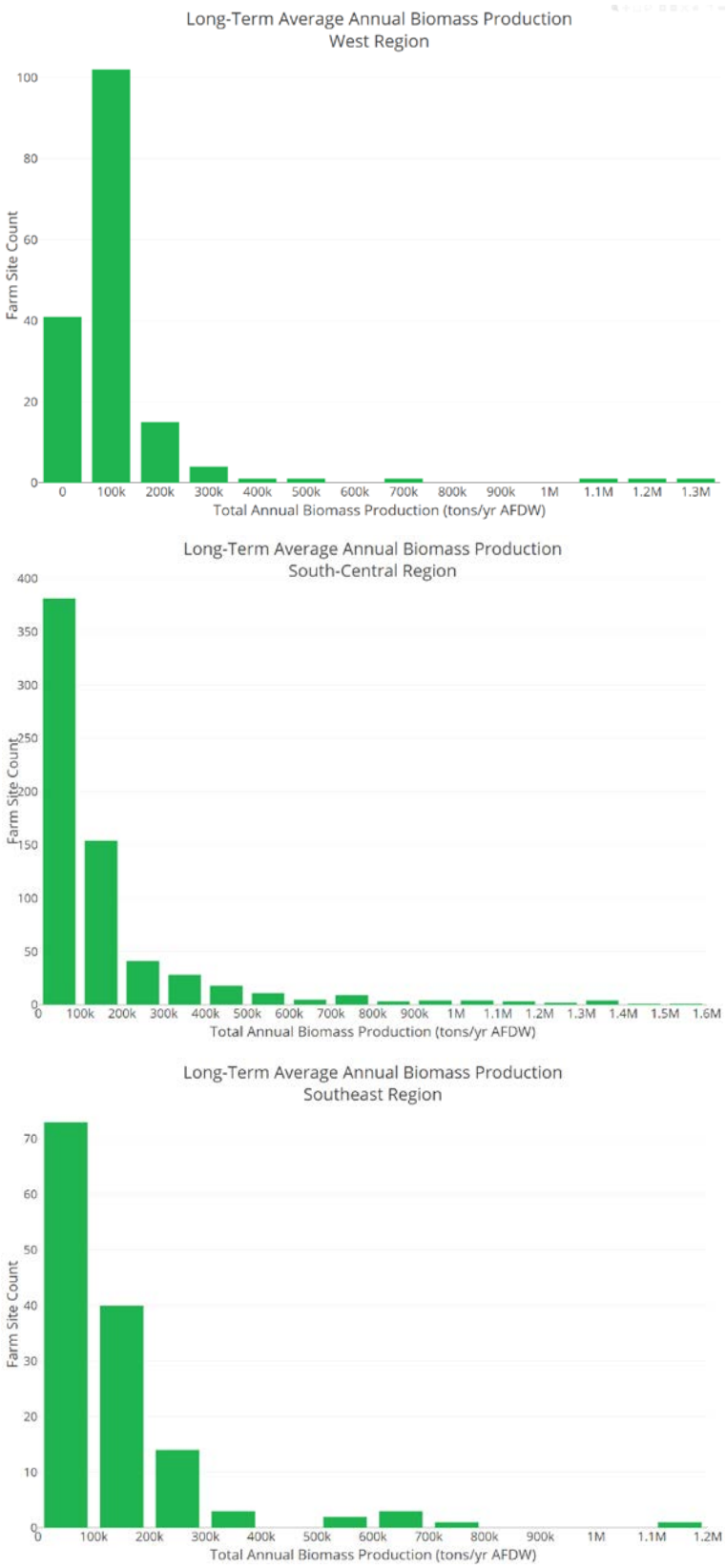

Figure 2.3.4. Histograms of the long-term total annual biomass production (tons/yr) per region. These plots reflect a combination of biomass productivity and available cultivation area.

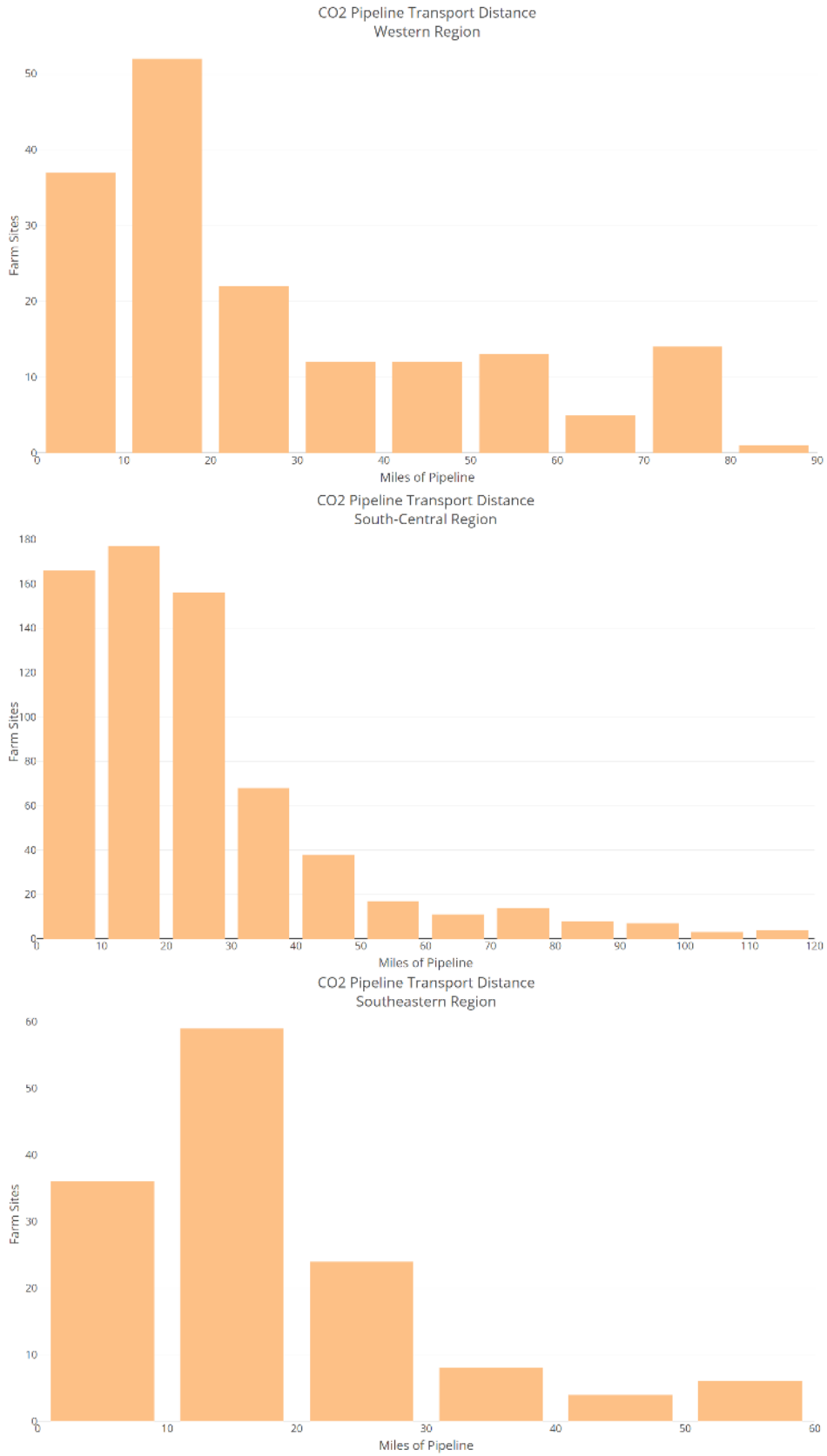

Figure 2.3.5. Histograms of CO_2 transport distance (miles) by region

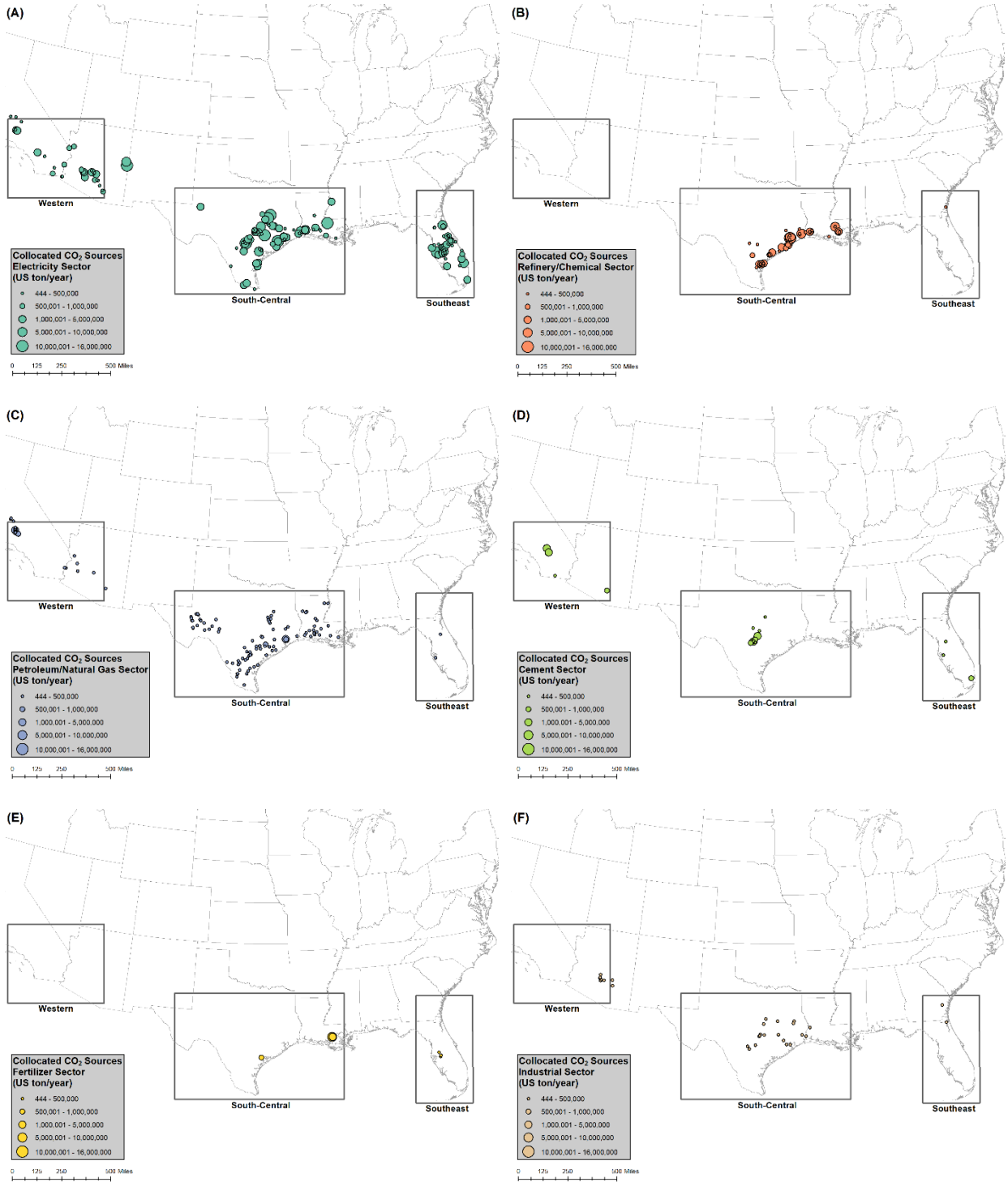
(A)
Western
South-Central
Southeast
Collocated CO_2 Sources
Electricity Sector
(US ton/year)
444 - 500,000
500,001 - 1,000,000
1,000,001 - 5,000,000
5,000,001 - 10,000,000
10,000,001 - 16,000,000
0 125 250 500 Miles
(B)
Western
South-Central
Southeast
Collocated CO_2 Sources
Refinery/Chemical Sector
(US ton/year)
444 - 500,000
500,001 - 1,000,000
1,000,001 - 5,000,000
5,000,001 - 10,000,000
10,000,001 - 16,000,000
0 125 250 500 Miles
(C)
Western
South-Central
Southeast
Collocated CO_2 Sources
Petroleum/Natural Gas Sector
(US ton/year)
444 - 500,000
500,001 - 1,000,000
1,000,001 - 5,000,000
5,000,001 - 10,000,000
10,000,001 - 16,000,000
0 125 250 500 Miles
(D)
Western
South-Central
Southeast
Collocated CO_2 Sources
Cement Sector
(US ton/year)
444 - 500,000
500,001 - 1,000,000
1,000,001 - 5,000,000
5,000,001 - 10,000,000
10,000,001 - 16,000,000
0 125 250 500 Miles
(E)
Western
South-Central
Southeast
Collocated CO_2 Sources
Fertilizer Sector
(US ton/year)
444 - 500,000
500,001 - 1,000,000
1,000,001 - 5,000,000
5,000,001 - 10,000,000
10,000,001 - 16,000,000
0 125 250 500 Miles
(F)
Western
South-Central
Southeast
Collocated CO_2 Sources
Industrial Sector
(US ton/year)
444 - 500,000
500,001 - 1,000,000
1,000,001 - 5,000,000
5,000,001 - 10,000,000
10,000,001 - 16,000,000
0 125 250 500 Miles

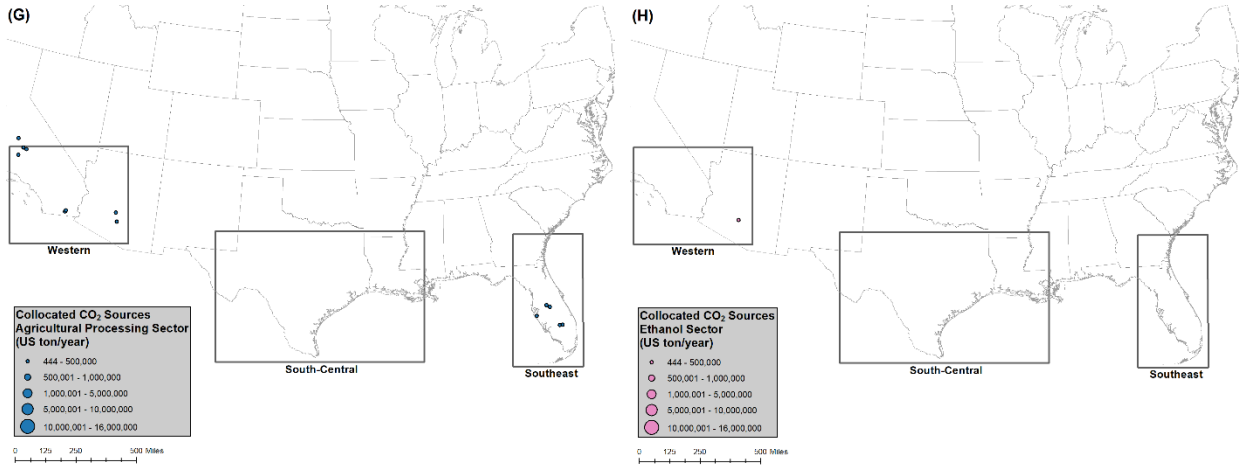

Figure 2.3.6. CO_2 point-source locations separated by production sector used for microalgae cultivation at captured and farm gate delivered price of ≤$75/tonne (≤$83/ton). The eight sectors included are ordered from A-H according to total CO_2 availability, with the electricity generation sector and ethanol sector representing the largest and smallest contributors respectively.

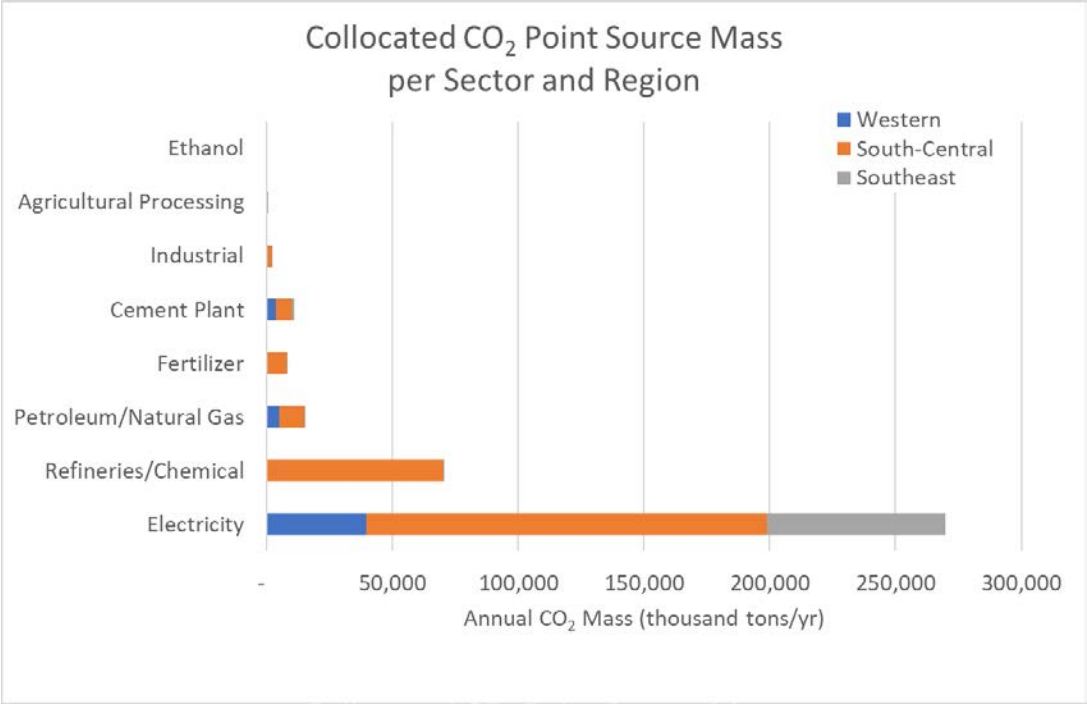

Figure 2.3.7. CO_2 point-source mass availability, broken out by production sector and region, as applied in this study for capture and transport to algae farms.

Direct Land Use Change (DLUC)

Direct land use emissions were also estimated through original land use data provided by PNNL and a location-based land use change (LUC) emissions factor (Eggleston et al. 2006; Quiroz et al. 2023). The net primary productivity data obtained from the Integrated Biosphere Simulator (IBIS) model in kg C/m^2 helped avoid areas with high carbon stocks and fluxes (Liu and Sleeter 2018). The LUC calculation specifically accounts for the carbon loss occurring in the landscape

due to the removal of aboveground and belowground biomass (Handler, Shi, and Shonnard 2017). Carbon emissions from LUC were calculated based on Equation 5. Detailed carbon emissions results from different sites can be found in Figure S4. Due to large uncertainties, the carbon emissions from DLUC were not included in overall GHG emissions, but rather are discussed separately in the Appendix.

$$LUC = EF_{LUC} \times Facility\ Size \times EA / LT / FP_{Annual} \quad \text{(Eq. 5)}$$

LUC – Annual land use change emissions per unit of fuel (g CO_2-eq./MJ of fuel)
EF_{LUC} – Land use change emissions factor (g CO_2/ha)
Facility Size – (ha)
EA – Energy allocation (%). For fuel only case: EA = 100%
LT – plant lifetime (years). LT of microalgae plant = 30 years.
FP_{Annual} – Annual fuel production (MJ/year)

Simulation of Algae Cultivation Costs Across Identified Sites

The algae farm TEA model was run for 980 individual locations spanning the full collection of sites depicted in Figure 2.3.2. This number of individual sites was reached after a downselection from all sites screened with the BAT model with the application of two filters: (1) discarding all cases with salinity of the makeup water above 40,000 mg/L and (2) removing all points with an estimated MBSP exceeding $1,000/ton AFDW. The analysis leveraged several parameters directly supplied by the BAT model, such as monthly productivities, farm size, evaporation rates, salinity of the input water, and delivered CO_2 costs. The water balance was then calculated using the NREL algae farm model as discussed above, thus determining the amount of saline water needed, the blowdown requirements, and brine production in the FO unit. This made use of associated BAT outputs for makeup water well CAPEX and pumping power, as well as CAPEX/power demands for the blowdown handling FO membrane and injection well, as those parameters are all dependent on the water balance of the facility and can be scaled from original BAT values by throughput. As noted above, a new feature in the present harmonization study relative to past studies is that the individual farm size was allowed to fluctuate to match the total available size dictated by BAT outputs (typically driven by local CO_2 availability). While this incurs an additional economy-of-scale difference between sites compared to the 2017 harmonization that assumed a fixed 5,000-acre farm size, it reflects the practical approach that would be taken at scale—i.e., building a single farm connected to a single conversion facility scaled to utilize all available CO_2 at that location, rather than multiple collocated farm/conversion facilities in close proximity. The resulting farm scales range between 1,000 and 38,500 acres based on production pond area, with an average size of 3,940 acres (the majority of sites fall between 1,000 and 5,000 acres).

Market Considerations for Protein Coproducts

Based on the high protein content of the algae PC product in this study, the primary potential market for this protein product is the protein ingredients market for food and feed supplement applications as listed in Table 2.3.2. This market mainly includes soy protein (plant-based) and whey protein (animal-based), which have comparable protein contents as the algae PC product of this study (see Table 2.2.9). The global market size of animal-based protein ingredients, which is mainly whey protein, is estimated based on the U.S. whey PC production rate and its market share in the global market (USDA 2022a; Grand View Research 2022a). Other potential markets

for algae protein products include animal meat, pet food, and animal feed. Some research has been conducted to substitute a portion of plant materials with microalgae or microalgae PC to produce meat analogues via extrusion (Caporgno et al. 2020; Martínez-Sanz et al. 2020; Fu et al. 2021). The assumed selling price of the algae protein product in this study is not competitive compared to lower-value products such as soy PC and the major animal feed, soybean meals, which are $0.59/lb (see Table 2.2.9) and about $0.20/lb, respectively (USDA 2022b). However, using microalgae does not incur competition for land against other food sources and can yield higher protein per unit area compared to soybean for protein production, which may make it a more attractive protein source considering near-term potential for farmland degradation (Bleakley and Hayes 2017; Koyande et al. 2019).

Table 2.3.2. Potential Global Market Sizes for Algae Protein Product With Different Application Targets

Market	2021 Global Market (million tons/yr)	2030 Forecast Global Market (million tons/yr)	Protein Content, wt %	Source
Protein ingredients (plant- and animal-based)	6.6	14	65 to over 90	Grand View Research (2022b); Bashi et al. (2019)
Whey protein	1.4	3.9	34 to over 80	Grand View Research (2022a); USDA (2022a)
Meat	125 (pork) 77 (beef)	n/a	21 (pork and beef)	Statista (2022); González, Frostell, and Carlsson-Kanyama (2011)
Pet food	37	n/a	17 to 58 (dry food)	Tyler (2022); Decision Innovation Solutions (2020)
Aquafeed	57	n/a	25 to 72	Glencross (2022); Miles and Chapman (2021)
Animal feed	1,370	n/a	46.5 to 48 (soybean meal)	Tyler (2022); USDA (2022b)

When algae HTL conversion with inclusion of protein extraction is employed for all sites, the total algae PC production rate is estimated at 51 million tons/yr, which exceeds the whey protein and total protein ingredients market sizes. Under this context, only a portion of the cultivation site groups could use their algae products for protein production, subject to the related protein market volume constraints with respect to saturating the markets. With the protein market saturated, algae biomass from the remaining sites is thus subsequently used for fuel production only. Alternatively, for a fuel production only pathway, whole algae without protein extraction was assumed to be converted to fuels via direct processing through HTL conversion and upgrading. Whole algae HTL conversion technology has been tested and evaluated by PNNL (Jiang et al. 2019; Zhu et al. 2021, 2023). The HTL product yields for whole algae without protein extraction are estimated based on the biochemical compositions (see Table 2.2.7) and the correlation equation developed by Jiang et al. (2019). The hydrotreating process of whole algae HTL biocrude is designed based on a 2022 published study for *Picochlorum celeri* HTL biocrude hydrotreating (Zhu et al. 2023). Based on different protein market constraints, three scenarios are evaluated in this study. Scenario 1 uses the market size of whey protein as the constraint for protein coproduction, Scenario 2 uses the protein ingredients (both plant- and animal-based) market size for this constraint, and Scenario 3 assumes fuel production only from whole algae:

- Scenario 1: Algae from part of the sites is used for fuel and protein production, subject to 2030 global whey protein market size limits; after the market is saturated, for the remaining site groups, algae is used for fuel production only.
- Scenario 2: Algae from part of the sites is used for fuel and protein production, subject to 2030 global protein ingredients market size limits; after the market is saturated, for the remaining site groups, whole algae is used for fuel production only.
- Scenario 3: Algae from all the sites is used for fuel production only (no protein extraction is included).

For scenarios with protein market size constraints, the resulting MFSPs presented further below for the fuel and protein production pathway were sorted from low to high, and the sites were selected based on the sequence until the given protein market size was saturated. Then the remaining sites switched to the fuel-only pathway and their MFSPs were also sorted from low to high. Based on different scenarios, different sites can use either the fuel and protein production pathway or the fuel-only one. An optimal case is also investigated by assuming the future protein market for algae PC products may be larger than 51 million tons/yr, and thus the HTL with protein extraction pathway could be used for all sites without reaching protein market limits. The current major protein source for food is animal meat, which has a much larger market size than the whey protein market assumed in Scenario 1. When assuming the total protein demand for food (including both protein ingredients and animal meat protein) as a constraint for algae protein production, all the sites could use their algae products for both fuel and protein production. Although soybeans are currently the major plant-based protein source, developing new sustainable and biodiverse protein products is essential to solve challenges including food security, land and water resource consumption, and protein allergenicity. Therefore, there is promising potential for algae protein products in the future, and their market size may not track constraints for the whey protein market alone. Future studies may benefit from consideration of expanding algal protein into animal meat protein markets, though in such a scenario competition with other vegetable-based protein sources (e.g., soy protein) would also need to be considered.

3 Results

3.1 Algal Biomass Production

As previously detailed, selected outputs from the BAT models were run through the algae farm TEA models based on site-specific details for monthly cultivation productivities, delivered CO_2 costs, makeup water demands and associated well CAPEX and pumping power, and saline blowdown removal rates, including CAPEX and power demands for FO membranes as well as injection disposal wells.

Table 3.1.1 presents a summary of key parameters organized by region. A large portion of the viable production sites identified were shown to be in the South-Central region (Texas and Louisiana), accounting for nearly 75% of the total area identified and 74% of the total microalgae biomass potential. However, the regions supporting the most economical algae production were largely concentrated in the Southeast (Florida and nominally Georgia, representing 11% of total area and 13% of total biomass potential), driven by higher biomass productivities, larger unit farms, and lower variability between productivities in summer versus winter. The remainder is produced in the Western region (California and Arizona), reflecting somewhat higher biomass costs at lower annual productivities and higher seasonal variability on average. Resulting MBSP estimates for each individual farm are mapped to the BAT-identified locations as shown in Figures 3.1.1 and 3.1.2 for MBSPs before and after seasonal storage, respectively.

Table 3.1.1. Key Metrics for Algae Farm Availability and Cultivation Productivity for Each U.S. Region

U.S. Region	Number of Individual Sites	Total Cultivation Area (acres)	Total Biomass Output (MM tons/yr AFDW)	Annual Productivity (g/m²/day AFDW)	Productivity Variability (max vs. min ratio)
Western	168	521,395	19.7	24.9	6.2
South-Central	675	2,903,983	112.6	25.8	5.7
Southeast	137	434,091	19.6	29.8	3.0
Total	**980**	**3,859,469**	**151.9**	**26.2**	**5.4**

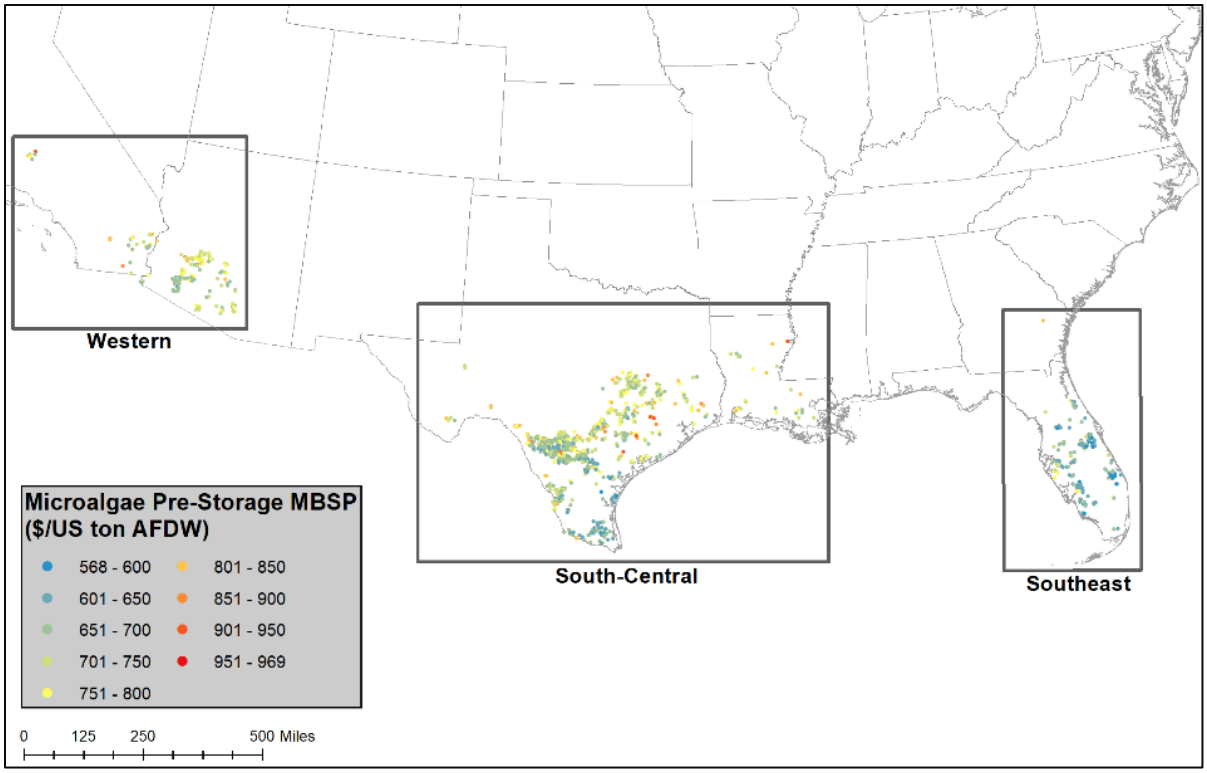

Figure 3.1.1. MBSP of individual sites *before* storage ($/U.S. dry ton AFDW, 2020 $). Rectangle areas represent the three regional categorizations.

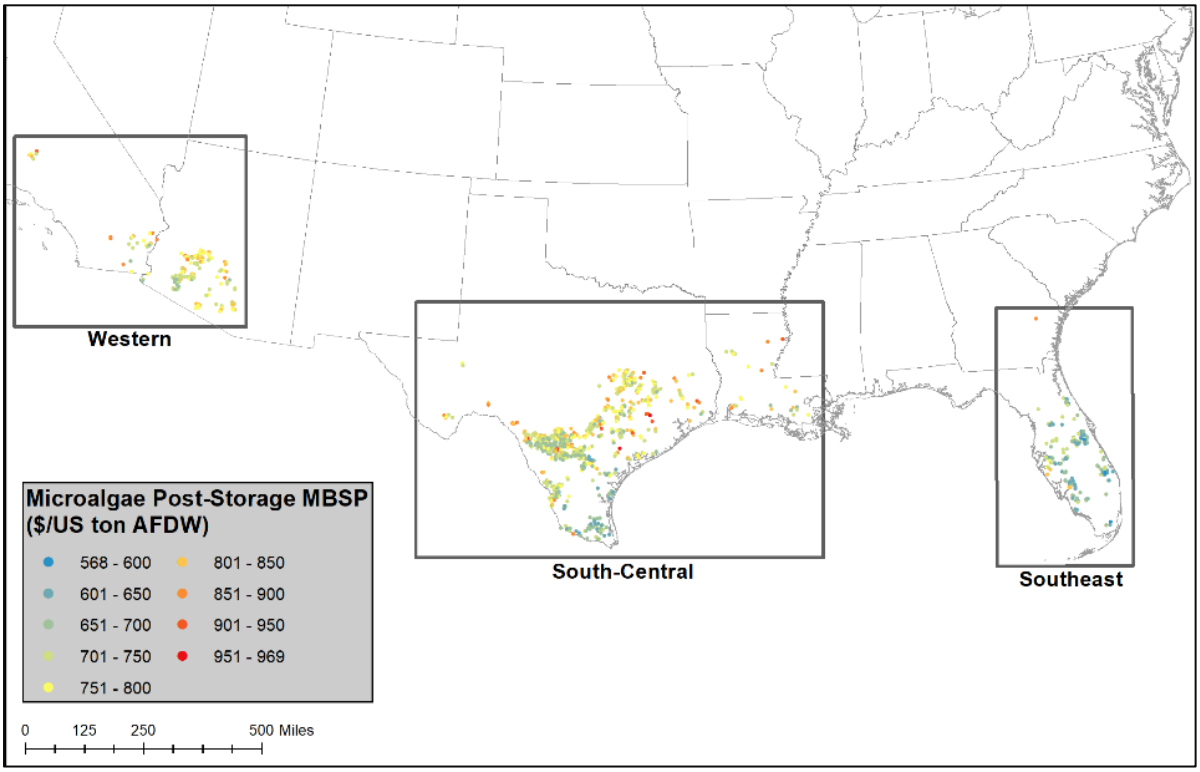

Figure 3.1.2. MBSP of individual sites *after* storage ($/U.S. dry ton AFDW, 2020 $). Rectangle areas represent the three regional categorizations.

Despite differences in the parameters that define algae cultivation (e.g., biomass productivity potential, salinity of the makeup water, salt disposal requirements, and delivered CO_2 costs between regions), the possibility of producing algal biomass at reasonable prices in all regions was demonstrated, at weighted average MBSPs of $674/ton AFDW and $701/ton AFDW (before and after seasonal storage, respectively) across the full site collection producing 152 MM tons AFDW algal biomass per year, as depicted in Figure 3.1.3. An alternative resource curve reflecting biomass dry weight and energy content metrics is presented in the Appendix (Figure S1). This scale translates to the ability to utilize roughly 270 million tons/yr of CO_2 captured from existing point sources across the United States. As noted above, the inclusion of seasonal storage aims to minimize the effect of seasonal production variability swings on the algae biomass conversion plant by storing excess peak seasonal biomass for use in lower-production seasons; thus, sites that exhibit higher seasonal variability swings during cultivation translate to incrementally higher MBSPs after storage (based on higher storage costs and degradation losses, though these effects are generally minimal). Figure 3.1.3 also details the cost breakdown for three representative cases of algae farms corresponding to low, medium, and high MBSPs along the full curve. Trends in overall MBSPs tend to follow an inverse correlation with cultivation productivities as expected (e.g., all bars in the breakdown plot of Figure 3.1.3 increase as productivity decreases due to lower biomass outputs), though with further factors such as salt management and farm size also weighing on individual farm costs as discussed below. An interesting finding from this work was that using an FO unit to process the blowdown stream incurs relatively low impacts on MBSP in the majority of sites, although FO and brine disposal costs increase considerably in sites with the highest blowdown requirements, driven by high makeup water salinity and/or evaporation rates. Coupled also with lower costs from the BAT model for injection disposal wells compared to previous algae farm TEA modeling assumptions (Klein and Davis 2022), the costs for salinity management in this work were generally seen to be lower than those in prior TEA modeling efforts, which utilized evaporation ponds followed by a fixed cost for injection disposal (a less granular approach based on sparse literature values), while also allowing for the recycling of a significant amount of freshwater to the algae farm.

Relative to the latest 2017 harmonization, which found the potential for producing roughly 100–200 million tons/yr of algal biomass at national scale based on freshwater or saline cultivation, respectively (Davis et al. 2018), the present harmonization update maintains a similar albeit slightly reduced biomass potential for saline-only cultivation at approximately 152 million tons/yr, now based on improved granularity for CO_2 availability and cost as well as blowdown water handling for high-saline-tolerant strains (55-ppt cultivation salinity threshold). The overall weighted average MBSP is also comparable to the prior saline case, with higher costs for often smaller-scale algae farms and higher nutrient demands for replete algae cultivation generally offset by reverting to minimally lined ponds as an n^{th}-plant assertion. Detailed breakdowns of the MBSPs and algae farm CAPEX for representative cases, alongside the main parameters used to define the cultivations, can be found in Tables S1–S8.

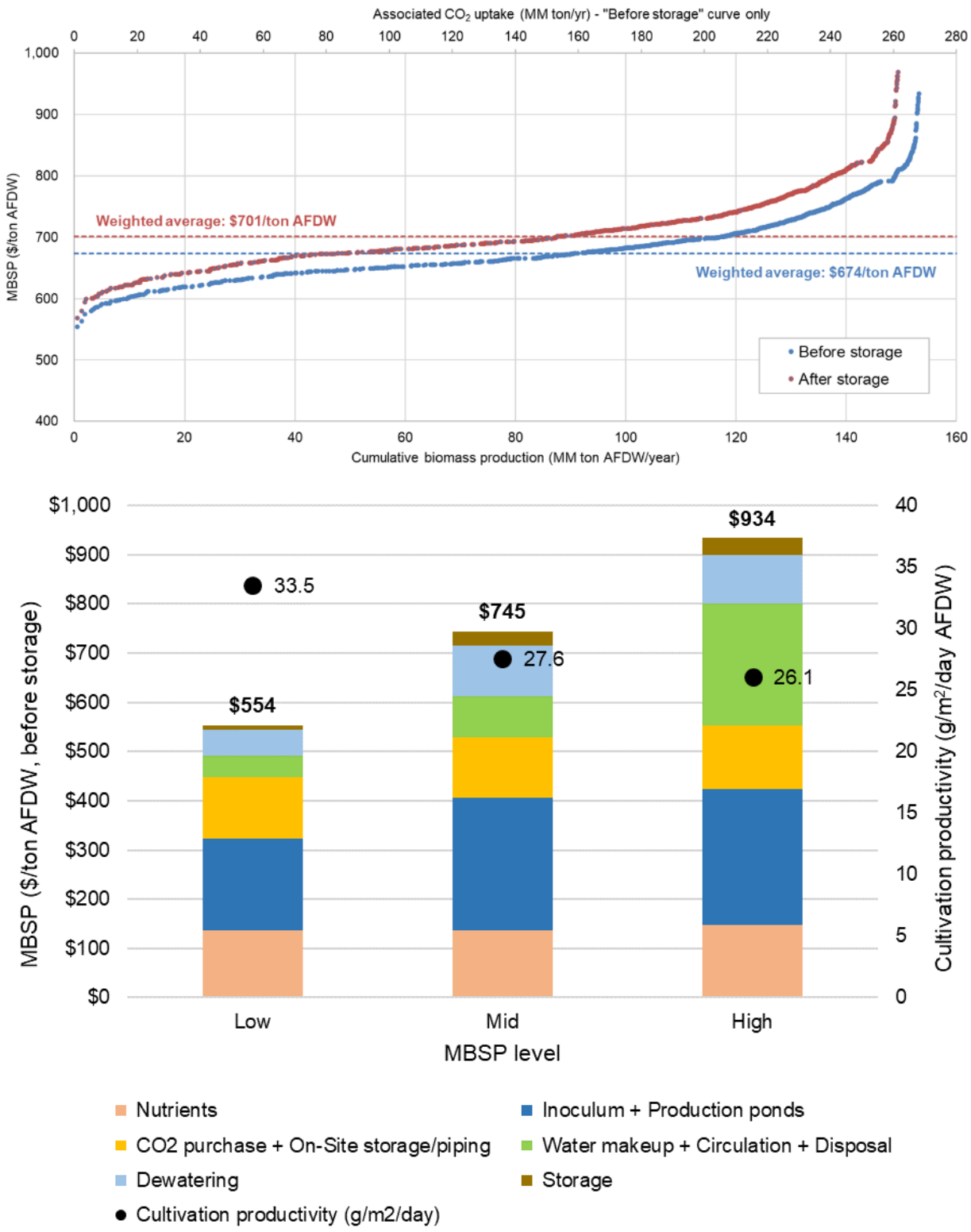

Figure 3.1.3. Cumulative national-scale biomass production potential and corresponding CO_2 uptake potential versus MBSP (top) and MBSP breakdowns for selected example farm sites (bottom)

Figure 3.1.4 provides additional insights on the drivers behind the MBSPs of the 980 individual sites. The majority of sites (i.e., 74% of the total) reflect MBSPs below $750/ton AFDW, while the remaining 26% fall between $750/ton and $940/ton. Consistent with prior findings (Davis et al. 2016, 2018), overall MBSPs tend to track closely with algae farm size and cultivation productivities (with an increase in either translating to lower MBSPs), reflected by the highest R^2 values in the correlation curves of Figure 3.1.4 for these two parameters typically following logarithmic correlations. Salt management also exhibits a notable driver in MBSPs, as evidenced by somewhat looser correlations for makeup water salinity and evaporation rate on a linear scale. Delivered CO_2 cost incurs a less significant influence on MBSP, though this is primarily dictated by limiting CO_2 availability to the $75/tonne ($83/ton) cutoff threshold applied here. Figure 3.1.4 also highlights more preferential cultivation parameters concentrated in the Southeast region (green markers), including higher productivity, larger farm sizes, and lower evaporation rates as a fraction of the total regional farm numbers, with the Western region (blue markers) generally exhibiting the inverse. This translates to a greater concentration of Southeastern sites falling toward the lower portion of the overall MBSP curve (Figure 3.1.4 A) and more Western sites somewhat more concentrated toward the higher portion of the curve, with the South-Central sites spanning the entire curve, as this region represents the majority of the full site collection.

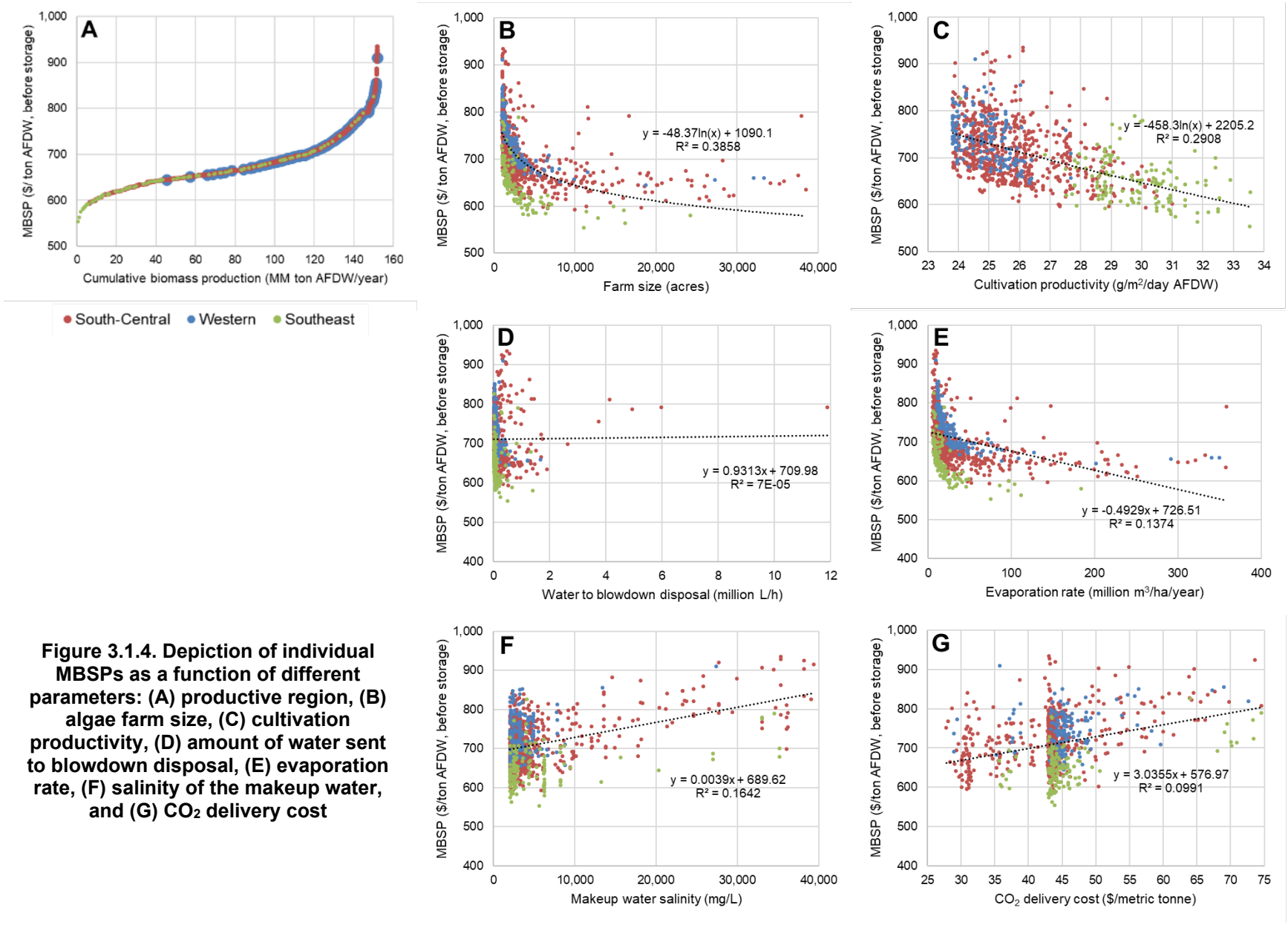

Figure 3.1.4. Depiction of individual MBSPs as a function of different parameters: (A) productive region, (B) algae farm size, (C) cultivation productivity, (D) amount of water sent to blowdown disposal, (E) evaporation rate, (F) salinity of the makeup water, and (G) CO_2 delivery cost

Figure 3.1.5 displays GHG emissions, fossil fuel energy, and freshwater consumption per ton biomass (AFDW) spanning CO_2 capture and transport through algae growth, prior to nutrient or CO_2 recycle, alongside corresponding MBSPs for each individual farm site. On the left-hand side, the results are sorted by increasing GHG emissions, while on the right-hand side, the results are arranged by MBSP. From Figure 3.1.5, GHG emissions per ton AFDW range from 942 kg to 1,718 kg; fossil energy consumption varies between 14,192 MJ and 23,789 MJ; and freshwater consumption spans from 4,435 to 7,695 liters per ton AFDW. The variations can be attributed to the diverse energy requirements for carbon capture and transport, as well as the varying nutrients and CO_2 consumption specific to each location. Beyond environmental impact variations across the locations, Figure 3.1.5 also illustrates that GHG emissions and MBSPs are not strongly correlated. For example, one of the stronger drivers in MBSP is farm size, which has no impact on GHGs, while energy demands for CO_2 sourcing exhibit much stronger influences on GHGs than they do on MBSPs.

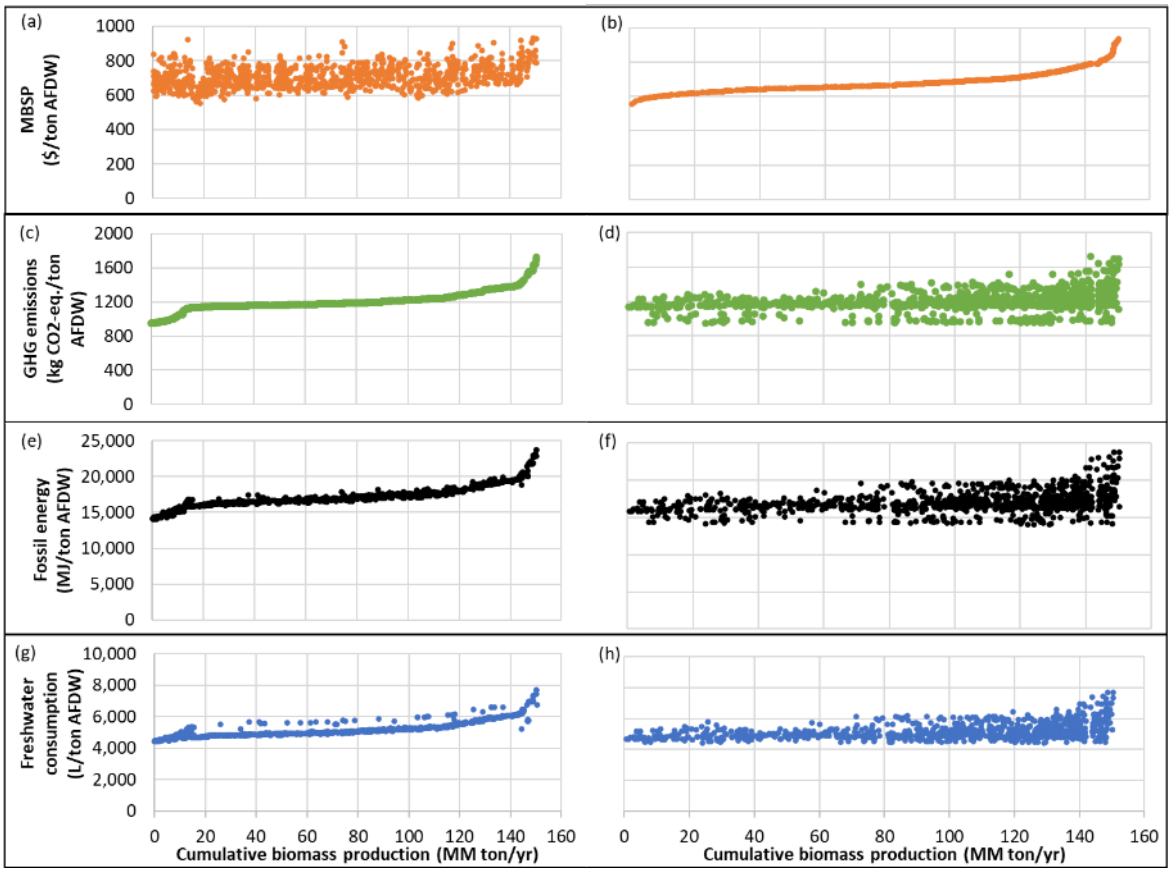

Figure 3.1.5. Cumulative algae biomass production and corresponding (a) MBSP, (c) GHG emissions, (e) fossil energy consumption, and (g) freshwater consumption sorted by GHG emissions; cumulative algae biomass production and corresponding (b) MBSP, (d) GHG emissions, (f) fossil fuel consumption, and (h) freshwater consumption sorted by MBSP, for algae farm biomass cultivation including CO_2 capture and transport, prior to nutrients and CO_2 recycling from downstream conversion.

Based on the curves above, the minimum, maximum, and weighted average GHG emissions, fossil energy usage, and freshwater consumption for algae cultivation are compared to those associated with soybean cultivation as shown in Table 3.1.2. The comparison reveals that

soybean production generates lower GHG emissions and requires less fossil energy per ton AFDW biomass. This disparity can be attributed to the increased energy consumption involved in sourcing CO_2 and facilitating algae cultivation and growth. However, freshwater consumption is considerably more favorable for saline algae cultivation, with all freshwater demands attributed to secondary effects associated with CO_2, nutrient, and energy sourcing (there is no direct freshwater consumption required in the algae farm itself). We also acknowledge that the environmental impacts arising from DLUC and indirect land use change (ILUC) may potentially increase the environmental footprint of soy PC, particularly when considering incremental future production, though these considerations are beyond the scope of this study.

Table 3.1.2. GHG Emissions, Fossil Energy Consumption, and Freshwater Consumption Comparison Between Algae and Soybean Production per Ton AFDW

	Saline Algae Growth (per ton AFDW)			Soybean Production (per ton AFDW)
	Min	Max	Weighted Average	
GHG emissions (kg/ton)	942	1,719	1,202	329
Fossil energy (MJ/ton)	14,063	23,789	17,247	1,568
Freshwater consumption (L/ton)	4,435	7,695	5,219	81,425

After subsequently accounting for recycling nutrients and CO_2 from downstream conversion, the LCA metrics presented above can result in improved environmental performance depending on the conversion scenario, as presented in Figure 3.1.6. Conversion operations can recycle more nutrients and CO_2 when producing only fuel, resulting in additional net cultivation demands for nutrients and CO_2 in scenarios including production of PC coproduct.

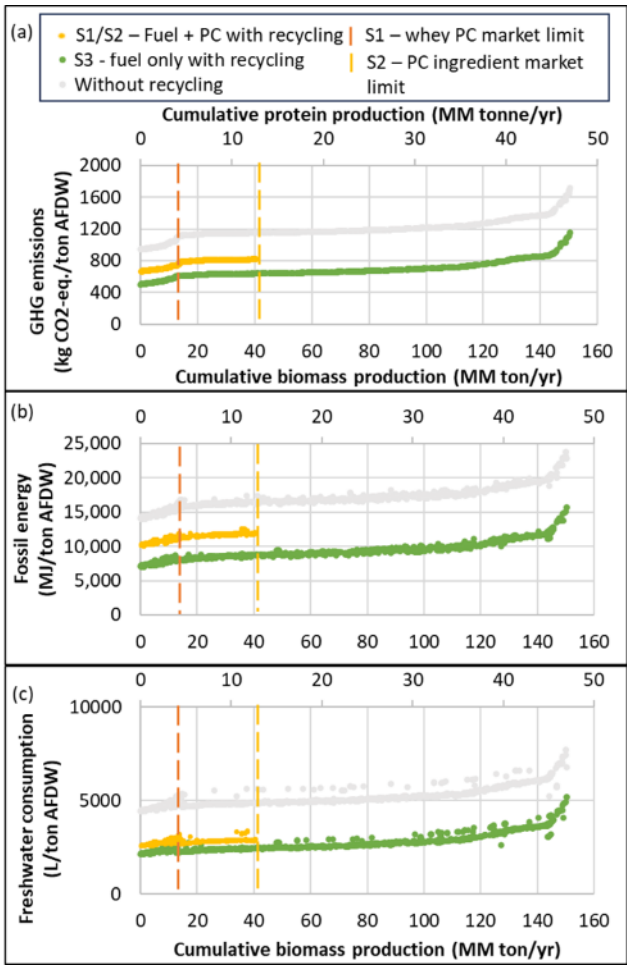

Figure 3.1.6. Environmental impacts: (a) GHG emissions (kg CO_2e/ton AFDW); (b) fossil fuel (MJ/ton AFDW); and (c) freshwater consumption (L/ton AFDW) comparison for algal biomass production (including CO_2 capture and transport) without (gray curve) and with (yellow/green curves) recycling of nutrients and CO_2 from downstream conversion, sorted by GHG emissions.

Green curve reflects fuel-only production (Scenario 3), while yellow curve reflects inclusion of algal PC coproduction up to market limits for whey PC replacement (Scenario 1; orange dashed line) or soy PC replacement representing the global protein ingredients market (Scenario 2; yellow dashed line).

LCA Considerations for CO_2 Sourcing

Results for the two allocation strategies considered are shown in Figure 3.1.7. In the cutoff approach, the CO_2 capture benefit is assigned to the biofuels with no distinction between the various capture configurations. The net emissions for high-purity sources (ethanol fermentation, renewable natural gas processing, and hydrogen/ammonia production) vary between 32 and 41 g CO_2e/MJ. These are slightly higher (by about 5 g CO_2e/MJ) compared to the results in Cai et al. (2021) and the supply chain sustainability analysis carried out by Argonne National Laboratory because of somewhat higher CO_2 capture energy, and also assuming compression of CO_2 to pipeline pressure across all cases employed in the present study. That said, high-purity sources are limited in volume. For instance, even an optimistic market for using CO_2 from ethanol fermentation could lead to an upper bound of 44 million tons AFDW algal biomass and 135,000 GGE biofuel. The net emissions when CO_2 is sourced from natural gas combined-cycle power plants is 41 g CO_2e/MJ, and for pulverized coal power plants is 39 g CO_2e/MJ of algae biofuel.

While DAC estimates are shown here as a stand-alone case in view of promising future potential for comparison purposes, DAC is otherwise outside the scope of this report and is not incorporated in any of the harmonization resource model outputs.

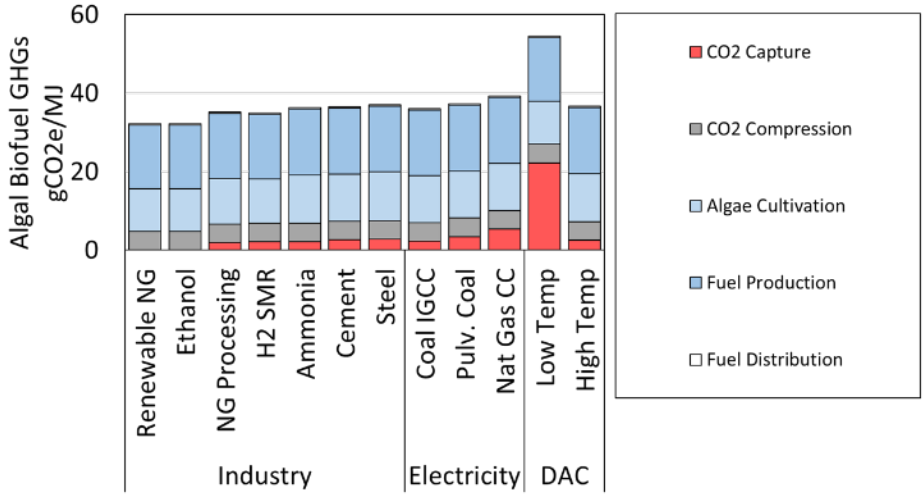

Figure 3.1.7. Impact of CO_2 sourcing on GHG emissions of algae biofuels using the cutoff or incremental approach. This figure represents a generic HTL example for fuel-only production based on Singh, Banerjee, and Hawkins (2023); site-specific results are shown in subsequent figures.

3.2 Algal Biofuel and Protein Concentrate

After incorporating outputs from the TEA farm models based on each individual site, the final product yields and MFSPs through HTL conversion for each site are estimated. Two conversion pathways, algae conversion to fuel and protein and conversion to fuel only, are first evaluated for each site independent of market limitations for the protein coproduct case. For each pathway, all sites were sorted from the lowest to highest MFSP values. The detailed process cost contributions for selected cases corresponding to the lowest, middle, and highest MFSPs for the two conversion pathways are depicted in Figure 3.2.1 (algal fuel and PC coproduction) and Figure 3.2.2 (algal fuel production only). The MFSPs for each site are greatly affected by the algae biomass feed flowrate cost (MBSP) from the upstream farm models, both tied to cultivation productivity. Lower biomass costs and higher algae feed flowrates lead to lower MFSPs. For the pathway with fuel and protein coproduction, the MFSPs for all sites range from \$0.28 to \$12.0/GGE, and the feedstock cost represents about 70% of the total production cost (excluding coproduct and nutrients credits). For the pathway with fuel only, the MFSPs for all sites range from \$6.72 to \$13.1/GGE, and the feedstock cost contributes 75%–80% of the total production cost. For the pathway with fuel and protein production, the protein extraction step contributes the largest fraction, 50%–60% (\$2.9–\$4.4/GGE), of the total conversion cost contributions to MFSP (excluding feedstock cost and credits). The high credits from protein coproduction outweigh the impacts of extra protein extraction costs and lower fuel yields, and thus lead to lower overall MFSPs than fuel production only. However, for the highest MFSPs of two pathways, the cost advantage of the fuel and protein pathway is limited. As algal feedstock MBSP increases and feed rate decreases (corresponding to lower cultivation productivity in the farm model), feedstock cost contributions to MFSP increasingly outweigh the protein coproduct

credits on a dollar-per-GGE basis, as the latter remains unchanged over the full range of sites, translating to nearly the same MFSP in the most extreme case reflected in Figures 3.2.1–3.2.2. Further cost and yield details for selected cases are provided in the Appendix (Tables S9–S12).

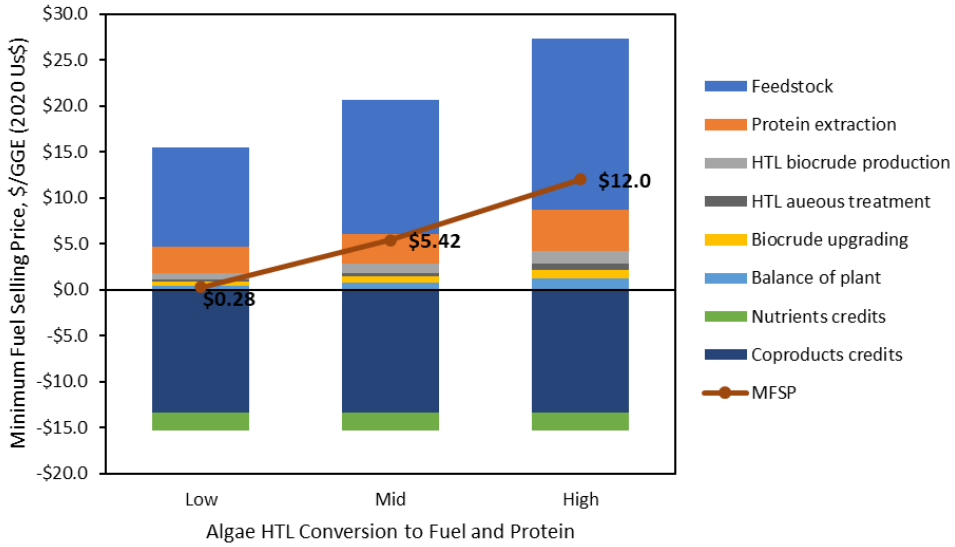

Figure 3.2.1. Process contributions to MFSP for algae HTL conversion to fuel and protein for the lowest, middle, and highest MFSP cases (excluding protein market volume limitations)

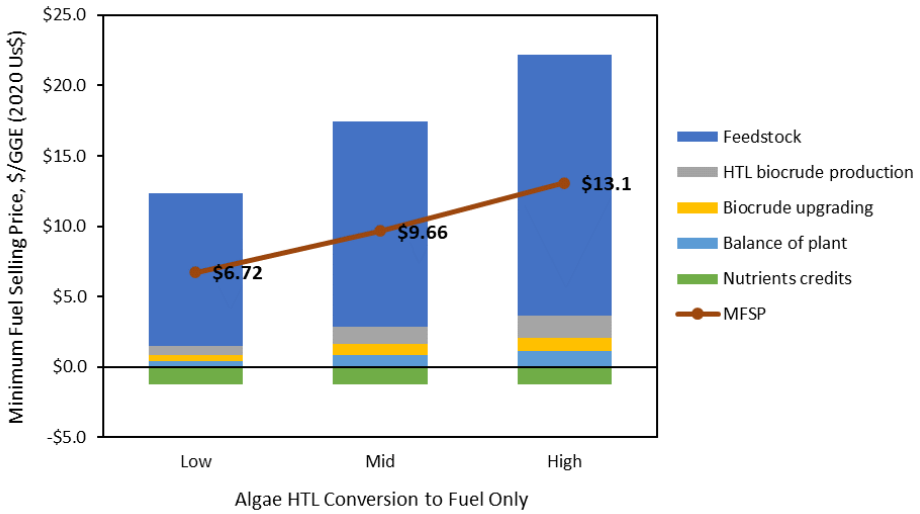

Figure 3.2.2. Process contributions to MFSP for algae HTL conversion to fuels only for the lowest, middle, and highest MFSP cases

The major TEA results for the three market volume scenarios described in Section 2.3, including MFSPs for each site, weighted average MFSP, and cumulative fuel and protein production rates, are depicted in Figures 3.2.3–3.2.5. The MFSP for each site is arranged in ascending order in the figures. The production rates for fuel and protein coproduct of each site are added to those of previous sites with lower MFSPs and then form the curves for cumulative fuel and coproduct outputs. The weighted average MFSP is calculated based on the MFSP and corresponding fuel production rate of each site and then averaged on the total fuel production rate of all sites.

Scenario 1 for fuel and protein coproduction with the whey protein market constraint has a cumulative weighted average MFSP of $8.49/GGE, with cumulative fuel and SAF production rates of 13.9 and 8.3 billion GGE/yr, respectively. When the cumulative protein production reaches the global whey protein market size, the MFSP reaches $1.28/GGE lower than the $2.5/GGE BETO goal of biofuels. The total algae PC production potential from all sites is estimated at 51 million tons/yr, and the whey protein market size is 7.4% of the total protein production potential. Therefore, with the whey protein market size constraint, about 7.4% of the total national algae production capacity can be used for generating market-competitive fuels with high-value protein coproduced. When configured to stop producing the protein coproduct upon reaching global market limits for whey PC, algae from the remaining sites reverted to fuel production only, and the MFSP jumped from $1.28/GGE (fuel plus protein) to $7.28/GGE (fuel only) and continued increasing to $13.1/GGE (max, fuel only) resulting from no protein credits.

Alternatively, Scenario 2 with the total protein ingredients market size constraint reflects cumulative fuel and SAF production rates of 12.6 and 7.5 billion GGE/yr, respectively, translating to a weighted average MFSP of $7.89/GGE (roughly $0.60/GGE lower than Scenario 1). When the cumulative protein production reaches the global protein ingredients market size, the MFSP reaches $2.17/GGE, still lower than BETO's historical $2.5/GGE goal. The protein ingredients market size is 26.9% of the total protein production potential of all sites. Thus, about 26.9% of the total algae production capacity could be used to generate cost-competitive fuels. When the cumulative algae PC output reached global market limits for protein ingredients, algae from the remaining sites reverted to fuel production only, and the MFSP jumped from $2.17/GGE (fuel and protein) to $7.79/GGE (fuel only) and continued increasing to $13.1/GGE (max, fuel only) resulting from no protein credits. Finally, Scenario 3 for fuel production only achieves cumulative fuel and SAF production rates of 14.4 and 8.6 billion GGE/yr, respectively, with a weighted average MFSP higher than the other two scenarios at $8.69/GGE (about $0.80/GGE higher than Scenario 2) given the lack of protein production cost and credits.

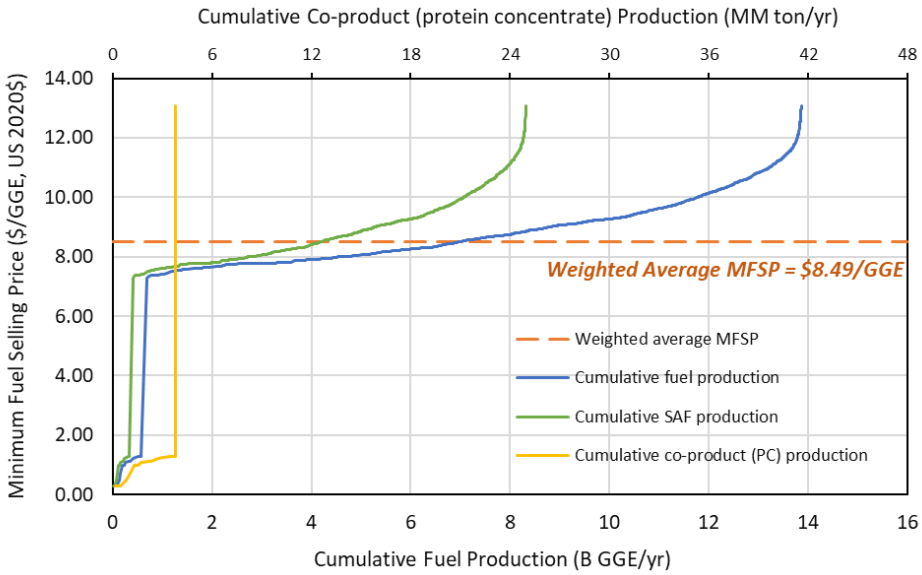

Figure 3.2.3. Algae HTL conversion cumulative fuel and protein coproduction outputs and corresponding MFSP (Scenario 1: global whey protein market size limit)

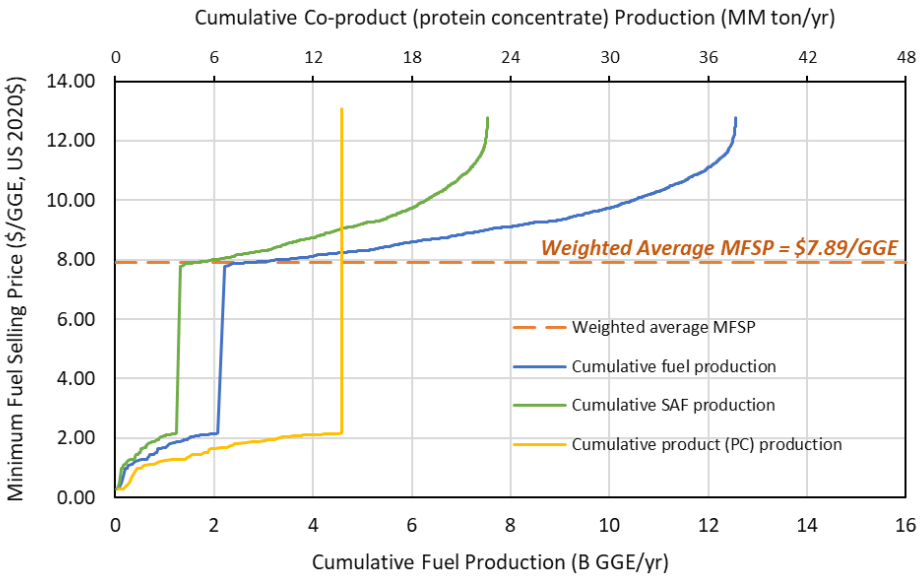

Figure 3.2.4. Algae HTL conversion cumulative fuel and protein coproduction outputs and corresponding MFSP (Scenario 2: global protein ingredients market size limit)

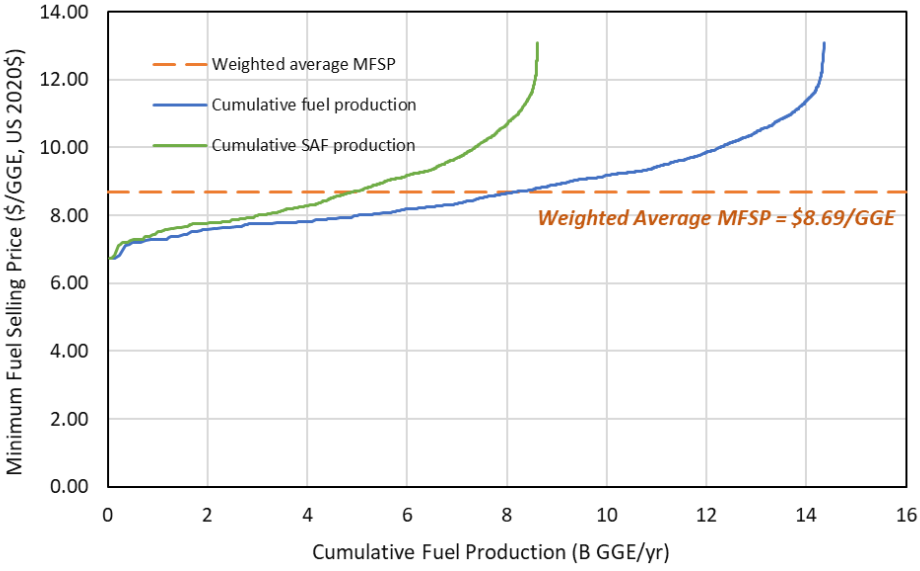

Figure 3.2.5. Algae HTL conversion cumulative fuel production outputs and corresponding MFSP (Scenario 3: fuel production only)

A summary of the three scenarios, as well as an alternative "optimal" case showing total fuel and protein coproduction rates and corresponding weighted average MFSPs, is depicted in Figure 3.2.6. The optimal case assumes the algae from all site groups may be used to produce both fuel and protein products without being subject to protein market limitations (i.e., assuming the protein market size is larger than the total algae PC production rate from the full collection of sites). The production rate of the algae PC coproduct is subject to the underlying protein market size constraint for the various scenarios, and it has significant impacts on the achievable MFSP.

When the assumed market size for the algae PC coproduct is not a limitation, algae from all site groups may be used to generate protein coproduct, which enables maintaining the high coproduct credit across the full collection of sites and a significantly lower MFSP of $3.72/GGE.

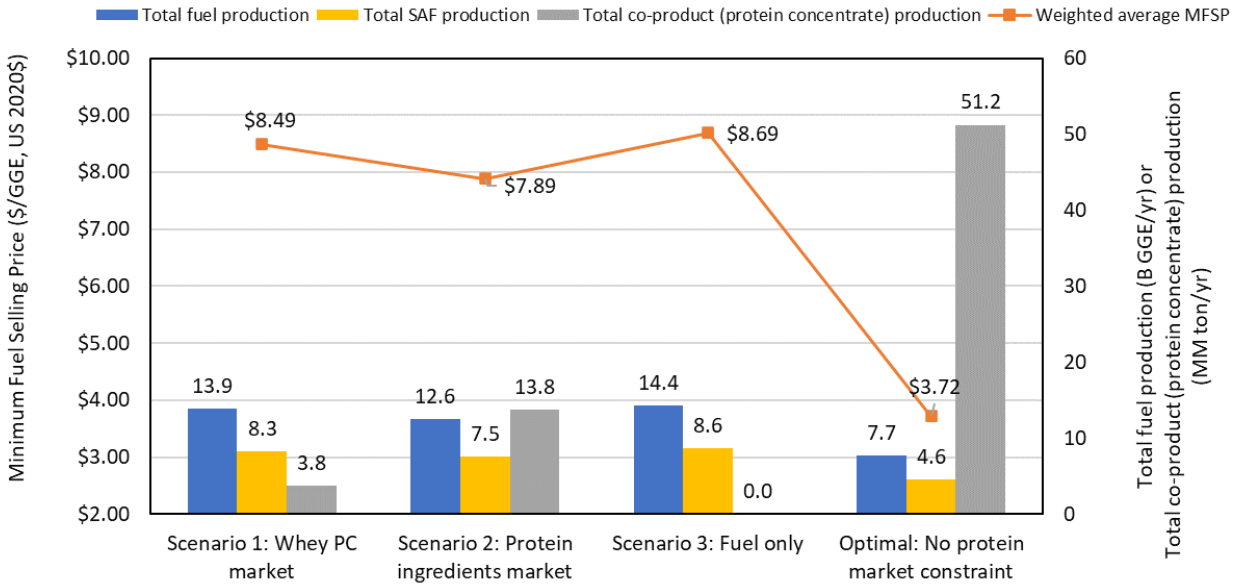

Figure 3.2.6. Algae HTL conversion—total fuel and protein coproduction outputs across the full site collection and corresponding weighted average MFSPs for the three case scenarios and an optimal case (no protein market volume constraints)

For LCA modeling, four coproduct calculation methods—mass allocation, economic value allocation, system expansion (displacement), and biorefinery-level analysis—have been considered in this study. As mentioned in the "Coproduct Handling in TEA and LCA Models" section, mass and economic value allocations are both "process-level"-based allocations. More specifically, processes exclusively associated with fuel production or PC production are allocated solely to fuel or PC, respectively. For processes used for both fuel and PC, they are assigned sub-allocation factors based on feedstock mass and economic values of the product, respectively. For the system expansion (displacement) method, it is assumed that the bio-coproduct microalgae PC can be used to replace whey PC, soy PC, or animal feed supplement, such as soybean meal or alfalfa meal. As a base case, a mass allocation method is selected to illustrate the environmental performance over the full collection of sites, either with or without inclusion of algae PC coproduction (excluding protein market volume constraints), depicted in Figure 3.2.7. In order to enhance comprehension of the environmental impact variances resulting from different coproduct calculation methods, Figure 3.2.8 presents the environmental results derived from allocation and system expansion (displacement) methods, while Figure 3.2.9 shows the results based on biorefinery-level analysis.

As depicted in Figure 3.2.7, the inclusion of microalgae PC coproduction exhibits slightly better performance in terms of GHG emissions when compared to fuel-only production. Specifically, GHG emissions from the scenario involving both microalgae PC and fuel production without market limitations range from 48 g/MJ to 90 g/MJ with the mass allocation method, whereas emissions from the fuel-only scenario range from 69 g/MJ to 118 g/MJ (Figure 3.2.7 (a) and (d)).

In other words, the credits gained from PC coproduction outweigh the additional energy and materials required for protein extraction and processing to PC coproduct, in terms of GHG emissions, when employing the mass allocation method. However, in the scenario that produces both fuel and PC without market limits, fossil energy consumption is comparable, but freshwater consumption is higher compared to the scenario that only produces fuel. The increase in freshwater consumption is primarily attributed to the water footprint embodied in increased net urea and DAP usage during algae growth, given lower nutrient recycle rates to cultivation when algae PC coproduction is included, as discussed previously (Figure 3.2.7 (c) and (f)). Namely, to produce 1 kg of urea and DAP, about 4.8 L and 37.0 L of freshwater are consumed, respectively.

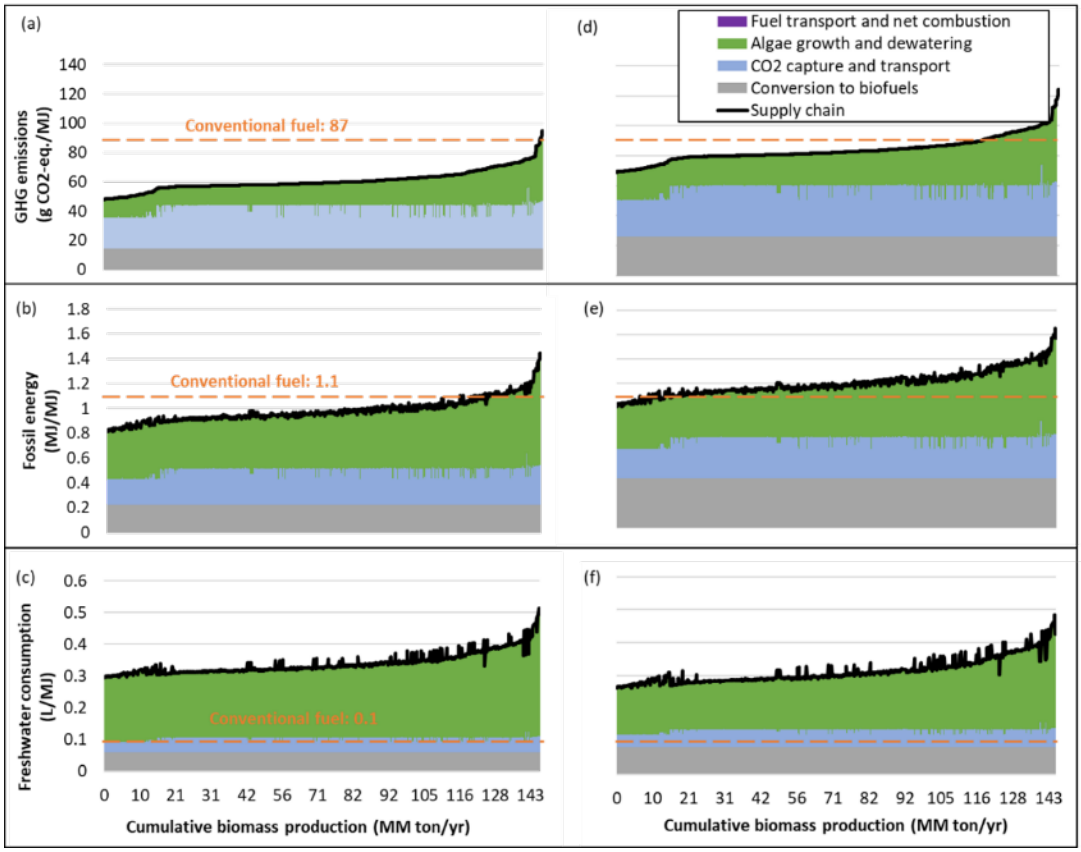

Figure 3.2.7. Life cycle (a) GHG emissions, (b) fossil energy use, and (c) freshwater consumption across all sites for the HTL pathway with both fuel and PC production by using mass allocation (no protein market constraints); compared to (d) GHG emissions, (e) fossil energy use, and (f) freshwater consumption for the HTL pathway with only fuel production.

In Figure 3.2.8, we compare three coproduct handling methods, using the site with median GHG emissions as an illustrative example. The system expansion (displacement) method demonstrates a scenario assuming soy PC is displaced in light of the considerations for whey PC being less likely to cease being produced given that whey PC itself is a byproduct (as discussed previously); further details on credits related to whey PC, soy PC, and animal feed can be found in Tables S29, S33, and S34 in the Appendix. From Figure 3.2.8, mass versus economic allocation methods produce similar trends, resulting in improved GHG emissions and fossil energy performance but higher water consumption when compared to petroleum diesel. The most favorable results are achieved with economic value allocation based on whey PC, followed

by mass allocation and then economic allocation based on soy PC. However, the displacement method based on soy PC displacement leads to higher GHG emissions and fossil fuel usage but significantly lower freshwater consumption compared to petroleum diesel. The results from the displacement method can be explained by water-intensive soybean farming but more GHG- and fossil-energy-efficient production of soy PC when compared with saline algae PC, as shown in Table 3.1.2.

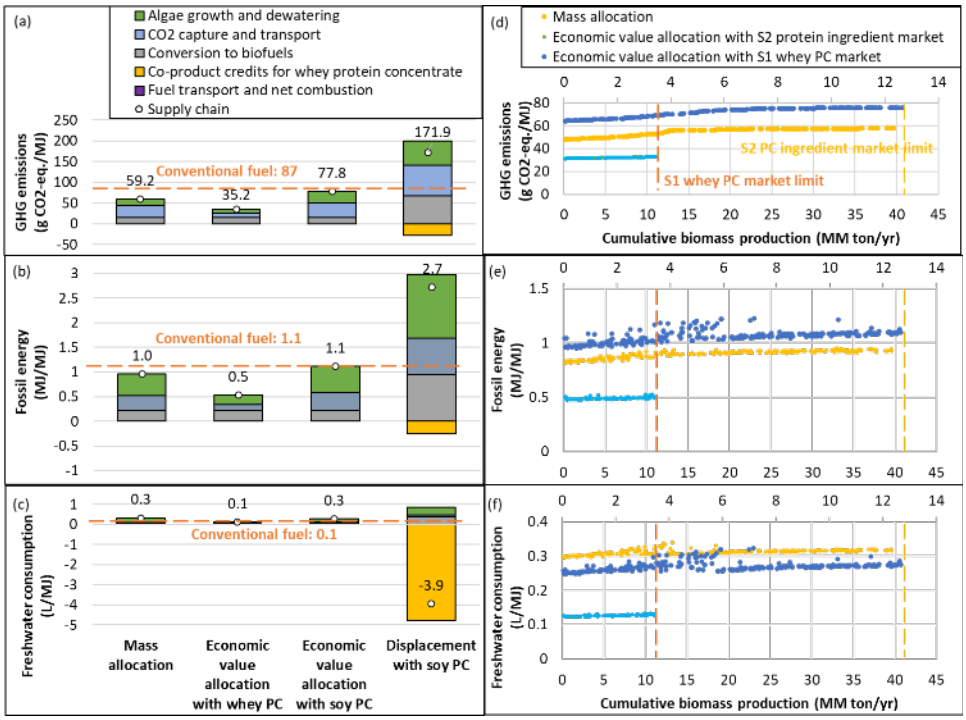

Figure 3.2.8. LCA results for (a) GHG emissions, (b) fossil energy use, and (c) freshwater consumption by using different coproduct handling methods for a single example site with median GHG emissions; LCA results over the full site collection for (d) GHG emissions, (e) fossil energy use, and (f) freshwater consumption reflecting algae PC coproduction constrained by whey PC market limits (orange dashed lines) or soy PC market limits representing the protein ingredients market (yellow dashed lines) with mass and economic value allocation methods.

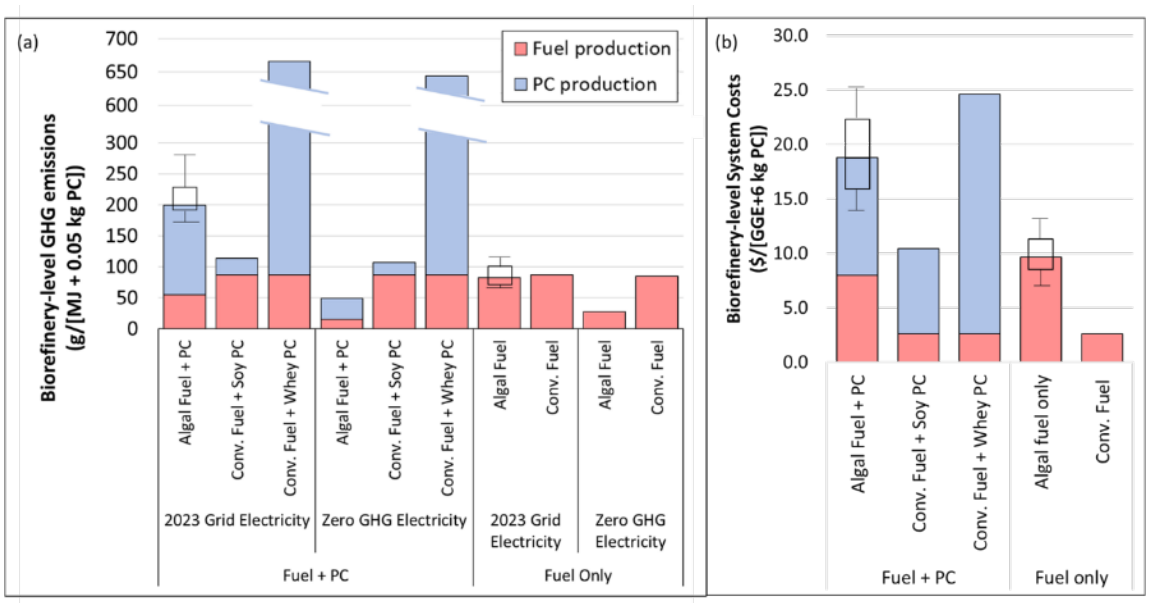

Figure. 3.2.9. Biorefinery-level comparison of (a) GHG emissions and (b) production costs between microalgal fuel plus PC coproduction versus conventional fuel and PC production and algal fuel-only production versus conventional fuel production with 2023 grid electricity and zero-GHG electricity (the box and whisker plots display the minimum, 10th percentile, 90th percentile, and maximum values).

Note: Conventional fuel cost is based on its wholesale price, while soy PC and whey PC costs are based on their projected market price.

The biorefinery-level analysis aims to quantify the total life cycle GHG emissions from all products and their potential GHG emission reductions when displacing conventionally made counterpart products. As shown in Figure 3.2.9 (a), the algal biorefinery results in lower GHG emissions compared to conventional fuel and whey PC production (−467 g CO_2e per MJ of fuel and 0.05 kg of PC production), but higher GHG emissions compared to conventional fuel and soy PC production (+85 g CO_2e per MJ of fuel and 0.05 kg of PC production). These differences are primarily due to more GHG-intensive operations for conventional whey PC than conventional soy PC production. However, these results could be significantly improved by replacing U.S. grid electricity with renewable energy that has zero carbon intensity produced on-site for the algal facility and upstream productions, which would reduce GHG emissions by 50% when compared to conventional fuel and soy PC production with zero-GHG electricity. However, it is worth noting that in real-world conditions, solar and wind energy may require energy storage systems, which can result in carbon intensity higher than zero. Although natural gas used in the HTL pathway could also be replaced with renewable natural gas, specific results are not provided here due to potential variations in GHG emissions based on different feedstocks and locations. Nevertheless, if the carbon intensity from natural gas consumption can be reduced to zero, GHG emissions from the algal biorefinery using zero-carbon-intensity electricity could further decrease by 50%. This highlights the significant role played by the carbon intensity of energy sources in the decarbonization of algal biorefineries. Figure 3.2.9 (a) also compares GHG emissions at the biorefinery level between algal fuel and conventional fuel. It reveals a slight decrease in emissions for algal fuel compared to conventional fuel (−4.6 g CO_2e/MJ). However, by replacing U.S. grid electricity with zero-carbon-intensity electricity for both algal and conventional fuel production, a GHG emissions reduction of 68% can be achieved when

comparing algal fuel to conventional fuel. From another perspective, it is noticeable that the electricity consumption for algal fuel is significantly lower than that for e-fuel. Specifically, 0.07–0.2 kWh of electricity is used per megajoule of algal fuel, and 0.7–2.2 kWh of electricity is used per megajoule of e-fuel (Li et al. 2023).

The biorefinery-level system costs are also analyzed here to illustrate the overall biorefinery-level costs and potential reductions. As shown in Figure 3.2.9 (b), an algal biorefinery with both fuel and PC production exhibits a higher algal biorefinery production cost compared to the wholesale price of conventional fuel (taking 5-year average wholesale prices for petroleum diesel, jet fuel, and naphtha as a reference: $2.6/GGE) and market price of soy PC, but a lower biorefinery production cost compared to the wholesale price of conventional fuel and market price of whey PC. In addition, if only producing fuel, the biorefinery algal fuel is more expensive than conventional fuel, even with minimum value. It is worth noting that the comparison relies on the wholesale price of conventional fuel and the market price of whey PC and soy PC, rather than the system costs. This is due to the limited data available on the production costs of whey PC and soy PC. Nevertheless, it is a common understanding that market prices or wholesale prices should exceed production costs, but the comparison results should remain unchanged because the additional costs associated with market prices or wholesale prices are unlikely to significantly affect the results. Based on the biorefinery-level analysis approach, algal PC does not enable an improvement in GHG emissions and production costs when compared with average soybean PC, although it does demonstrate a significant improvement when compared to whey PC. However, as discussed previously, it is important to reiterate that the current whey PC market is quite limited, and as whey is a byproduct of cheese production, its production would not necessarily be hindered by replacement with algal PC. Nevertheless, if electricity and natural gas can be replaced with more sustainable energy sources such as solar, wind, and renewable natural gas, the GHG emissions from the algal biorefinery could be significantly reduced, potentially resulting in lower GHG emissions than those associated with conventional fuel and soy PC production.

4 Conclusions and Key Findings

This work reiterates the potential for substantial contributions to national-scale biomass volumes that can be produced from microalgae, enabled by CO_2 capture from currently existing point sources, unencumbered land that does not compete with food, and saline groundwater. Based on more refined details in locating and procuring such resources relative to prior studies, this harmonization analysis identified roughly 150 million tons per year AFDW of algal biomass production potential capturing 268 million tons of CO_2 from 3.9 million acres of open ponds across the CONUS at an average production cost (MBSP) of $674/ton based on future productivity performance goals. MBSPs for individual farm sites varied between $554 and $934 per ton as a function of farm size, cultivation productivity, degree of variability in seasonal productivity swings, delivered CO_2 cost, and saline water handling expenses. The addition of long-term seasonal storage to equalize monthly biomass flows to downstream conversion added roughly $30/ton to these figures. Without conflicting against prior harmonizations focused on high-lipid biomass cultivation in large farms, the results presented here for biomass production translate to higher fuel costs, lower fuel yields, and higher GHG emissions based on high-protein algae cultivation using generally smaller farms (3,900 acres on average), but accordingly may be viewed as a more near-term scenario for algae. The associated GHG emissions for biomass production vary between 942 and 1,718 kg CO_2e per ton AFDW biomass, with an average over the full collection of sites at 1,198 kg CO_2e/ton. Similar to cost results, GHG emissions vary by site, driven by biomass yields (productivity), makeup/blowdown water handling energy demands, nutrient consumption, and CO_2 capture energy for delivery to the farm specific to typical CO_2 concentrations in the flue gas from each point source industry.

Moving to downstream conversion, the TEA of algae HTL with protein extraction pretreatment demonstrated encouraging potential for SAF and concentrated protein production from algae conversion. Based on different protein market size constraints, up to 7.4% (whey protein market) or 26.8% (protein ingredients market) of the total national algae production capacity could be used to generate cost-competitive (<$2.5/GGE) fuels driven by high credits from protein coproduction. The lowest weighted average MFSP for the full national-scale collection of sites was estimated to be $7.89/GGE when producing protein up to the protein ingredients market size limit, and the highest MFSP was $8.69/GGE for fuel production only. The scenario taking algae to fuel only could enable a maximum total fuel production potential of 14.4 billion GGE/yr, which includes a SAF production rate of 8.6 billion GGE/yr, for the full collection of sites. Under the most optimal scenario, a maximum PC production potential of 51 million tons/yr could be reached nationally from all sites without protein market size constraints, which would bring average MFSPs down to $3.72/GGE, albeit with lower total fuel production potential of 7.7 billion GGE/yr. Considering the large protein market needs for food/feed applications and the potential for large-scale microalgae production reported here, the market for algae protein products as an alternative to other food-based proteins has potential to grow and become more competitive in the future.

In this study, mass allocation was used as the primary method to compare life cycle environmental impacts. GHG emissions from fuel and PC coproduction, without market limits, range from 48 to 90 g CO_2e/MJ, with a weighted average of 61 g/MJ. In contrast, GHG emissions from fuel-only production range from 69 to 118 g/MJ, with a weighted average of 85 g/MJ, compared to conventional fuels at 87 g/MJ. These results indicate that the GHG emissions

allocated to algal PC production outweigh the effects of increased emissions from PC production and the greater nutrient requirements in algae cultivation given lower nutrient recycle with PC coproduction. Alternatively, taking a biorefinery-level analysis approach in LCA, an algal biorefinery with PC coproduction does not achieve an improvement in GHG emissions when compared to conventional fuel and soy PC production in light of conventional soy production being less GHG-intensive (though considerably more water-intensive than saline algae cultivation). However, it does demonstrate a significant improvement when compared to conventional fuel and whey PC production, with a caveat that the current market for whey PC is small, and being a byproduct of the cheese industry, its production would not be hindered by replacement with algal protein. Electricity and natural gas consumption across the integrated facility represent the primary contributors to GHG emissions. By using renewable electricity and natural gas with zero carbon intensity, biorefinery-level GHG emissions could be reduced by roughly 77%, resulting in lower GHG emissions than even conventional fuel and soy PC production. Alternatively, an algal biorefinery with only fuel production achieves moderate reductions in GHG emissions when compared to conventional fuel benchmarks, though again through the implementation of zero carbon intensity electricity and natural gas, biorefinery-level GHG emissions for the fuel only scenario could similarly be reduced by roughly 70%.

In addition to replacing conventional electricity and natural gas with renewable energy, future analysis efforts can benefit by exploring passive CO_2 sourcing, namely DAC and biogenic CO_2 sources. These are particularly important for a low-carbon algal fuel production system under future industrial decarbonization advancements that may result in fewer fossil point sources for CO_2 capture. Additionally, optimizing nutrient recycling from conversion to cultivation is essential. Finally, exploring other coproduct options could lead to improved GHG emissions and cost metrics beyond the scope of this analysis around protein for food/feed applications, such as production of bioplastics from algal proteins (or other food scenarios such as meat alternatives). Beyond these considerations, moving away from high-protein cultivation in favor of high-lipid algal compositional targets can significantly improve both costs and GHG emissions for algal biorefinery systems by way of higher fuel yields and alternate coproduct opportunities, though recognizing that may represent a longer-term scenario to maintain comparable cultivation productivity performance.

References

Aguirre-Villegas, H., et al. 2012. "Life cycle impact assessment and allocation methods development for cheese and whey processing." *Transactions of the ASABE* 55 (2): 613–627.

Al-Malah, K.I. 2016. "Aspen Process Economic Analyzer (APEA)." In *Aspen Plus*®. Edited by K.I. Al-Malah. Hoboken, NJ: Wiley, 523–564.

Bacenetti, J., L. Bava, A. Schievano, and M. Zucali. 2018. "Whey protein concentrate (WPC) production: Environmental impact assessment." *Journal of Food Engineering* 224: 139–147.

Baker, S.E., J.K. Stolaroff, G. Peridas, S.H. Pang, H.M. Goldstein, F.R. Lucci, W. Li, E.W. Slessarev, J. Pett-Ridge, F.J. Ryerson, and J.L. Wagoner. 2020. *Getting to neutral: options for negative carbon emissions in California.* Livermore, CA: Lawrence Livermore National Laboratory. LLNL-TR-796100.

Bashi, Z., R. McCullough, L. Ong, and M. Ramirez. 2019. *Alternative proteins: The race for market share is on*. McKinsey & Company.

Bauer, J., C. Rowan, A. Barkhurst, J. Digiulio, K. Jones, M. Sabbatino, K. Rose, and P. Wingo. 2018. "NATCARB." National Energy Technology Laboratory Energy Data eXchange. edx.netl.doe.gov/dataset/natcarb.

Beal, C.M., R.E. Hebner, M.E. Webber, R.S. Ruoff, A.F. Seibert, and C.W. King. 2012. "Comprehensive evaluation of algal biofuel production: experimental and target results." *Energies* 5 (6): 1943–1981.

Becker, E.W. 2007. "Micro-algae as a source of protein." *Biotechnology Advances* 25: 207–210.

Bleakley, S., and M. Hayes. 2017. "Algal proteins: extraction, application, and challenges concerning production." *Foods* 6 (5): 33.

Bwapwa, J.K., A. Anandraj, and C. Trois. 2018. "Microalgae processing for jet fuel production." *Biofuels, Bioproducts and Biorefining* 12 (4): 522–535.

Bylund, G. 1995. "Chapter 15: Whey Processing." In *Dairy Processing Handbook*. Edited by Teknotext AB. Lund, Sweden: Tetra Pak Processing Systems AB.

Cai, H., J. Han, M. Wang, R. Davis, M. Biddy, and E. Tan. 2018. "Life-cycle analysis of integrated biorefineries with co-production of biofuels and bio-based chemicals: co-product handling methods and implications." *Biofuels, Bioproducts and Biorefining*, 12(5), pp.815-833.

Cai, H., L. Ou, M. Wang, R. Davis, A. Dutta, K. Harris, M.R. Wiatrowski, E. Tan, A. Bartling, B. Klein, and D. Hartley. 2021. *Supply Chain Sustainability Analysis of Renewable Hydrocarbon Fuels via Indirect Liquefaction, Ex Situ Catalytic Fast Pyrolysis, Hydrothermal Liquefaction, Combined Algal Processing, and Biochemical Conversion: Update of the 2020 State-of-Technology Cases*. Lemont, IL: Argonne National Laboratory. ANL/ESD-21/1 Rev. 1.

Caporgno, M.P., and A. Mathys. 2018. “Trends in Microalgae Incorporation into Innovative Food Products with Potential Health Benefits.” *Front. Nutr.* 5 (58).

Caporgno, M.P., L. Böcker, C. Müssner, E. Stirnemann, I. Haberkorn, H. Adelmann, S. Handschin, E.J. Windhab, and A. Mathys. 2020. “Extruded meat analogues based on yellow, heterotrophically cultivated *Auxenochlorella protothecoides* microalgae.” *Innovative Food Science & Emerging Technologies* 59: 102275.

Carter, B., H. Patel, D.M. Barbano, and M. Drake. 2018. “The effect of spray drying on the difference in flavor and functional properties of liquid and dried whey proteins, milk proteins, and micellar casein concentrates.” *Journal of Dairy Science* 101: 3900–3909.

Carullo, D., B.D. Abera, M. Scognamiglio, F. Donsì, G. Ferrari, and G. Pataro. 2022. “Application of Pulsed Electric Fields and High-Pressure Homogenization in Biorefinery Cascade of C. vulgaris Microalgae.” *Foods* 11: 471.

Coday, B.D., L. Miller-Robbie, E.G. Beaudry, J. Munakata-Marr, and T.Y. Cath. 2015. “Life cycle and economic assessments of engineered osmosis and osmotic dilution for desalination of Haynesville shale pit water.” *Desalination* 369: 188–200.

Coleman, A.M., J.M. Abodeely, R.L. Skaggs, W.A. Moeglein, D.T. Newby, E.R. Venteris, and M.S. Wigmosta. 2014. “An integrated assessment of location-dependent scaling for microalgae biofuel production facilities” *Algal Research* 5: 79–94. doi: 10.1016/j.algal.2014.05.008.

Cooney, G., J. Benitez, U. Lee, and M. Wang. 2022. “Clarification to Recent Publication - Incremental Approach for the Life-Cycle Greenhouse Gas Analysis of Carbon Capture and Utilization.” Lemont, IL: Argonne National Laboratory. greet.es.anl.gov/files/ccu_lca_memo.

Cronin, D.J., S. Subramaniam, C. Brady, A. Cooper, Z. Yang, J. Heyne, C. Drennan, K.K. Ramasamy, and M.R. Thorson. 2022. “Sustainable Aviation Fuel from Hydrothermal Liquefaction of Wet Wastes.” *Energies* 15: 1306.

Davis, R., D. Fishman, E.D. Frank, M.S. Wigmosta, A. Aden, A.M. Coleman, et al. 2012. *Renewable diesel from algal lipids: an integrated baseline for cost, emissions, and resource potential from a harmonized model*. Golden, CO: National Renewable Energy Laboratory.

Davis R., J. Markham, C. Kinchin, N. Grundl, E. Tan, and D. Humbird. 2016. *Process Design and Economics for the Production of Algal Biomass: Algal Biomass Production in Open Pond Systems and Processing Through Dewatering for Downstream Conversion*. Golden, CO: National Renewable Energy Laboratory.

Davis, R., J.N. Markham, C.M. Kinchin, C. Canter, J. Han, Q. Li, et al. 2018. *2017 Algae Harmonization Study: Evaluating the Potential for Future Algal Biofuel Costs, Sustainability, and Resource Assessment from Harmonized Modeling*. Golden, CO: National Renewable Energy Laboratory. NREL/TP-5100-70715. https://doi.org/10.2172/1468333.

De Godos, I., J.L. Mendoza, F.G. Acién, E. Molina, C.J. Banks, S. Heaven, and F. Rogalla. 2014. "Evaluation of carbon dioxide mass transfer in raceway reactors for microalgae culture using flue gases." *Bioresource Technology* 153: 307–314.

Decision Innovation Solutions. 2020. *Pet Food Production and Ingredient Analysis*. Urbandale, IA: Decision Innovation Solutions. ifeeder.org/wp-content/uploads/200218-Pet-Food-Report.pdf.

Devi, M.A., G. Subbulakshmi, K.M. Devi, and L.V. Venkataraman. 1981. "Studies on the proteins of mass-cultivated, blue-green alga (Spirulina platensis)." *Journal of Agricultural and Food Chemistry* 29 (3): 522–525.

Djekic, I., J. Miocinovic, I. Tomasevic, N. Smigic, and N. Tomic. 2014. "Environmental life-cycle assessment of various dairy products." *Journal of Cleaner Production* 68: 64–72.

Eggleston, H.S., L. Buendia, K. Miwa, T. Ngara, and K. Tanabe. 2006. *2006 IPCC guidelines for national greenhouse gas inventories*.

Escobar, N., E.J. Tizado, E.K. zu Ermgassen, P. Löfgren, J. Börner, and J. Godar. 2020. "Spatially-explicit footprints of agricultural commodities: Mapping carbon emissions embodied in Brazil's soy exports." *Global Environmental Change* 62, p.102067.

Esposito, E., L. Dellamuzia, U. Moretti, A. Fuoco, L. Giorno, and J.C. Jansen. 2019. "Simultaneous production of biomethane and food grade CO_2 from biogas: An industrial case study." *Energy & Environmental Science* 12 (1): 281–289.

Eustance, E., Y.J.S. Lai, T. Shesh, and B.E. Rittmann. 2020. "Improved CO_2 utilization efficiency using membrane carbonation in outdoor raceways." *Algal Research* 51: 102070.

Farhadian, O., L. Daghighi, and E.E. Dorche. 2013. "Effects of microalgae and alfalfa meal on population growth and production of a freshwater rotifer, *Euchlanis dilatata* (Rotifera: Mongononta)." *Journal of the World Aquaculture Society* 44 (1): 86–95.

Flysjö, A., M. Thrane, and J.E. Hermansen. 2014. "Method to assess the carbon footprint at product level in the dairy industry." *International Dairy Journal* 34 (1): 86–92.

Fu, Y., T. Chen, S.H.Y. Chen, B. Liu, P. Sun, H. Sun, and F. Chen. 2021. "The potentials and challenges of using microalgae as an ingredient to produce meat analogues." *Trends in Food Science & Technology* 112: 188–200.

Gifuni, I., L. Lavenant, J. Pruvost, and A. Masse. 2020. "Recovery of microalgal protein by three-steps membrane filtration: Advancements and feasibility." *Algal Research* 51: 102082.

Glencross, B. 2022. "Marine ingredients maintain a strategic role, but we need additional bulk nutrients for aquaculture growth." *International Aquafeed*, April 2022.

González, A.D., B. Frostell, and A. Carlsson-Kanyama. 2011. "Protein efficiency per unit energy and per unit greenhouse gas emissions: potential contribution of diet choices to climate change mitigation." *Food Policy* 36 (5): 562–570.

González-García, S., É.G. Castanheira, A.C. Dias, and L. Arroja. 2013. "Environmental performance of a Portuguese mature cheese-making dairy mill." *Journal of Cleaner Production* 41, pp.65-73.

Grand View Research. 2022a. *Protein Ingredients Market Size, Share & Trends Analysis Report By Product (Plant Proteins, Animal/Dairy Proteins, Microbe-based Proteins, Insect Proteins), By Application, By Region, And Segment Forecasts, 2021 - 2028*. San Francisco, CA: Grand View Research. www.grandviewresearch.com/industry-analysis/protein-ingredients-market.

Grand View Research. 2022b. *Whey Protein Market Size, Share & Trends Analysis Report By Type (WPI, WPC, WPH), By Application (Sports Nutrition, Dietary Supplements, Beverages), By Region, And Segment Forecasts, 2022 – 2030*. San Francisco, CA: Grand View Research. www.grandviewresearch.com/industry-analysis/whey-protein-market.

Grant, C.A., and A.L. Hicks. 2018. "Comparative life cycle assessment of milk and plant-based alternatives." *Environmental Engineering Science* 35 (11): 1235–1247.

Grossmann, L., J. Hinrichs, and J. Weiss. 2020. "Cultivation and downstream processing of microalgae and cyanobacteria to generate protein-based technofunctional food ingredients." *Critical Reviews in Food Science and Nutrition* 60 (17): 2961–2989.

Gutiérrez-Antonio, C., A.G. Cruz, A.G. RomeroIzquierdo, F.I. Gómez-Castro, and S. Hernández. 2018. "Modeling, simulation and intensification of hydroprocessing of micro-algae oil to produce renewable aviation fuel." *Clean Technologies and Environmental Policy* 20 (7): 1589–1598.

Handler, R.M., R. Shi, and D.R. Shonnard. 2017. "Land use change implications for large-scale cultivation of algae feedstocks in the United States Gulf Coast." *Journal of Cleaner Production* 153: 15–25.

Hazlebeck, D. 2023. "Enhanced algae productivity in CO_2 direct air capture." Presented at the 2023 BETO Peer Review, April 4, 2023, Denver, CO.

Hemighaus, G., T. Boval, J. Bacha, F. Barnes, M. Franklin, L. Gibbs, N. Hogue, J. Jones, D. Lesnini, J. Lind, and J. Morris. 2007. *Aviation Fuels Technical Review*. San Ramon, CA: Chevron Products Company.

Huesemann, M., S. Edmundson, S. Gao, S. Negi, T. Dale, A. Gutknecht, H. E. Daligault, et al. 2023. "DISCOVR strain pipeline screening–Part I: Maximum specific growth rate as a function of temperature and salinity for 38 candidate microalgae for biofuels production." *Algal Research* 71: 102996.

Huntley, M. E., Z. I. Johnson, S. L. Brown, D. L. Sills, L. Gerber, I. Archibald, S. C. Machesky, J. Granados, C. Beal, and C. H. Greene. 2015. "Demonstrated large-scale production of marine microalgae for fuels and feed." *Algal Research* 10: 249–265.

Integrated Environmental Control Model Team. 2019. *Pulverized Coal-Fired Power Plants and Air Pollution Controls*. Pittsburgh, PA: Department of Engineering and Public Policy, Carnegie Mellon University. www.uwyo.edu/iecm/_bfiles/documentation/201903_iecmtd_cp-apc-rev-a.pdf.

International Dairy Federation. 2022. *The IDF global Carbon Footprint standard for the dairy sector*. shop.fil-idf.org/products/the-idf-global-carbon-footprint-standard-for-the-dairy-sector.

International Energy Agency. 2022. *Direct Air Capture 2022*. Paris: International Energy Agency. www.iea.org/reports/direct-air-capture-2022.

Jiang, Y., S.B. Jones, Y. Zhu, L. Snowden-Swan, A.J. Schmidt, J.M. Billing, and D. Anderson. 2019. "Techno-economic uncertainty quantification of algal-derived biocrude via hydrothermal liquefaction." *Algal Research* 39: 101450.

Kim, D., G. Thoma, D. Nutter, F. Milani, R. Ulrich, and G. Norris. 2013. "Life cycle assessment of cheese and whey production in the USA." *The International Journal of Life Cycle Assessment* 18 (5): 1019–1035.

Klein, B., and R. Davis. 2022. *Algal Biomass Production via Open Pond Algae Farm Cultivation: 2021 State of Technology and Future Research*. Golden, CO: National Renewable Energy Laboratory. NREL/TP-5100-82417.

Klein, B., and R. Davis. 2023. *Algal Biomass Production via Open Pond Algae Farm Cultivation: 2022 State of Technology and Future Research*. Golden, CO: National Renewable Energy Laboratory. NREL/TP-5100-85661.

Koyande, A.K., K.W. Chew, K. Rambadu, Y. Tao, D. Chu, and P. Show. 2019. "Microalgae: A potential alternative to health supplementation for humans." *Food Science and Human Wellness* 8 (1): 16–24.

Kristensen, T., K. Søegaard, J. Eriksen, and L. Mogensen. 2015. "Carbon footprint of cheese produced on milk from Holstein and Jersey cows fed hay differing in herb content." *Journal of Cleaner Production* 101, pp.229-237.

Kuo, C.M., J.F. Jian, Y.L. Sun, T.H. Lin, Y.C. Yang, W.X. Zhang, H.F. Chang, J.T. Lai, J.S. Chang, and C.S. Lin. 2018. "An efficient photobioreactors/raceway circulating system combined with alkaline-CO_2 capturing medium for microalgal cultivation." *Bioresource Technology* 266: 398–406.

Lamminen, M., A. Halmemies-Beauchet-Filleau, T. Kokkonen, S. Jaakkola, and A. Vanhatalo. 2019. "Different microalgae species as a substitutive protein feed for soya bean meal in grass silage based dairy cow diets." *Animal Feed Science and Technology* 247: 112–126.

Langley, N.M., S.T.L. Harrison, and R.P. Van Hille. 2012. "A critical evaluation of CO_2 supplementation to algal systems by direct injection." *Biochemical Engineering Journal* 68: 70–75.

Li, Y., E. Zhou, L. Tao, K.H. Baek, P. Sun, and A. Elgowainy. 2023. *Near-Term Electricity Requirement and Emission Implications for Sustainable Aviation Fuel Production with CO_2-to-Fuels Technologies*. Golden, CO: National Renewable Energy Laboratory. NREL/TP-6A20-84838.

Linares, R.V., Z. Li, V. Yangali-Quintanilla, N. Ghaffour, G. Amy, T. Leiknes, and J.S. Vrouwenvelder. 2016. "Life cycle cost of a hybrid forward osmosis–low pressure reverse osmosis system for seawater desalination and wastewater recovery." *Water Research* 88: 225–234.

Liu, J., and B.M. Sleeter. 2018. "Simulated 1km resolution 1971-2015 ecosystem carbon variables from the IBIS model (2017/09/12)." U.S. Geological Survey. www.usgs.gov/data/simulated-1km-resolution-1971-2015-ecosystem-carbon-variables-ibis-model-20170912.

Manzocchi, E., B. Guggenbühl, M. Kreuzer, and K. Giller. 2020. "Effects of the substitution of soybean meal by spirulina in a hay-based diet for dairy cows on milk composition and sensory perception." *Journal of Dairy Science* 103 (12): 11349–11362.

Martínez-Sanz, M., E. Larsson, K.B. Filli, C. Loupiac, A. Assifaoui, A. López-Rubio, and P. Lopez-Sanchez. 2020. "Nano-/microstructure of extruded Spirulina/starch foams in relation to their textural properties." *Food Hydrocolloids* 103: e105697.

Middleton, R. S., et al. 2014. "CO_2 deserts: Implications of existing CO_2 supply limitations for carbon management." *Environ. Sci. Technol.* 48 (19): 11713–11720.

Miles, R.D., and F.A. Chapman. 2012. *The benefits of fish meal in aquaculture diets*. FA122. Institute of Food and Agricultural Sciences, University of Florida.

Massachusetts Institute of Technology. 2016. "LaBarge Fact Sheet: Carbon Dioxide Capture and Storage Project." Carbon Capture and Sequestration Technologies Program, Massachusetts Institute of Technology. sequestration.mit.edu/tools/projects/la_barge.html.

National Renewable Energy Laboratory (NREL). 2023. "Biorefinery Analysis Process Models – Algae Production via Open Pond Cultivation: NREL Algae Farm Model (Excel TEA Tool)." www.nrel.gov/extranet/biorefinery/aspen-models/.

Neumann, C., S. Velten, and F. Liebert. 2018. "The graded inclusion of algae (*Spirulina platensis*) or insect (*Hermetia illucens*) meal as a soybean meal substitute in meat type chicken diets impacts on growth, nutrient deposition and dietary protein quality depending on the extent of amino acid supplementation." *Open Journal of Animal Sciences* 8 (2) 163–183.

Niccolai, A., et al. 2019. "Microalgae of interest as food source: Biochemical composition and digestibility." *Algal Research* 42: 101617.

Ou, L., S. Banerjee, H. Xu, A.M. Coleman, H. Cai, U. Lee, M.S. Wigmosta, and T.R. Hawkins. 2021. "Utilizing high-purity carbon dioxide sources for algae cultivation and biofuel production in the United States: Opportunities and challenges." *J. Clean. Prod.* 321: 128779.

Parimi, N.S., M. Singh, J.R. Kastner, K.C. Das, L.S. Forsberg, and P. Azadi. 2015. "Optimization of protein extraction from Spirulina platensis to generate a potential co-product and a biofuel feedstock with reduced nitrogen content." *Front. Energy Res.* 3: 30.

Panagopoulos, A., K.-J. Haralambous, and M. Loizidou. 2019. "Desalination brine disposal methods and treatment technologies-A review." *Science of the Total Environment* 693: p. 133545.

Penner, J.E., D.H. Lister, D.J. Griggs, D.J. Dokken, and M. McFarland (eds.). 1999. *Aviation and the Global Atmosphere.* Cambridge, UK: Cambridge University Press.

Pereira, H., M. Sardinha, T. Santos, L. Gouveia, L. Barreira, J. Dias, and J. Varela. 2020. "Incorporation of defatted microalgal biomass (*Tetraselmis* sp. CTP4) at the expense of soybean meal as a feed ingredient for juvenile gilthead seabream (*Sparus aurata*)." *Algal Research* 47: 101869.

Philis, G., E.O. Gracey, L.C. Gansel, A.M. Fet, and C. Rebours. 2018. "Comparing the primary energy and phosphorus consumption of soybean and seaweed-based aquafeed proteins–a material and substance flow analysis." *Journal of Cleaner Production* 200: 1142–1153.

Pilorgé, H., N. McQueen, D. Maynard, P. Psarras, J. He, T. Rufael, and J. Wilcox. 2020. "Cost analysis of carbon capture and sequestration of process emissions from the US industrial sector." *Environmental Science & Technology* 54 (12): 7524–7532.

Procházková, G., I. Brányiková, V. Zachleder, and T. Brányik. 2014. "Effect of nutrient supply status on biomass composition of eukaryotic green microalgae." *Journal of Applied Phycology* 26 (3): 1359–1377.

Putt, R., M. Singh, S. Chinnasamy, and K.C. Das. 2011. "An efficient system for carbonation of high-rate algae pond water to enhance CO_2 mass transfer." *Bioresource Technology* 102 (3): 3240–3245.

Qin, P., T. Wang, Y. Luo. 2022. "A review on plant-based proteins from soybean: Health benefits and soy product development." *Journal of Agriculture and Food Research* 7: 100265.

Quiroz, D., J.M. Greene, B. J. Limb, and J.C. Quinn. 2023. "Global life cycle and techno-economic assessment of algal-based biofuels." *Environmental Science & Technology* 57 (31): 11541–11551.

Ravindran, V., M.R. Abdollahi, and S.M. Bootwalla. 2014. "Nutrient analysis, metabolizable energy, and digestible amino acids of soybean meals of different origins for broilers." *Poultry Science* 93 (10): 2567–2577.

Saadaoui, I., R. Rasheed, A. Aguilar, M. Cherif, H.A. Jabri, S. Sayadi, and S.R. Manning. 2021. "Microalgal-based feed: promising alternative feedstocks for livestock and poultry production." *Journal of Animal Science and Biotechnology* 12: 76.

Safi, C., G. Olivieri, R. P. Campos, N. Engelen-Smit, W. J. Mulder, L. A. M. van den Broek, and L. Sijtsma. 2017. "Biorefinery of microalgal soluble proteins by sequential processing and membrane filtration." *Bioresource Technology* 225: 151–158.

Safi, C., L.C. Rodriguez, W.J. Mulder, N. Engelen-Smit, W. Spekking, L.A.M. Van den Broek, G. Olivieri, and L. Sijtsma. 2017. "Energy consumption and water-soluble protein release by cell wall disruption of *Nannochloropsis gaditana*." *Bioresource Technology* 239: 204–210.

Sajjadi, B., W. Y. Chen, A. A. A. Raman, and S. Ibrahim. 2018. "Microalgae lipid and biomass for biofuel production: A comprehensive review on lipid enhancement strategies and their effects on fatty acid composition." *Renewable and Sustainable Energy Reviews* 97: 200–232.

Schoenung, S.M., R.A. Efroymson, and M.H. Langholtz. 2019. *Considerations for the Design of a Gas Transport System for Co-location of Microalgae Cultivation with CO_2 Sources*. Oak Ridge, TN: Oak Ridge National Laboratory. ORNL/TM-2019/1130.

Sheehan, J., V. Camobreco, J. Duffield, M. Graboski, and H. Shapouri. 1998. *Life cycle inventory of biodiesel and petroleum diesel for use in an urban bus*. Golden, CO: National Renewable Energy Laboratory. NREL/SR-580-24089.

Singh, U., S. Banerjee, and T.R. Hawkins. 2023. "Implications of CO_2 Sourcing on the Life-Cycle Greenhouse Gas Emissions and Costs of Algae Biofuels." *ACS Sustainable Chemistry & Engineering* 11 (39): 14435–14444.

Skone, T. J., M. Mutchek, M. Krynock, S. Moni, S. Rai, J. Chou, D. Carlson, et al. 2022. *Carbon Dioxide Utilization Life Cycle Analysis Guidance for the U.S. DOE Office of Fossil Energy and Carbon Management, Version 2.0*. Pittsburgh, PA: National Energy Technology Laboratory. netl.doe.gov/energy-analysis/details?id=30f43c4f-2e95-4afa-8a0e-e49168ada191.

Snowden-Swan, L., S. Li, M. Thorson, A. Schmidt, D. Cronin, Y. Zhu, T. Hart, M. Santosa, S. Fox, T. Lemmon, and M. Swita. 2022. *Wet Waste Hydrothermal Liquefaction and Biocrude Upgrading to Hydrocarbon Fuels: 2022 State of Technology*. Richland, WA: Pacific Northwest National Laboratory. PNNL-33622.

Song, G., S. Edmundson, M. Huesemann, A. Gutknecht, L.M.L. Laurens, S. Van Wychen, K. Pittman, and M. Greer. 2023. "DISCOVR strain screening pipeline – Part III: Strain evaluation in outdoor raceway ponds." *Algal Research* 70:102990.

Soto-Sierra, L., P. Stoykova, and Z.L. Nikolov. 2018. "Extraction and fractionation of microalgae-based protein products." *Algal Research* 36: 175–192.

Statista. 2022. "Global animal protein consumption by type 2021." Accessed October 2022. www.statista.com/statistics/1025784/human-consumption-of-protein-by-type-worldwide/.

Sun, N., R. Skaggs, M.S. Wigmosta, A. Coleman, M.H. Huesemann, and S.J. Edmundson. 2020. "Growth Modeling to Evaluate Alternative Cultivation Strategies to Enhance National Microalgal Biomass Production." *Algal Research* 49: 101939. doi:10.1016/j.algal.2020.101939.

Thiel, G.P., E.W. Tow, L.D. Banchik, and H.W. Chung. 2015. "Energy consumption in desalinating produced water from shale oil and gas extraction." *Desalination* 366, pp.94-112.

Thoma, G., J. Popp, D. Nutter, D. Shonnard, R. Ulrich, M. Matlock, D.S. Kim, et al. 2013. "Greenhouse gas emissions from milk production and consumption in the United States: A cradle-to-grave life cycle assessment circa 2008." *International Dairy Journal* 31: S3–S14.

Tyler, J. 2022. "Global pet food production up 8.2% in 2021." *Pet Food Processing*.

U.S. Department of Agriculture (USDA). 2015. *Whey Protein Concentrate (WPC)*. Washington, D.C.: USDA, AMS, Agricultural Analytics Division for the USDA National Organic Program. www.ams.usda.gov/sites/default/files/media/Whey%20Protein%20Concentrate%20TR.pdf.

USDA. 2021. *Dairy Market Statistics 2020 Annual Summary*. Washington, D.C.: Agricultural Marketing Service.

USDA. 2022a. *Dairy Products 2021 Summary*. Washington, D.C.: National Agricultural Statistics Service.

USDA. 2022b. *National Grain and Oilseed Processor Feedstuff Report*. Minneapolis, MN: AMS Livestock, Poultry & Grain Market News.

U.S. Department of Energy (DOE). 2020. *Bioenergy Technologies Office R&D State of Technology 2020*. Washington, D.C.: DOE. DOE/EE-2531. bioenergykdf.net/sites/default/files/2022-05/BETO-2020-SOT_FINAL_5-11-22.pdf.

U.S. DOE. 2021. "Memorandum of Understanding: Sustainable Aviation Fuel Grand Challenge." Sept. 8, 2021. www.energy.gov/sites/default/files/2021-09/S1-Signed-SAF-MOU-9-08-21_0.pdf.

U.S. DOE. 2022. *Industrial Decarbonization Roadmap*. Washington, D.C.: DOE. DOE/EE-2635.

U.S. DOE. 2023. "Carbon Negative Shot." www.energy.gov/fecm/carbon-negative-shot.

U.S. Department of Homeland Security. 2019. "Homeland Infrastructure Foundation-Level Data (HIFLD)." hifld-geoplatform.opendata.arcgis.com/.

U.S. Environmental Protection Agency. 2020. "Greenhouse Gas Reporting Program (GHGRP)." www.epa.gov/ghgreporting.

U.S. Food and Drug Administration. 2022. "Cheeses and Related Cheese Products." CFR Title 21, Chapter I, Subchapter B, Part 133. www.accessdata.fda.gov/scripts/cdrh/cfdocs/cfcfr/CFRSearch.cfm?CFRPart=133&showFR=1.

Venteris, E.R., R. McBride, A.M. Coleman, R. Skaggs, and M.S. Wigmosta. 2014. "Siting algae cultivation facilities for biofuel production in the United States: trade-offs between growth rate, site constructability, water availability, and infrastructure" *Environmental Science & Technology* 48 (6): 3559–3566. doi:10.1021/es4045488.

Wang, Y., S.M. Tibbetts, and P.J. McGinn. 2021. "Microalgae as Sources of High-Quality Protein for Human Food and Protein Supplements." *Foods* 10: 3002.

Wiatrowski, M., R. Davis, and J. Kruger. 2022. *Algal Biomass Conversion to Fuels via Combined Algae Processing (CAP): 2021 State of Technology and Future Research*. Golden, CO: National Renewable Energy Laboratory. NREL/TP-5100-82502.

Wigmosta, M.S., A.M. Coleman, E.R. Venteris, and R.L. Skaggs. 2017. "Microalgae Feedstocks for Aviation Fuels." In *Green Aviation: Aircraft Technology, Alternative Fuels and Public Policy, Sustainable Energy Developments Series*. Edited by E.S. Nelson and D.R. Reddy. New York: CRC Press, Taylor & Francis Group. ISBN 9780415620987.

Xu, H., U. Lee, A.M. Coleman, M.S. Wigmosta, N. Sun, T. Hawkins, and M. Wang. 2020. "Balancing water sustainability and productivity objectives in microalgae cultivation: siting open ponds by considering seasonal water-stress impact using AWARE-US." *Environmental Science & Technology* 54 (4): 2091–2102. doi:10.1021/acs.est.9b05347.

Yoo, E., U. Lee, G. Zang, P. Sun, A. Elgowainy, and M. Wang. 2022. "Incremental approach for the life-cycle greenhouse gas analysis of carbon capture and utilization." *J. CO_2 Util.* 65: 102212. doi.org/10.1016/j.jcou.2022.102212.

Zhang, J., H. Yuan, Y. Deng, I.M. Abu-Reesh, Z. He, and C. Yuan. 2019. "Life cycle assessment of osmotic microbial fuel cells for simultaneous wastewater treatment and resource recovery." *The International Journal of Life Cycle Assessment* 24 (11): 1962–1975.

Zhu, Y., K.O. Albrecht, D.C. Elliott, R.T. Hallen, and S.B. Jones. 2013. "Development of Hydrothermal Liquefaction and Upgrading Technologies for Lipid-Extracted Algae Conversion to Liquid Fuels." *Algal Research* 2 (4): 455–464.

Zhu, Y., S.B. Jones, A.J. Schmidt, H.M. Job, J.M. Billing, J.R. Collett, K.R. Pomraning, et al. 2021. *Microalgae Conversion to Biofuels and Biochemical via Sequential Hydrothermal Liquefaction (SEQHTL) and Bioprocessing: 2020 State of Technology*. Richland, WA: Pacific Northwest National Laboratory. PNNL-30124.

Zhu, Y., S.B. Jones, A.J. Schmidt, J.M. Billing, D.M. Santosa, and D.B. Anderson. 2020. "Economic impacts of feeding microalgae/wood blends to hydrothermal liquefaction and upgrading systems." *Algal Research* 51: 102053.

Zhu Y., Y. Xu, A.J. Schmidt, M.R. Thorson, D.J. Cronin, D.M. Santosa, S.J. Edmundson, et al. 2023. *Microalgae Hydrothermal Liquefaction and Biocrude Upgrading: 2022 State of Technology*. Richland, WA: Pacific Northwest National Laboratory. PNNL-34032.

Appendix

TEA Result Details for Algae Farm Models

Table S1. Seasonal Parameters for a Site With Low MBSP

Parameter	Summer	Fall	Winter	Spring	Average
Productivity (g/m^2/day)	43.7	30.7	21.8	37.9	**33.5**
Evaporation rate (cm/day)	0.59	0.39	0.31	0.57	**0.46**
Pond blowdown volume (m^3/h)	650	425	344	644	**515**
Pond freshwater input from FO (m^3/h)	1,329	934	665	1,154	**1,020**
Saline groundwater input (m^3/h)	11,612	7,718	6,074	11,191	**9,149**
Brine water for deep-well injection (m^3/h)	292	205	146	253	**224**

Table S2. Seasonal Parameters for a Site With Medium MBSP

Parameter	Summer	Fall	Winter	Spring	Average
Productivity (g/m^2/day)	43.5	25.4	11.3	30.0	**27.6**
Evaporation rate (cm/day)	0.96	0.51	0.31	0.74	**0.63**
Pond blowdown volume (m^3/h)	62	32	20	48	**41**
Pond freshwater input from FO (m^3/h)	129	76	34	89	**82**
Saline groundwater input (m^3/h)	1,812	975	578	1,387	**1,188**
Brine water for deep-well injection (m^3/h)	28	17	7	20	**18**

Table S3. Seasonal Parameters for a Site With High MBSP

Parameter	Summer	Fall	Winter	Spring	Average
Productivity (g/m^2/day)	43.0	23.9	9.6	27.9	**26.1**
Evaporation rate (cm/day)	0.91	0.47	0.27	0.66	**0.58**
Pond blowdown volume (m^3/h)	790	410	237	579	**504**
Pond freshwater input from FO (m^3/h)	648	336	194	474	**413**
Saline groundwater input (m^3/h)	2,469	1,281	737	1,806	**1,573**
Brine water for deep-well injection (m^3/h)	142	74	43	104	**91**

Table S4. Additional Nonseasonal Parameters for Selected MBSP Scenarios

Parameter	MBSP Scenario		
	Low	Medium	High
Salinity of makeup water (mg/L)	5,597	3,289	27,622
Groundwater well – CAPEX (MM$)	0.09	0.95	1.80
Groundwater well – average power requirement (kW)	816	1,183	2,462
Groundwater well – total OPEX (MM$/yr)	0.44	0.64	1.33
FO unit – CAPEX (MM$)	33.07	3.22	16.1
FO unit – average power requirement (kW)	6,844	550	2,771
FO unit – total OPEX (MM$/yr)	4.68	0.38	1.90
Deep-well injection – CAPEX (MM$)	1.47	0.39	1.80
Deep-well injection – average power requirement (kW)	32	5	16
Deep-well injection – total OPEX (MM$/yr)	0.49	0.04	0.20

Table S5. MBSP Breakdown for a Representative Site With Low MBSP

Item	Unit	Quantity	Total Cost ($/U.S. ton AFDW)
Cultivation			
Urea	kg/h	10,835	97.1
DAP	kg/h	3,194	36.3
CO_2 supply	kg/h	146,956	105.3
Electricity	kW	19,462	18.9
Saline water	m^3/h	8,976	0.0
Inoculum			
Urea	kg/h	311	2.8
DAP	kg/h	81	0.9
CO_2 supply	kg/h	3,194	2.3
Electricity	kWh	532	0.5
Saline water	m^3/h	173	0.0
Chiller	GJ/h	30	2.5
Dewatering			
Electricity	kW	3,435	3.3
Salinity Management			
Electricity	kW	7,692	7.5
Other costs	-	-	2.6
Other			
Labor	-	-	25.4
Maintenance	-	-	10.4
Insurance		-	11.2
Capital depreciation	-	-	53.0
Income tax	-	-	18.0
Return on investment	-	-	156.0
Total MBSP	**-**	**-**	**553.6**
Algae biomass production	**kg AFDW/h**	**63,623**	**-**

Table S6. MBSP Breakdown for a Representative Site With Medium MBSP

Item	Unit	Quantity	Total Cost ($/U.S. ton AFDW)
Cultivation			
Urea	kg/h	870	97.1
DAP	kg/h	257	36.2
CO_2 supply	kg/h	11,806	103.3
Electricity	kW	1,769	21.4
Saline water	m^3/h	1,166	0.0
Inoculum			
Urea	kg/h	25	2.8
DAP	kg/h	7	0.9
CO_2 supply	kg/h	258	2.3
Electricity	kWh	51	0.6
Saline water	m^3/h	22	0.0
Chiller	GJ/h	3	3.0
Dewatering			
Electricity	kW	276	3.3
Salinity Management			
Electricity	kW	1,737	21.0
Other costs	-	-	2.6
Other			
Labor	-	-	110.5
Maintenance	-	-	15.4
Insurance		-	15.3
Capital depreciation	-	-	74.0
Income tax	-	-	24.0
Return on investment	-	-	211.0
Total MBSP	**-**	**-**	**745.2**
Algae biomass production	**kg AFDW/h**	**5,112**	**-**

Table S7. MBSP Breakdown for a Representative Site With High MBSP

Item	Unit	Quantity	Total Cost ($/U.S. ton AFDW)
Cultivation			
Urea	kg/h	882	104.4
DAP	kg/h	258	38.6
CO_2 supply	kg/h	11,759	109.2
Electricity	kW	1,864	23.9
Saline water	m^3/h	1,552	0.0
Inoculum			
Urea	kg/h	26	3.1
DAP	kg/h	7	1.0
CO_2 supply	kg/h	265	2.5
Electricity	kWh	59	0.8
Saline water	m^3/h	21	0.0
Chiller	GJ/h	3	3.4
Dewatering			
Electricity	kW	260	3.3
Salinity Management			
Electricity	kW	5,250	67.4
Other costs	-	-	14.0
Other			
Labor	-	-	117.3
Maintenance	-	-	18.4
Insurance		-	20.3
Capital depreciation	-	-	97.0
Income tax	-	-	32.0
Return on investment	-	-	277.0
Total MBSP	**-**	**-**	**934.3**
Algae biomass production	**kg AFDW/h**	**4,816**	**-**

Table S8. CAPEX Breakdown for Selected Sites

MBSP Scenario	Low	Medium	High
Algae farm size (acres)	11,052	1,080	1,136
Algae farm section	Installed cost (MM 2020 $) [a]		
Production ponds	391.2	38.5	54.6
Inoculum	28.5	2.8	3.0
CO_2 storage	26.0	1.8	1.8
Water circulation	37.4	4.6	6.4
Dewatering	112.6	14.9	14.9
Storage	14.8	4.0	4.6
Total installed cost	**610.5**	**66.6**	**85.2**
Warehouse	9.6	1.1	1.3
Site development	36.0	3.9	4.0
Additional piping	5.1	0.7	0.7
Total direct cost (TDC)	**661.1**	**72.2**	**91.2**
Indirect cost			
Proratable expenses	31.3	3.6	4.2
Home office & construction fees	71.4	8.0	9.7
Field expenses	33.2	3.8	4.5
Project contingency	66.1	7.2	9.1
Other costs (startup, permits, etc.)	25.5	3.0	3.4
Total indirect cost	2,227.5	25.5	31.0
Fixed capital investment	**888.7**	**97.7**	**122.1**
Working capital	44.4	4.9	6.1
Land	50.5	4.9	5.2
Total capital investment	**983.6**	**107.5**	**133.5**

[a] Methodology and rationale consistent with the assumptions in Davis et al. (2016) and with the modifications detailed in this report.

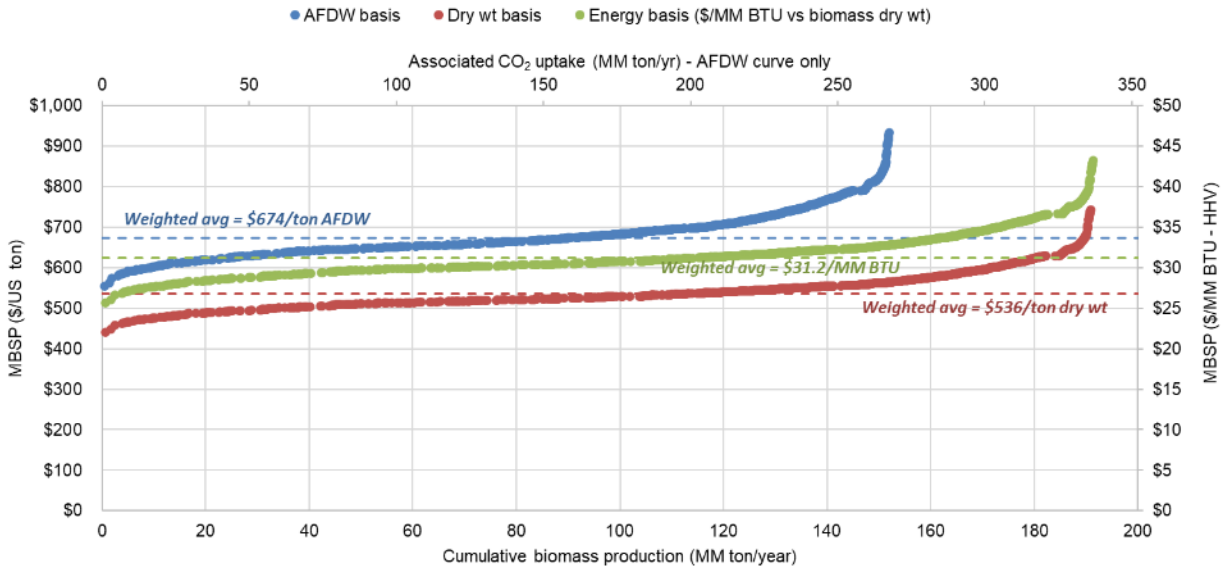

Figure S1. Biomass cost versus resource curves reflecting TEA modeling for individual farms: MBSP before storage in dollars per ton AFDW (blue curve), dollars per ton dry weight (red curve), and dollars per MM Btu higher heating value (HHV) energy content (green curve; dry weight biomass basis). Top axis for CO_2 uptake potential corresponds to the blue AFDW curve only.

TEA Result Details for Algae HTL Conversion

Table S9. Detailed Cost Results of Selected Cases for the Algae HTL Conversion to Fuel and Protein System

Processing Area Cost Contributions & Key Technical Parameters	Metric	Low, Fuel + PC	Mid, Fuel + PC	High, Fuel + PC
Fuel selling price	$/GGE	$0.28	$5.42	$12.02
Conversion contribution	$/GGE	($10.58)	($9.17)	($6.58)
Production diesel	MM GGE/yr	5.0	1.2	0.4
Production SAF	MM GGE/yr	17.2	4.0	1.3
Production naphtha	MM GGE/yr	6.4	1.5	0.5
Diesel yield (AFDW feedstock basis)	GGE/U.S. ton feedstock	9.1	9.1	9.1
Jet fuel yield (AFDW feedstock basis)	GGE/U.S. ton feedstock	31	31	31
Naphtha yield (AFDW feedstock basis)	GGE/U.S. ton feedstock	12	12	12
Production PC	1,000 U.S. tons/yr	190	44	14
Natural gas usage - total (AFDW algae basis)	scf/U.S. ton feedstock	1,023	1,023	1,023
Feedstock				
Total cost contribution	$/GGE fuel	$10.86	$14.59	$18.60
Feedstock type		Algae only	Algae only	Algae only
Feedstock cost (AFDW basis)	$/U.S. ton feedstock	$565	$760	$968
Protein Extraction				
Total cost contribution	$/GGE fuel	$2.91	$3.26	$4.44
Capital cost contribution	$/GGE fuel	$1.42	$1.58	$2.27
Operating cost contribution	$/GGE fuel	$1.48	$1.68	$2.16
HTL Biocrude Production				
Total cost contribution	$/GGE fuel	$0.64	$0.99	$1.43
Capital cost contribution	$/GGE fuel	$0.42	$0.63	$0.89
Operating cost contribution	$/GGE fuel	$0.22	$0.36	$0.54
LHSV	vol/h/vol	4.0	4.0	4.0
HTL biocrude yield (AFDW)	lb/lb PEA feed	0.41	0.41	0.41
HTL Biocrude Hydrotreating to Finished Fuels				
Total cost contribution	$/GGE fuel	$0.48	$0.69	$0.95
Capital cost contribution	$/GGE fuel	$0.26	$0.39	$0.54
Operating cost contribution	$/GGE fuel	$0.22	$0.30	$0.41
Mass yield on dry HTL biocrude	lb/lb biocrude	0.83	0.83	0.83
HTL Aqueous Phase Treatment				
Total cost contribution	$/GGE fuel	$0.18	$0.36	$0.61
Capital cost contribution	$/GGE fuel	$0.13	$0.24	$0.39
Operating cost contribution	$/GGE fuel	$0.05	$0.12	$0.22
Balance of Plant				
Total cost contribution	$/GGE fuel	$0.47	$0.79	$1.24
Capital cost contribution	$/GGE fuel	$0.26	$0.46	$0.73
Operating cost contribution	$/GGE fuel	$0.22	$0.34	$0.52
Credits				
Coproduct credit	$/GGE fuel	(13.37)	(13.37)	(13.37)
Nutrient recycle credit	$/GGE fuel	(1.89)	(1.89)	(1.89)

Table S10. Detailed Cost Results of Selected Cases for the Algae HTL Conversion to Fuel-Only System

Processing Area Cost Contributions & Key Technical Parameters	Metric	Low, Fuel Only	Middle, Fuel Only	High, Fuel Only
Fuel selling price	$/GGE	$6.72	$9.66	$13.07
Conversion contribution	$/GGE	$0.25	$1.63	$2.40
Production diesel	MM GGE/yr	12.9	1.2	0.6
Production SAF	MM GGE/yr	44	4	2
Production naphtha	MM GGE/yr	16.7	1.6	0.8
Diesel yield (AFDW feedstock basis)	GGE/U.S. ton feedstock	17	17	17
SAF yield (AFDW feedstock basis)	GGE/U.S. ton feedstock	58	58	58
Naphtha yield (AFDW feedstock basis)	GGE/U.S. ton feedstock	22	22	22
Natural gas usage - fuel production (AFDW basis)	scf/U.S. ton feedstock	4,409	4,409	4,409
Feedstock				
Total cost contribution	$/GGE fuel	$6.47	$8.03	$10.68
Feedstock type		Algae only	Algae only	Algae only
Feedstock cost (AFDW basis)	$/U.S. ton blend	$580	$720	$957
HTL Biocrude Production				
Total cost contribution	$/GGE fuel	$0.60	$1.19	$1.52
Capital cost contribution	$/GGE fuel	$0.38	$0.72	$0.89
Operating cost contribution	$/GGE fuel	$0.22	$0.47	$0.63
LHSV	vol/h/vol	4.0	4.0	4.0
HTL biocrude yield (AFDW)	lb/lb feed	0.39	0.39	0.39
HTL Biocrude Hydrotreating to Finished Fuels				
Total cost contribution	$/GGE fuel	$0.46	$0.81	$0.99
Capital cost contribution	$/GGE fuel	$0.24	$0.44	$0.53
Operating cost contribution	$/GGE fuel	$0.22	$0.37	$0.46
Mass yield on dry HTL biocrude	lb/lb biocrude	0.79	0.79	0.79
Balance of Plant				
Total cost contribution	$/GGE fuel	$0.42	$0.85	$1.11
Capital cost contribution	$/GGE fuel	$0.19	$0.45	$0.58
Operating cost contribution	$/GGE fuel	$0.23	$0.40	$0.52
Credits				
Nutrient recycle credit	$/GGE fuel	(1.22)	(1.22)	(1.22)

Table S11. Capital Cost Results of the Algae HTL Conversion to Fuel and Protein System

Installed Cost	**Million $ (2020 U.S. $)**	**% of Total Installed Cost**
Protein extraction	$49.3	48%
HTL	$19.7	19%
Biocrude upgrading to finished fuels	$12.2	12%
Aqueous phase treatment	$7.50	7.3%
Hydrogen generation	$7.68	7.5%
Balance of plant	$6.60	6.4%
Total installed cost	**$103**	**100%**
Warehouse (1% of inside battery limit [ISBL])	$1.03	--
Site development (9% of ISBL)	$9.27	--
Additional piping (4.5% of ISBL)	$3.99	--
TDC	**$117**	--
Indirect cost		**--**
Prorated expenses (10% of TDC)	$11.7	--
Home office & construction fees (20% of TDC)	$23.5	--
Field expenses (10% of TDC)	$11.7	--
Project contingency (10% of TDC)	$11.7	--
Other costs (startup, permits, etc.) (5% of TDC)	$5.87	--
Total indirect cost	**$64.5**	**--**
Fixed capital investment	**$182**	--
Working capital (5% of fixed capital investment)	$9.09	--
Total capital investment	**$191**	**--**

Note: The capital cost listed in this table as an example is for the case with median value of MFSPs for all sites. For sites with different algae production rates, the capital cost results are different due to variance in plant scales.

Table S12. Operating Cost Results of the Algae HTL Conversion to Fuel and Protein System

Raw Materials	Unit Price (2020 U.S. $)	Unit	Consumption (per GGE fuel)	Cost (MM$/yr)
Algae feedstock cost	760 [a]	$/ton AFDW	0.019	96.9
Natural gas	3.32	$/1,000 scf	0.047	1.04
Cooling tower chemicals	36.3	$/ton-yr cooling	0.00025	0.06
Sulfuric acid	0.047	$/lb	0.38	0.12
Flocculant	229	$/ton	0.00022	0.33
NaOH	0.26	$/lb	0.015	0.03
HCl	0.49	$/lb	0.0029	0.01
Hydrogen plant catalyst	2.20	¢/1,000 scf H_2	0.11	0.02
Hydrotreating main bed catalyst	11.3	$/lb	0.0011	0.08
Hydrotreating guard bed fill	17.8	$/lb	0.0030	0.36
HDN catalyst	17.8	$/lb	0.00047	0.06
Hydrocracking catalyst	17.8	$/lb	0.000081	0.01
Sum				**99.0**
Utilities				
Water makeup	0.40	$/tonne	0.017	0.02
Electricity	7.31	¢/kwh	11.3	3.12
Sum				**3.14**
Credits				
PC (coproduct)	1.00	$/lb	13.4	−88.8
Urea (N recycle equivalent)	0.29	$/lb	4.69	−4.45
CO_2 (C recycle equivalent)	0.02	$/lb	26.6	−4.13
DAP (P recycle equivalent)	0.36	$/lb	1.65	−3.96
Sum				**−101**
Total Variable Operating Costs				**−0.78**

[a] Note: Algae feedstock and other variable operating costs listed in this table as an example are for the case with median value of MFSPs for all sites. For sites with different algae production rate and feedstock cost, the operating cost results are different.

LCI Details

Upstream LCI for FO Membrane

Table S13. LCI of FO Membrane Fabrication

Material Inputs (kg)		Sources	Notes
Viscose fiber with extrusion	2.74E-02	Section 1.1	Membrane active layer
Glass fiber reinforced plastic with calendering	2.55E-01	GREET2, literature	Membrane support layer
Polyurethane, flexible foam	2.46E-01	GREET1	Glue
Polyvinyl chloride with extrusion	7.31E-02	GREET1	Sealant tape
Polypropylene with extrusion	5.70E-02	GREET1	Filament tape
Polystyrene with calendaring	3.97E-01	GREET1, literature	Feed spacer
Freshwater	1.70E+00		Routine cleaning
Stainless steel	1.48E-02	GREET2	Feed strainer housing/basket
Acrylonitrile butadiene styrene with injection molding	2.51E-03	GREET1, literature	Pressure vessel middle membrane connector
Polyvinyl chloride with injection molding	4.26E-03	GREET1	Pressure vessel and adaptors
Hot rolled steel	8.49E-01	GREET2	Tube
Galvanized steel	1.71E-02	GREET2	Tube
High-density polyethylene with injection molding	3.95E-01	GREET1	Tanks
Glass fiber reinforced polymer with injection molding	4.15E-01	GREET2, literature	Pressure vessels
Output (kg)			
FO membrane	1.00E+00		
Infrastructure	1.75E+00		
Wastewater	1.70E+00		

Upstream LCI for Whey PC Production

The LCI of whey PC was obtained from Bacenetti et al. (2018) and incorporated into the GREET model. Detailed input material and energy consumption for producing 1 kg of whey PC can be found in Table S14. Whey PC 35%, whey PC 60%, and whey PC 80% reflect different whey protein concentrations available in the market (approximately 35%, 60%, and 80% protein content on a dry mass basis, respectively). Here, three replacement approaches are considered, taking into account dry mass, protein content, and digestible protein. A 100% replacement ratio was achieved when mass was used as the matching unit. The replacement ratios by using protein content and digestible protein are summarized in Table 2.2.10.

Liquid whey is the main feedstock for whey PC production and is a coproduct of cheese making and casein manufacturing in the dairy industry (Bacenetti et al. 2018). The LCI of upstream

liquid whey production was calculated based on two sources using the GREET model (Kim et al. 2013; Aguirre-Villegas et al. 2012). The first LCI source was obtained from Kim et al. (2013) and provides detailed LCI of liquid whey production using mixed allocation methods. The first allocation method is the default solid weight allocation of milk solids in each coproduct, while the second involves a survey sent to plant operators to estimate allocation. Plant-specific allocation is employed if provided by the plants. If neither of the first two methods is applicable, revenue-based allocation is utilized when the input fraction is not clearly identified. The adjusted LCI data for liquid whey production from Kim et al. (2013) can be found in Table S15. GHG emissions from liquid whey production were calculated using the GREET model, as they were not available in the literature (Kim et al. 2013). In addition, the LCIs of upstream milk and cream production were obtained from literature (Grant and Hicks 2018; Djekic et al. 2014), and environmental impacts were calculated using the GREET model. Detailed LCI of milk and cream production and associated upstream inventories can be found in this Appendix.

In addition, GHG emissions from liquid whey production were calculated from the LCI for cheese production obtained from literature and three allocation methods—economic value, solid content, and nutritional value—by using the GREET model, since the environmental impacts of liquid whey production are not provided in literature (Aguirre-Villegas et al. 2012). The inventory used for liquid whey production in this study only includes the reception and storage stages of fluid milk and making vats, since pasteurization is considered part of milk production and whey PC production. These two steps cannot be further divided, and the three allocation methods (economic, solid content, and nutritional value) were used to allocate the environmental impacts arising from cheese and liquid whey production, as provided in the literature. Detailed LCI data for cheese and liquid whey production, as well as the corresponding allocation factors from Aguirre-Villegas et al. (2012), can be found in Tables S16 and S17, respectively. The allocation methods utilized in these two references adhere to the guidance provided by the International Dairy Federation (2022). The system was divided into subsystems whenever feasible, and allocation factors were employed when subdivision was not possible.

Milk and cream are two main raw materials for cheese and liquid whey production, as shown in Tables S18 and S24. The milk used to produce cheese is assumed to be pasteurized milk since all the cheese regulated by the U.S. Food and Drug Administration must either be made from pasteurized milk or aged at least 60 days (U.S. Food and Drug Administration 2022). In addition, the functional unit for milk production is 1 kg of fat- and protein-corrected milk (FPCM), which standardizes milk to 4% fat and 3.3% protein.

The LCI of 1 kg FPCM in the United States was obtained from the literature, where milk production is based on Wisconsin condition (Grant and Hicks 2018). The composition of produced milk is 3.5% fat and 3.0% protein, and 1 kg of milk production is equal to 0.9968 kg of FPCM. A detailed conversion equation is listed below (Thoma et al. 2013), and the LCI of 1 kg FPCM production is shown in Table S18. The LCIs of alfalfa feed production of immature cows and mature cows and corn silage feed were obtained from literature (Grant and Hicks 2018) and adjusted to the GREET model, and detailed information can be found in Tables S19–S22. The produced milk needs to be further pasteurized to be used in cheese production, and the material and energy consumption for processing milk was adjusted from literature and summarized in Table S23 (Grant and Hicks 2018). The transportation from milk production plant to cheese production plant was estimated from chemical transportation by medium-/heavy-duty truck in

the GREET model, and the transportation of animal feed (alfalfa feed, corn silage, and cotton feed) from farm to collection stack and from collection stack to milk production plants was added based on corn transportation data obtained from the GREET model.

$$FPCM = \frac{0.0929F + 0.05882P + 0.192}{0.0929 \times (4\%) + 0.05882 \times (3.3\%) + 0.192} = \frac{0.092F + 0.05882P + 0.192}{0.7576} \quad \text{(S1)}$$

Cream is another ingredient to make cheese, which is not available in the current GREET model. The LCI of cream was obtained from Djekic et al. (2014), and detailed inventory for cream production is summarized in Table S24. Cream is usually coproduced with milk, and it is assumed that the transportation of cream from the production plant to cheese production factory is the same as milk.

Table S14. Input Material and Energy Consumption to GREET for Producing 1 kg of Whey PC

Input	Unit	WPC35	WPC60	WPC80
Whey (6% dry weight)	kg/kg of whey PC	45.8	80.0	112.8
Electricity	kWh/kg of whey PC	0.49	0.56	0.55
Natural gas	MJ/kg of whey PC	3.6	3.8	3.8
Water consumption	kg/kg of whey PC	0.0	1.3	3.1

Table S15. Input of 1 kg of Liquid Whey Production (Dry Mass Basis)

Input	Quantities	Notes
Fluid milk, FPCM	7.82E+00	New GREET model, pasteurized milk (detailed information is in the Appendix)
Cream	1.44E-02	New GREET model (detailed information is in the Appendix)
Nitric acid, 50% in H_2O (kg)	7.45E-05	
Sodium hydroxide, 50% in H_2O (kg)	1.20E-05	
Purchased water, municipal (kg)	3.95E+00	
Electricity (kWh)	1.34E-01	
Heat, natural gas (MJ)	5.25E+00	
Heat, propane/butane (MJ)	1.78E-02	
Heat, light oil (#2) (MJ)	1.71E-04	
Heat, heavy oil (#5 or #6) (MJ)		
Transportation (km)	1.50E+02	

Table S16. LCI of Cheese and Liquid Whey Production

Input	Quantities	Units
Pasteurized milk	1.02E+01	kg
Thermal energy	7.39E-01	MJ
Electricity	5.40E-02	kWh
Output		
Cheese	1.00E+00	kg
Liquid whey	9.22E+00	kg

Table S17. Allocation Percentages

Product	Total Solids	Nutritional Content	Economic Value
Cheese	50%	69%	88%
Liquid whey	50%	31%	12%

Table S18. LCI of 1 kg FPCM Production

Input	Quantity	Unit	Notes
Water	5.42E+00	kg	GREET
Electricity	6.75E+01	Btu	GREET
Alfalfa silage (immature cows)	9.04E-02	kg	New model, Table S19
Alfalfa silage (mature cows)	2.29E-01	kg	New model, Table S20
Corn silage	2.18E-01	kg	New model, Table S21
Cotton seed	5.73E-02	kg	New model, Table S22
Corn grain	1.89E-01	kg	GREET
Soybean meal	2.54E-02	kg	GREET
Corn grain (ground, dry)	4.01E-03	kg	New model (corn silage)
Distiller's dried grains with solubles	4.62E-03	kg	GREET
Energy from diesel burned in machinery	3.67E+01	Btu	GREET
Output			
FPCM	1.00E+00	kg	
Methane, biogenic	8.52E-03	kg	
Ammonia	2.14E-03	kg	
Nitrogen oxide	9.72E-05	kg	
CO_2, biogenic	5.23E-01	kg	
N_2O	3.69E-04	kg	

Table S19. LCI of 1 kg Alfalfa Feed Production for Immature Cows (Dry Mass, Adjusted Based on Available Fertilizer in GREET Model)

Input	Quantity	Unit
Herbicides	4.20E-04	kg
Pesticides	1.00E-04	kg
Energy from diesel burned in machinery	8.51E+02	Btu
P_2O_5, fertilizer	6.51E-03	kg
K_2O, fertilizer	3.14E-02	kg
$CaCO_3$, fertilizer	1.62E-01	kg
Output		
Alfalfa feed for immature cows (dry matter)	1.00E+00	kg

Table S20. LCI of 1 kg Alfalfa Feed for Mature Cows (Adjusted Based on Available Fertilizer in GREET Model)

Input	Quantity	Unit
Herbicides	4.20E-04	kg
Pesticide	1.00E-04	kg
Energy from diesel burned in machinery	5.78E+02	Btu
P_2O_5	6.51E-03	kg
K_2O	3.14E-02	kg
$CaCO_3$	1.62E-01	kg
Output		
Alfalfa feed for mature cows (dry matter)	1.00E+00	kg

Note: Seed production is excluded from the inventory based on Grant and Hicks (2018)

Table S21. LCI of 1 kg Corn Silage Feed (Dry Mass)

Input	Quantity	Unit
Nitrogen fertilizer	7.15E-03	kg
P_2O_5, fertilizer	5.16E-03	kg
Energy from diesel burned in machinery	6.47E+02	Btu
Pesticides	3.00E-04	kg
$CaCO_3$, lime fertilizer	2.97E-02	kg
K_2O, fertilizer	1.24E-02	kg
Output		
Corn silage (dry mass)	1.00E+00	kg

Table S22. LCI of 1 kg Cotton Seed Production

Input	Quantity	Unit
P_2O_5, fertilizer	2.12E-02	kg
Energy from diesel burned in machinery	9.69E-02	MJ
Electricity	3.47E-02	kWh
Liquified petroleum gas, at refinery	2.70E-02	L
Herbicides	0.00055	kg
Pesticides	0.00012	kg
$CaCO_3$, fertilizer	6.00E-03	kg
K_2O, fertilizer	1.62E-02	kg
Nitrogen, fertilizer	1.85E-02	kg
Natural gas	7.00E-07	m^3
Output		
Cotton feed (dry mass)	1.00E+00	kg

Table S23. Material and Energy Inputs for Milk Processing (Pasteurizing)

Input	Quantity	Unit
Milk	1.00E+00	kg
Natural gas (industrial boiler)	7.12E+01	Btu
Liquified petroleum gas (industrial boiler)	2.03E+00	Btu
Gasoline (combustion)	2.30E+01	Btu
Transport distance	4.08E-01	tkm

Table S24. LCI of Cream Production

Inputs	Quantity	Unit
Raw milk	3.78E+00	kg
Water	2.33E+00	kg
NaOH	1.48E-03	kg
HNO_3	1.30E-04	kg
Electricity	3.18E+02	Btu
Natural gas	2.61E+02	Btu
Output		
Cream	1.00E+00	kg
Wastewater	6.71E+00	kg

LCI of Soy PC

The soy PC is extracted from soybean. The LCI of soybean (13% water) farming, harvesting, and transportation to a soy PC production plant was obtained from the GREET model. The LCI of soy PC extraction from soybean (13% water) was obtained from Philis et al. (2018), and the LCI data were allocated based on mass or price as shown in Table S25. The protein content for soy PC is 62% according to literature (Philis et al. 2018), and it is assumed that the algae-based protein coproduct with protein content of approximately 72% can be used to replace it with three replacement metrics: mass, protein content, and digestible protein. The replacement ratio can be found in Table 2.2.10. Detailed LCI based on mass and price allocation can be found in Table S26.

The soy PC is investigated here to represent the protein ingredient market. Algal protein coproducts can also be used to replace other compounds, such as animal feed supplement, animal feed, and food and beverages. The LCI and LCAs of animal feed supplement, such as soybean meal and alfalfa meal supplement, were also investigated here for comparison purposes, and detailed information can be found in the next section.

Table S25. Mass and Price Allocation for Soy PC

Product	Mass Allocation	$ Allocation
Soy PC, 8% water	49.8%	75.4%
Soybean, hulls	6.8%	0.8%
Soybean, crude oil	16.6%	20.7%
Soybean, molasses	26.8%	3.1%

Table S26. LCI of Soybean PC Production With Mass and Price Allocation

Inputs	Mass Allocation	$ Allocation	Units
Soybean (water content 13%)	9.23E-01	1.40E+00	kg
Diesel, extraction	3.58E+02	5.42E+02	Btu
Electricity, extraction	9.44E+02	1.43E+03	Btu
Natural gas, extraction	6.30E+02	9.53E+02	Btu
Process water	2.31E-01	3.49E-01	kg
Output			
Soybean PC, 8% water	1.00E+00	1.00E+00	kg
Wastewater	1.53E-01	2.32E-01	kg

Soybean PC is the main product, and multiple coproducts are generated in the production process. To assess the environmental impacts associated with soybean PC production, allocation methods have been utilized. However, it is important to note that these allocation methods can introduce uncertainties. To address this, both mass and economic value allocation methods have been employed to estimate GHG emissions. Furthermore, it should be acknowledged that the inclusion of ILUC can influence the environmental outcomes, adding further variability to the results. The ILUC carbon emissions caused by the increasing demand for soybean PC will contribute to the overall carbon footprint, particularly considering the deforestation associated with soy production. LUC has been identified as the primary contributor to carbon emissions in Brazil, accounting for approximately 36% of the country's total emissions in 2010–2015 (Escobar et al. 2020). Consequently, the incorporation of ILUC carbon emissions will increase the GHG emissions associated with soybean PC production, resulting in higher environmental credits for soybean PC. However, the consideration of ILUC falls outside the scope of this project, and we will explore the variation in GHG emissions with ILUC inclusion in other future work. To provide an understanding of the additional environmental credits that can be achieved through the increased GHG emissions of soybean production, we also estimated the GHG emissions generated from soybean PC by doubling the GHG emissions of soybean production. The results can be found in the "LCA Result Details and Supporting Information" section in the Appendix.

LCI of Animal Feed Supplement

In recent years, microalgae have been considered as a valuable feed supplement or substitute for conventional protein sources, such as soybean meal, alfalfa meal, fishmeal, and rice bran. As one scenario in this report, it is assumed that microalgae solid coproduct from HTL can be used to replace animal feed supplement, and the environmental credits by using solid coproduct to replace animal feed supplement, including fossil energy, water consumption, and GHG emissions, are evaluated.

It has been found that replacing animal feed supplement with microalgae protein does not incur significant impacts on feed intake, overall growth, or yield (e.g., milk yield), regardless of whether microalgae is used as a feed supplement or substitution for conventional protein sources (Table S27). It is noticeable that different microalgae species may lead to different performances, since they have different compositions. However, for simplification purposes, it is assumed that when the microalgae species (*Tetraselmis striata*) used in this study serves as animal feed supplement, it has similar performance with other microalgae species used to replace soybean

meal or alfalfa meal in different cases. In addition, compared with microalgae, solid microalgae-based protein coproduct does not contain significant fermentable carbohydrates or lipids, the latter of which are transformed into SAF and renewable diesel. However, the main reason for using microalgae for animal feed supplement is the high protein and amino acids, and the protein and amino acids in solid coproduct are intact and can be used to replace soybean meal or alfalfa meal. Mass, protein content, and digestible protein were used to calculate the replacement ratios by using microalgae protein coproduct to replace soybean meal or alfalfa meal. A 100% replacement ratio was achieved when mass was used as the matching unit. The replacement ratio by using protein content and digestible protein can be found in Table 2.2.10.

Table S27. Literature Review on the Replacement of Animal Feed Supplement With Microalgae

Microalgae Species	Animals	Percentage of Replacement	Function	Effects on Growth or Yield	Reference
Tetraselmis sp. CTP4 (defatted)	Juvenile gilthead seabream (*Sparus aurata*)	10% of dehulled SBM [a] is replaced with defatted microalgal biomass	Substitution of protein source	Not significant	Pereira et al. (2020)
Spirulina platensis	Meat type chicken	50%, 75%, and 100% of SBM is replaced with SPI [b]	Substitution of protein source	Not significant	Neumann, Velten, and Liebert (2018)
Spirulina (*Arthrospira platensis*)	Dairy cow	6% SBM is replaced with 5% of SPI	Feed supplement	Not significant	Manzocchi et al. (2020)
Spirulina platensis, *Chlorella vulgaris*, and *Nannochloropsis gaditana*	Dairy cow	16.5% SBM is replaced with 10% SPI, 11.9% CHL,[c] or 7.1% CHL-NAN [d]	Feed supplement		Lamminen et al. (2019)
Scenedesmus quadricauda and *Chlorella vulgaris*	Freshwater rotifer, *E. dilatata*	100% of alfalfa meal is replaced with SQ [e] or CHL	Substitution of protein source	Not significant	Farhadian, Daghighi, and Dorche (2013)

[a] Soybean meal
[b] *Spirulina platensis*
[c] *Chlorella vulgaris*
[d] Mixture of *Chlorella vulgaris* and *Nannochloropsis gaditana* (1:1 on dry matter basis)
[e] *Scenedesmus quadricauda*.

LCA Result Details and Supporting Information

LCA Results for the FO Membrane

The LCA results for the FO membrane are presented in Table S28. No comparisons with the literature were made due to limited available data.

Table S28. Fossil Energy, Water Consumption, and GHG Emissions From the FO Membrane System To Treat 1 L of Water

	FO Membrane System	Unit
Fossil energy	5.62E-03	MJ/L of treated water
Water consumption	2.39E-04	gal/L of treated water
GHG emissions	7.17E-01	g CO_2e/L of treated water

LCA Results and Validation for Whey PC

The calculated results of whey PC were compared with findings from literature sources, as shown in Figure S2 and Table S29. The analysis revealed that a wide range of GHG emissions can be attributed to three main factors: the allocation factor, GHG emissions from cheese production, and the consumption of liquid whey in whey PC production. When comparing the results, GHG emissions from cheese production were found to vary from 4.7 to 14.4 kg CO_2e/kg of cheese production, while the liquid whey consumption exhibited variability based on assumptions regarding the protein content of liquid whey. Although the latter two factors contribute to the uncertainties in whey PC production, the allocation methods employed play the most significant role in introducing uncertainties. As shown in Table S30, GHG emissions resulting from liquid whey production ranged from 0.74 to 8.51 kg CO_2e/kg of dry mass of liquid whey. Consequently, the environmental credits attributed to whey PC production were presented as a range, with the average value obtained from the economic allocation method (14.6 kg CO_2e/kg), the minimum value obtained by excluding the impacts from liquid whey production (0.9 kg CO_2e/kg), and the maximum value obtained through the solid content allocation method (46.3 kg CO_2e/kg).

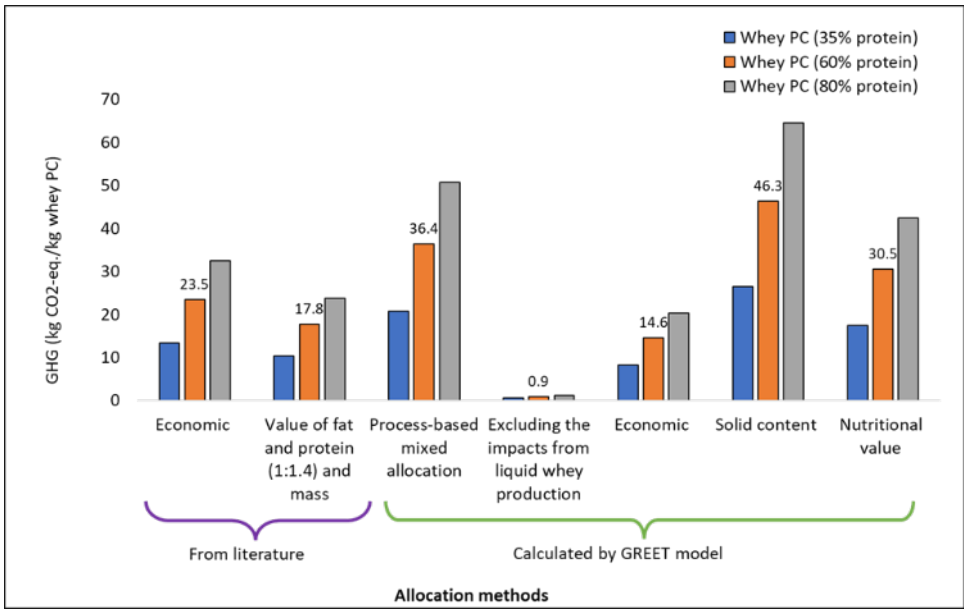

Figure S2. Comparison of GHG emission results with the literature

Table S29. Comparison of GHG Emission Results With Literature

	GHG Emissions from Literature		**Results Calculated by GREET Model**				
Allocation methods	Economic	Value of fat and protein (1:1.4) and mass	Process-based mixed	Excluding the impacts from liquid whey production	Economic	Solid content	Nutritional value
Whey PC (35% protein)	13.3	10.4	20.8	0.5	8.2	26.0	17.1
Whey PC (60% protein)	**23.5**	**17.8**	**36.4**	**0.9**	**14.4**	**45.4**	**29.9**
Whey PC (80% protein)	32.5	23.7	50.7	1.2	20.0	63.3	41.6
References	Bacenetti et al. (2018)	Allocation based on the value of fat and protein (1:1.4) (Flysjö, Thrane, and Hermansen 2014)	Kim et al. 2013		Aguirre-Villegas et al. (2012)	Aguirre-Villegas et al. (2012)	Aguirre-Villegas et al. (2012)

Table S30. LCA Results Validation With Literature for 1 kg of Liquid Whey

Parameter	GHG Emissions	Units	Notes	Reference
Production of barley (ready for use at the farm)	0.74	kg CO_2e/kg of barley dry mass	System expansion	Kristensen et al. (2015)
Whey powder	0.56	kg CO_2e/kg whey powder	Economic allocation (cheese: 7.49 kg CO_2e/kg; 7% is allocated to whey powder)	González-García et al. (2013)
Whey powder	2.55	kg CO_2e/kg whey powder	Mass allocation (33% is allocated to whey powder)	González-García et al. (2013)
Liquid whey	7.35	kg CO_2e/kg liquid whey (dry mass)	Process-based mixed allocation method and GREET (cheese: 8.34 kg CO_2e/kg)	Kim et al. (2013)
Liquid whey	8.51	kg CO_2e/kg liquid whey (dry mass)	LCI and solid content allocation and GREET (cheese: 4.71 kg CO_2e/kg)	Aguirre-Villegas et al. (2012)
Liquid whey	5.28	kg CO_2e/kg liquid whey (dry mass)	LCI and nutritional value allocation and GREET (cheese: 6.50 kg CO_2e/kg)	Aguirre-Villegas et al. (2012)
Liquid whey	2.04	kg CO_2e/kg liquid whey (dry mass)	LCI and economic value allocation and GREET (cheese: 8.28 kg CO_2e/kg)	Aguirre-Villegas et al. (2012)

LCA Results and Validation of Upstream Data for Liquid Whey Production

The LCIs of liquid whey production were obtained from two sources (Kim et al. 2013; Aguirre-Villegas et al. 2012), and detailed inventories can be found in Tables S15 and S16. To ensure the data quality of liquid whey production, the LCA results for its upstream data were also compared. The main upstream feedstock for cheese and liquid whey production are milk and cream, and the LCA results for these two were compared with literature results and shown in Tables S31 and S32.

Table S31. LCA Results Validation With Literature for 1 kg of FPCM Production

	This Study	Mean Value (Grant and Hicks 2018) [a]	Mean Value (Till Milk Production) (Grant and Hicks 2018)
Fossil energy (MJ/kg FPCM)	2.4	3.0	~2.6
GHG (g/kg FPCM)	0.8	2.8	~1.3

[a] The values given by Grant and Hicks (2018) are cradle-to-gate data, which include the impacts from retail. The impacts from cradle to milk production (excluding retail) are estimated from the figure obtained from Grant and Hicks.

Table S32. LCA Results Validation With Literature for 1 kg of Cream Production

	This Study	Djekic et al. (2014)
GHG (g/kg cream)	3.0	3.52–4.53

LCA Results and Validation for Soy PC

As shown in Table S33, the LCA results of soybean PC were compared with the results of soybean meal and soybean production in the GREET model and soybean production in Brazil

from literature (Escobar et al. 2020). It should be noted that the current upstream data used in this study for soybean PC production are based on average U.S. conditions. However, it is likely that the microalgae PC coproduct will be used to replace marginal soybean PC due to increasing demand. Therefore, the microalgae PC coproduct will be utilized as a replacement for soybean PC or soybeans produced in countries like Brazil, which is the world's largest soybean exporter. From the comparison, the GHG emissions from soybean production with U.S. average data is about half of those with Brazil average data, which can be explained by the inclusion of LUC carbon emissions. Consequently, the environmental credits attributed to soybean PC production were also presented as a range, with the minimum value obtained through mass allocation (0.5 kg CO_2e/kg), the average value obtained through economic allocation (0.7 kg CO_2e/kg), and the maximum value obtained by doubling the GHG emissions of soybean production and applying economic allocation (1.2 kg CO_2e/kg).

Table S33. LCA Results Validation With Literature for 1 kg of Soy PC (62% Protein Content) (Philis et al. 2018; Escobar et al. 2020)

	This Study (Soybean PC, 62% Protein Content)		U.S. Average		Brazilian Average
	Mass Allocation	Economic Allocation	Soybean Meal	Soybean	Soybean
GHG (g CO_2e/kg)	454.3	687.4	476.4	345.3	690
Fossil energy (MJ/kg)	4.3	6.5	3.4	1.6	
Water consumption (L/kg)	79.5	120.4	85.9	85.6	

Environmental Impacts Comparison Between Whey PC and Soy PC

As shown in Figure S3, GHG emissions are compared between whey PC and soybean PC. It is clear that whey PC has higher GHG emission credits than soybean PC with current allocation and assumptions. However, the specific products that the microalgae PC coproducts will replace remain uncertain. The decision will depend on many factors, such as the rising demand for protein, public acceptance, current production, and trade conditions of existing products, as well as the economic benefits associated with meeting the increasing protein demand. Furthermore, careful consideration has been given to the assessment of environmental impact uncertainties and variations arising from allocation methods and ILUC. It should be noted that soybean PC may potentially provide more substantial environmental credits as a result of higher carbon emissions resulting from ILUC. By replacing whey PC and soybean PC, the range of environmental credits obtained provides us with a more comprehensive understanding of the potential environmental benefits. This approach allows for a clearer perspective on the extent of environmental credits that can be achieved.

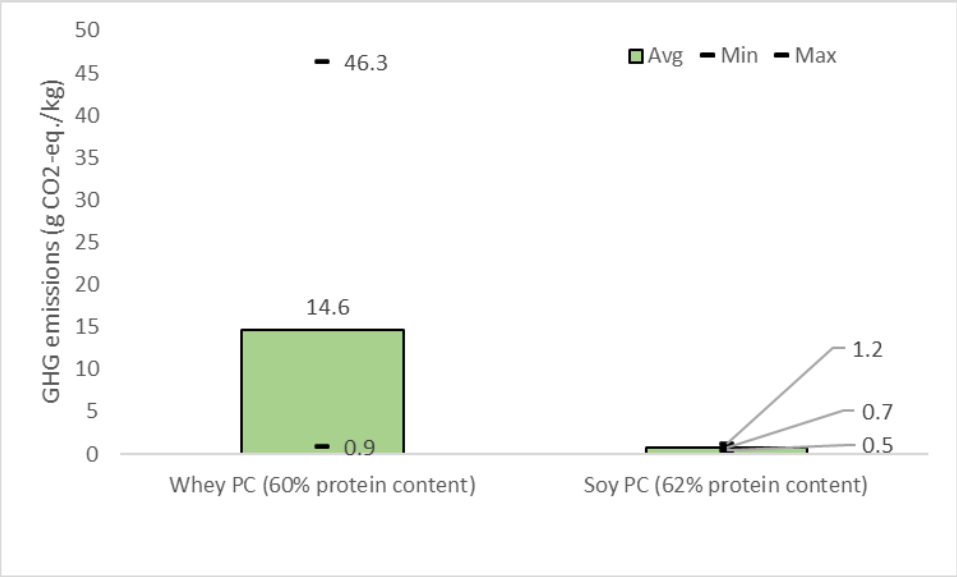

Figure S3. GHG emissions credit average, minimum, and maximum values estimated from different methods

LCA Results for Soybean Meal and Alfalfa Meal

Table S34. Fossil Energy, Water Consumption, and GHG Emissions From Soybean Meal and Alfalfa Meal

	Soybean Meal	Alfalfa Meal
GHG (g CO_2e/kg)	476.4	227.2
Fossil fuel (MJ/kg)	3.4	3.8
Water consumption (gal/kg)	22.7	169.0

Direct Land Use Change

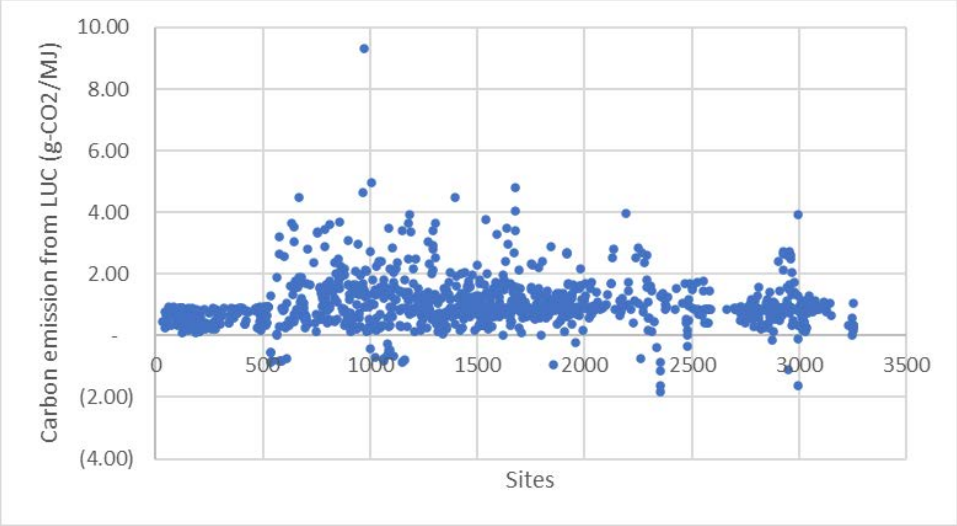

Figure S4. Carbon emissions from LUC (from original use to algae pond)

As shown in Figure S4, the maximum DLUC carbon emissions (9.3 g CO_2e/MJ) are generated from Pierson, Florida, due to 59% of original land from deforestation. The average LUC carbon

emissions from all sites are 1.0 g CO_2e/MJ, which is relatively small compared to the emissions from the supply chain.

LCI of the System and Associated GHG Emissions

Table S35. LCI of the System and Associated GHG Emissions in Site 1670 (With Median GHG Emissions)

CO_2 capture, transport, and compression (per kg CO_2)				
Item	**Units**	**Quantity**	**GHG (g CO_2e/unit)**	**Total GHG (g CO_2e/kg CO2)**
Capture (kWh/kg CO_2)	kWh	0.30	1,057	316
Transport (kWh/kg CO_2)	kWh	0.0012	1,057	1.3
CO_2 capture, transport, and compression (per kg CO_2)				317
Algae growth (per kg AFDW, with recycling)				
Item	**Units**	**Quantity**	**GHG (g CO_2e/unit)**	**Total GHG (g CO_2e/kg AFDW)**
Resource consumption				
Electricity (kWh/kg AFDW)	kWh	0.58	440	253
CO_2 (kg/kg AFDW)	kg	1.7	317	525
Urea (kg/kg AFDW)	kg	0.059	1,222	72
$(NH_4)_2HPO_4$ (kg/kg AFDW)	kg	0.010	1,741	18
FO membrane unit	kg	0.007		
Total process water input (freshwater)	kg	278		
Output stream				
Water in biomass product stream (kg/kg AFDW)	kg	9.0		
Water sent to blowdown (kg/kg AFDW)	kg	228		
Conversion				
Item	**Units**	**Quantity (units/MJ RDe [a])**	**GHG (g CO_2e/unit)**	**Total GHG (g CO_2e/MJ RDe)**
Biomass input				
Algae biomass (kg AFDW/MJ RDe)	kg	0.14	868	124
Fuel products				
Renewable diesel (MJ/MJ RDe)	MJ	0.17		
Naphtha (MJ/MJ RDe)	MJ	0.22		
SAF (MJ/MJ RDe)	MJ	0.60		
Gasoline (MJ/MJ RDe)	MJ	0		
Total (MJ fuels)	MJ	1		
Coproducts				
PC production	kg	0.050	14,616	−579
Energy inputs				
Electricity demand (kWh/MJ RDe)	kWh	0.092	440	41
Natural gas (Utility) (MJ/MJ RDe)	MJ	0.20		
Natural gas (H_2 production) (MJ/MJ RDe)	MJ	0.15		
Natural gas (summer/spring algae drying) (MJ/MJ RDe)	MJ			
Total natural gas (MJ/MJ Rde)	MJ	0.35	45	16

Chemicals and water demand	Units	Quantity (units/MJ RDe [a])	GHG (g CO_2e/unit)	Total GHG (g CO_2e/MJ RDe)
Sulfuric acid (kg/MJ RDe)	kg	0.0014	43	0.061
Hydrotreatment catalyst (kg/MJ RDe)	kg	1.7E-05	3192	0.055
Hydrocracking catalyst (kg/MJ RDe)	kg	3.0E-07	3192	9.6E-04
Membrane flocculant (kg/MJ RDe)	kg	0.0016	1272	2.0
NaOH (kg/MJ RDe)	kg	5.5E-05	1241	6.8E-02
Water (process demands) (gal/MJ RDe)	gal	0.036	0	0
HCl (kg/MJ RDe)	kg	1.1E-05	1985	2.1E-02
CO_2 capture, transport, and compression (g per MJ RDe)				73
Algae growth (g per MJ RDe)				49
Conversion (g per MJ RDe)				67
Coproduce credits (g per MJ RDe)				-27
Overall (g CO_2e/MJ RDe)				162

[a] Renewable diesel equivalent.